Analytical and Experimental Study of Turbulent Flow Drag Reduction and Degradation with Polymer Additives

By

© Xin Zhang

A Thesis submitted to the

School of Graduate Studies

in partial fulfillment of the requirements for the degree of

Doctor of Philosophy

Faculty of Engineering and Applied Science

Memorial University of Newfoundland

May 2020

St. John's Newfoundland

Abstract

Flow friction reduction by polymers is widely applied in the oil and gas industry for flow enhancement or to save pumping energy. The huge benefit of this technology has attracted many researchers to investigate the phenomenon for 70 years, but its mechanism is still not clear. The objective of this thesis is to investigate flow drag reduction with polymer additives, develop predictive models for flow drag reduction and its degradation, and provide new insights into the drag reduction and degradation mechanism.

The thesis starts with a semi-analytical solution for the drag reduction with polymer additives in a turbulent pipe flow. Based on the FENE-P model, the solution assumes complete laminarization and predicts the upper limitation of drag reduction in pipe flows. A new predictive model for this upper limit is developed considering viscosity ratios and the Weissenberg number - a dimensionless number related to the relaxation time of polymers. Next, a flow loop is designed and built for the experimental study of pipe flow drag reduction by polymers. Using a linear flexible polymer - polyethylene oxide (PEO) - in water, a series of turbulent flow experiments are conducted. Based on Zimm's theory and the experimental data, a correlation is developed for the drag reduction prediction from the Weissenberg number and polymer concentration in the flow. This correlation is thoroughly validated with data from the experiments and previous studies as well.

To investigate the degradation of drag reduction with polymer additives, a rotational turbulent flow is first studied with a double-gap rheometer. Based on Brostow's assumption, i.e., the degradation rate of drag reduction is the same as that of the molecular weight decrease, a correlation of the degradation of drag reduction is established, along with the proposal of a new theory that the degradation is a first-order chemical reaction based on the polymer chain scission.

Then, the accuracy of the Brostow's assumption is examined, and extensive experimental data indicate that it is not correct in many cases. The degradation of drag reduction with polymer additives is further analyzed from a molecular perspective. It is found that the issue with Brostow's theory is mainly because it does not consider the existence of polymer aggregates in the flow. Experimental results show that the molecular weight of the degraded polymer in the dilute solution becomes lower and the molecular weight distribution becomes narrower. An improved mechanism of drag reduction degradation considering polymer aggregate is proposed - the turbulent flow causes the chain scission of the aggregate and the degraded aggregate loses its drag-reducing ability. Finally, the mechanism of drag reduction and degradation is examined from the chemical thermodynamics and kinetics. The drag reduction phenomenon by linear flexible polymers is explained as a non-spontaneous irreversible flow-induced conformational-phase-change process that incorporates both free polymers and aggregates. The entire non-equilibrium process is due to the chain scission of polymers. This theory is shown to agree with drag reduction experimental results from a macroscopic view and polymer behaviours from microscopic views.

The experimental data, predictive models, and theories developed in this thesis provide useful new insights into the design of flow drag reduction techniques and further research on this important physical phenomenon.

Acknowledgements

I would like to thank my supervisor, Prof. Xili Duan, for his guidance and help throughout this thesis. At the beginning of this work, I once felt lost and did not know how to solve the research problems, and even had difficulty in writing papers and communicating with other people. Dr. Duan provided useful help in all these aspects. Without his help, I could not complete my Ph.D. program. I also wish to thank my co-supervisor, Prof. Yuri Muzychka, for his help in fluid mechanics theories and discussions to improve my research work. I am grateful to Prof. Kevin Pope and Prof. Yan Zhang for their valuable suggestions on my research. Besides, I also thank Prof. Anand Yethiraj from the department of physics and physical oceanography at the Memorial University of Newfoundland for the use of rheometer, and Prof. Zongming Wang from the department of chemical engineering at the China University of Petroleum (East China) for helping me to establish the flow loop. I am also grateful to the financial support from the Memorial University of Newfoundland and the NL Innovation Council. Last, I wish to thank my parents who always support me for my Ph.D.

Contents

List of Figures

List of Tables

List of Symbols

a	Monomer length	m
C^*	Overlap concentration	ppm
C_P	Concentration of DRAs	ppm
$\vec{c}$	Conformation tensor of the polymer	-
d	Diameter	m
De	Deborah number	-
$DR\%$	Drag reduction	-
E_a	Activation energy	J/mol
f	Friction factor	-
G	Modulus	Pa
G'	Storage modulus	Pa
G''	Loss modulus	Pa
I	Unit tensor	-
k	Chemical reaction rate constant	s^{-1}
k_0	Pre-exponential factor	s^{-1}
l	Maximum length of the polymer; length of the pipe	m
M	Average molecular weight	g/mol
N	Polymerization degree	-
N_A	Avogadro constant	mol^{-1}
P	Pressure drop along a certain direction	Pa
Q	Flow rate	L/min
$\vec{Q}$	End-to-end vector of the polymer	-

R_G	Radius of gyration of polymer	m
R_H	Radius of hydrodynamics of polymer	m
$\dot{r}$	Shear rate	s^{-1}
Re	Reynolds number	-
Re_b	Reynolds number based on bulk velocity	-
t	Time	s
T	Absolute temperature; torque	k; N·m
$\vec{T}$	Stress tensor of the polymers	-
t_P	Observation time	s
$\vec{u}$	Velocity vector	-
U_b	Bulk velocity	$m \cdot s^{-1}$
Wi	Weissenberg number	-
x	Distance	m

Greek symbols

α	Ratio of drag reduction; order of chemical reaction	-
β	Ratio of viscosity	-
δ	Uncertainty	-
$\mathcal{E}$	Roughness of pipe	m
λ	Relaxation time	s
μ	Viscosity	Pa·s
ρ	Density	$kg \cdot m^{-3}$

Chapter 1 Introduction of Drag Reduction by Polymers

1.1 Drag Reduction Research History

Some significant discoveries are often out of expectations, and drag reduction by polymers is one example. Toms found this remarkable phenomenon while he did not aim to research the pressure drop in the middle of 1946 (Toms, 1948). He was studying the degradation of polymer (polymethyl methacrylate) in a dilute solution (Chlorobenzene as the solvent) in a turbulent pipe flow, and the pressure drop was measured by a mercury u-tube manometer. Amazingly, Toms found that the pressure drop with polymers was lower than the one without polymers. Then he wished to find an explanation about this phenomenon from published works but failed since no work regarding it was released before. As a chemist, Toms did not understand this phenomenon. After he found this phenomenon, Oldroyd, another principal researcher in drag reduction by polymers, showed great interest in it. As a researcher in the Research Laboratory of Courtaulds with a mathematical background, Oldroyd mentioned that this phenomenon might be related to the modification of near-wall structure in turbulent flow (Toms, 1948 and 1977).

Before Toms observed the drag reduction phenomenon, Brautlecht & Sethi (1933) and Forrest & Grierson (1931) found that in pumping paper pulps, adding dilute suspensions could reduce the friction in the pipe. However, they used a figure to indicate this phenomenon but did not point out that it was the drag reduction phenomenon induced by chemical additives. Thus, the finding of the drag reduction phenomenon was still credited to Toms. In 1948, Toms presented his findings in the 1st International Congress on Rheology in Scheveningen Netherlands (Toms, 1948). However, this important finding did not receive much attention after it was published for the first time (Toms, 1977).

Figure 1-1 is the summary of Nadolink & Haigh's work (1995), who summarized the publication number about drag reduction by additives. It includes journal papers, conference papers, technical reports, book chapters, presentations and theses. In total, approximately 5000 papers were published from 1948 to 1995. Data of the publication number after 1995 are not available.

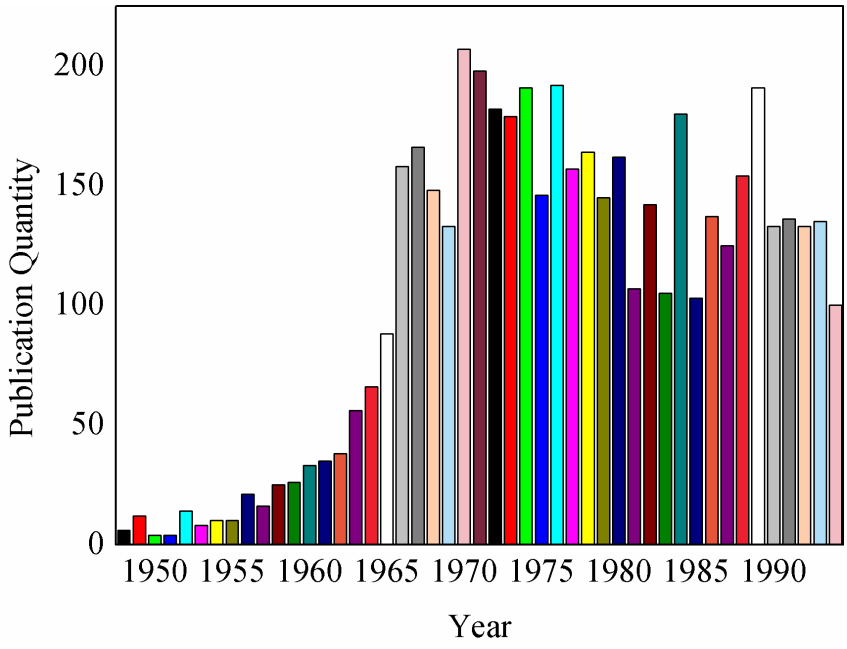

Figure 1-1 Summary of publications regarding drag reduction by additives

Figure 1-1 indicates that, from 1948, when this phenomenon was published, to the 1960s, before the oil crisis, this critical research area received little attention since few publications regarding this topic were released. But from the 1960s, this phenomenon received remarkably notice, and this was shown in the publication number because of the energy crisis in the late 1960s (oil embargo, 1967) and early 1970s (the first oil crisis, 1973) (Daoudi & Dajani, 1984; Houthakker, 1983). These energy crises forced oil companies to develop technologies to save

budget in every aspect of the oil and gas industry, including transportation. In this case, researchers received more funding from governments and companies in this area, and published more papers since these two energy crisis.

1.1.1 Top Three Achievements of Drag Reduction Research

The top three achievements of drag reduction by polymers in the author's view are the following ones:

- 1970s': Virk's maximum drag reduction (Virk et al., 1970; Virk, 1975)

In the 1970s, Virk summarized the drag reduction data in several works and proposed the famous Virk's asymptote (maximum drag reduction line by polymers). This asymptote is independent of polymer type, polymer concentration and viscosity etc. and only dependent on the Reynolds number. After Virk released this result, researchers started to use this maximum drag reduction line as a reference to show that all friction factors in drag-reducing flows should be less than the one predicted by Virk's asymptote which will be shown later. This result is also the most widely-accepted conclusion in the drag reduction research. The paper in 1970 is cited by more 300 times and the paper in 1975 is cited more than 1300 times.

- 1980s': Application in Alaska (Burger et al., 1980 and 1982)

The Trans-Alaska Pipeline System (TAPS) is the most successful application of drag reduction by polymers. In the 1970s, as mentioned above, the harsh situation for oil and gas industry forced oil companies to use new technologies to save the budget and increase oil output. In this condition, Alaska Pipeline Service Company first did several laboratory-scale experiments in 2.54 and 5.04 cm diameter pipes. After these tests, they did more tests in larger scale pipes (35.6 cm-diameter). They were looking for the relationship between the drag reduction in a small diameter pipeline and the drag reduction in a large-scale application (122

cm-diameter). The detailed information can be found in the two references mentioned above. This application is successful, but the empirical correlation and its method are not very scientific since they only used empirical coefficients to establish the correlation without reasonable interpretations.

- 1990s': De Gennes's Nobel Prize lecture about soft matter (De Gennes, 1992)

De Gennes (1932-2007) was a leading soft-matter scientist who won the Nobel Prize in 1991. In his Nobel-prize winning speech about soft matter, he also mentioned the drag reduction by polymers. This presentation is the most famous work for the drag reduction by polymers as an individual research topic. In this speech, he defined the concept of soft matter (complex fluid) with two features, complexity and flexibility, which also works for drag reduction by polymers.

1.2 Drag Reduction Applications

How much energy or cost is saved by oil companies in polymer drag reduction technology? Table 1.1 summarizes the drag reduction application in the oil-gas industry. On average, the drag reduction is about 20% based on the drag reduction definition in Eq. 1-1 (ΔP_P and ΔP_S are the pressure drop with and without polymers (pure solvents) under the same flow rate).

$$DR\% = \frac{\Delta P_S - \Delta P_P}{\Delta P_S} \times 100\% \tag{1-1}$$

If the drag reduction defined in Eq. 1-1 cannot represent how much energy is saved by companies, there is an alternative method to show how much this effect can help companies to reduce costs. The flow rate increase ($FI\%$) is a function of drag reduction in Eq. 1-2 (Burger et al., 1980 and 1982).

$$FI\% = \frac{1}{(1 - DR\%)^{0.55} - 1} \times 100\% \tag{1-2}$$

FI% describes the flow rate increase percentage if the pumping power remains the same. From Table 1-1, it can be seen that the flow increase is significant, especially for the Alaska pipeline, the most important drag reduction application. The flow increase is 560 m^3/h approximately from Eq. 1-2, more than 30,000,000 bbl/y (barrels oil per year). It means that this drag reduction technology provides an "extra" 1.8 billion US dollar per year based on the current oil price, i.e., approximately 60 US dollars per barrel. This technology offers a substantial economic benefit to the oil gas company.

There is also a positive side-effect of using drag-reducing polymers – the anti-corrosion effect in the transportation pipeline (Schmitt et al., 2001; Sedahmed et al., 1979, 1984 and 1999; Zahran et al., 1997 and 1998). This means that once polymers are used in transportation, not only pressure drop is decreased, but also the corrosion by the crude oil decreases. This side effect can lead to fewer replacements of pipeline and increase oil transportation safety.

Besides the application in oil and gas industry, drag reduction by polymers can also be applied in the other areas, i.e. irrigation (Khalil et al., 2002; Phukan et al., 2001), heating in building (to reduce the heat loss) (Kotenko et al., 2019; Myska & Mik, 2003), firefighting (Fabula et al., 1971; Figueredo et al., 2003), reservoir hydraulic fracturing (Ibrahim et al., 2018; Nguyen et al., 2018; Shah et al., 2010; Nguyen et al., 2018), and municipal wastewater transportation (Sellin, 1978 and 1983), even in drinking water transportation without affecting drinking water quality (Edomwonyi-Out et al., 2018). This drag reduction effect can also be used in blood pressure control. However, due to the potential toxicity of polymer to human, this application is still in the lab stage, not in the human experiment (Coleman et al., 1987; Faruqui et al., 1978; Hutchison et al., 1987; Kameneva et al., 2004; Polimeni et al., 1985 and 1989; Sawchuk et al., 1999; Unthank et al., 1992).

Previous sections mentioned the application of drag reduction in internal flows. Even in external flow, such as the shipbuilding industry, the phenomenon is still useful. White (1966) first argued that the drag-reducing effect of polymers could reduce the resistance of submarine vessel. Chahine et al. (1993) and Khomyakov & Elyukhina (2019) followed this view and used polymers to reduce the friction between the propeller of ship and sea water. Not only frictions, but also noise made by the propeller could be decreased by polymers (Oba et al., 1978; Reitzer et al., 1976).

Table 1-1 Summary of application drag reduction by polymers in the industry

Reference	Location	Liquid	Polymer name (Commercial name)	Concentration (ppm)	Inner diameter (cm)	Length (km)	Flow rate (m^3/h)	Drag reduction (%)	Flow increase (%)	Flow increase (Million bbl/year)	Saving (Million US $/year)	Cost of polymers (Million US dollar/year)
Burger et al., 1980 and 1982	Alaska, U.S.	Crude oil	NA (CDR)	5-20	122	1287	7950	12 on average	7	30	1830	0.17-0.68
Cao et al., 2018	Shandong, China	Crude oil	Poly-α-olefin	20-30	20	15	226	16-33	10	1.2	70	0.11-0.17
Carradine et al., 1983	Montana, U.S.	Gasoline	NA (CDR)	14	20	96	207	28	20	1.9	130	0.076
		Diesel		5			196	26	18	1.9	110	0.026
Lescarboura et al., 1971	Oklahoma, U.S.	Crude oil	NA	230	21	46	276	18	11	1.6	100	1.66
				250	31	52	559	17	11	3.4	200	3.67
Muth et al., 1985	Conoco Inc., U.S.	Gasoline	NA (CDR)	NA	20	97	199	28	24	2.6	150	NA
		Fuel oil			15	80		20	14	2.3	90	NA
Muth et a., 1986	Kansas. U.S.	Crude oil	NA (CDR)	38	41	262	713	23	15	5.9	350	0.71
Yang et al., 2018	Sichuan, China	Diesel	Poly-α-olefin	6-16	51	130	1232	28-55	20-55	13-37	820-2240	0.19

Note: oil price is 60 US dollar per barrel and drag reducing polymer price is 3 US dollar/kg based on the current price. Even if the investment of polymer injection stations is 10 million US dollars (an estimation), there is still important benefit from the drag reduction technology.

1.3 Thesis Objective, Structure and Highlights

The objective of this thesis is to investigate flow drag reduction with polymer additives, develop predictive models for flow drag reduction and its degradation, and provide new insights into the drag reduction and degradation mechanism. The relationship between these different aspects and the thesis structure is shown in Figure 1-2.

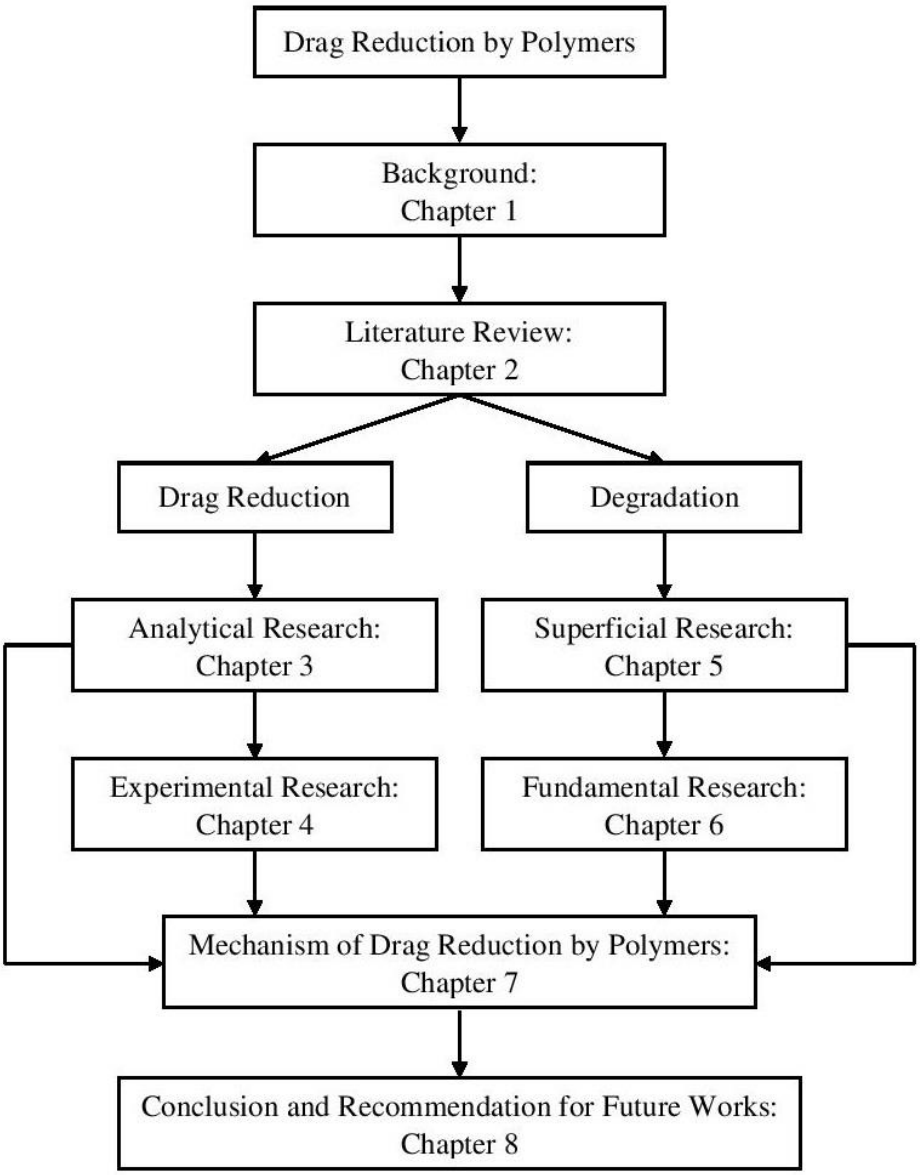

Figure 1-2 Thesis structure

- Chapter 1 (background): a short history of drag reduction, applications and thesis structure are repsented.
- Chapter 2 (literature review) : a review of relavent literature for the reserch topic is represented.
- Chapter 3 (analytical research about the semi-analytical solution of drag reduction): from governing equations for drag reduction by polymers and several assumptions, a semi-analytical solution to predict the drag reduction is developed and it is validated by experimental data.
- Chapter 4 (experimental research about the drag reduction prediction using Zimm's relaxation theory): an experimental study in a flow loop is peformed to investigate the drag reduction by polymers based on Zimm's relaxation theory.
- Chapter 5 (correlation and mechanism of drag reduction degradation): degradation of drag reduction is studied to develop a correlation and a new degradation mechanism from chemical reaction view is provided.
- Chapter 6 (fundmental research about the correctness of the widely-accepted Brostow's assumption): experimental data are used to show the inaccuracy of Brostow's theory. An improvded degradation mechanism of drag reduction is then proposed.
- Chapter 7 (proposed mechanism of drag reduction and degradation): chemical thermodynamics and kinetics are introduced to propose a new drag reduction and degradation mechanism by polymers.
- Chapter 8 (conclusions and recommendation for future work): conclusions in previous chapters are summarised and the future work recommendations are provided.

The novelty and highlight of this thesis are summarized as follows:

- A semi-analytical solution is proposed from the FENE-P model and validated by experimental results.
- The definition of the relaxation time and Weissenberg number are clarified, and a correlation of drag reduction prediction is provided from the polymer relaxation.
- The degradation of drag reduction is explained as a first-order chemical reaction, and this view is supported by experimental data.
- A revised mechanism of degradation of drag reduction is provided, which incorporates the degradation of free polymer and degradation of polymer aggregate.
- The mechanism for flow drag reduction and degradation is proposed based on the observation of molecular behavior in the microscope and validated by the experimental data.

Chapter 2 Literature Review

2.1 Drag Reduction

2.1.1 The Problem of Drag Reduction Mechanism

For every research topic, one of the fundamental problems is to understand the mechanism of the phenomenon. On the topic of drag reduction by polymers, researchers also hope to find the mechanism to completely understand this phenomenon. However, such a mechanism is still not available even this has been investigated for more than 70 years. The detailed reasons will be shown in the following section.

On the application side, the aim of the drag reduction research has been to help the design of oil transportation. Most studies use a flow loop to simulate this process. In the flow loop experiment, the velocity (flow rate), concentration of polymers, polymer type, molecular weight, pipe diameter and temperature can be changed to investigate how these parameters affect the drag reduction. In the drag reduction study, friction factor is often used to manifest the resistance in drag-reducing flow. Friction factor, f, is defined in Eq. 2-1. In this equation, d is the pipe diameter; ΔP is the pressure drop; l is the pipe length; ρ is the fluid density; U_b is the bulk velocity.

$$f = \frac{d\Delta P}{2l\rho U_b^2} \tag{2-1}$$

Figure 2-1 shows a typical result of drag reduction research by drag-reducing agents, also known as the most acknowledged result, polymer or surfactant in a pipe or channel flow. The friction factor in the drag-reducing flow should be enveloped by several lines: friction of laminar flow and its extension (Eq. 2-2, $Re \leq 2300$ in pipe or channel flows), friction factor of fully turbulent flow by Blasius equation (Eq. 2-3, $4000 \leq Re \leq 10^5$ in pipe or channel flows), friction

factor by Virks's asymptote (maximum drag reduction line by polymers, first introduced by Virk et al. in 1970, Eq. 2-4, $4000 \leq Re \leq 4\times10^4$ in pipe or channel flows) and friction factor by Zakin's asymptote (maximum drag reduction line by surfactants, first introduced by Zakin et al. in 1996, Eq. 2-5, $4000 \leq Re \leq 4\times10^4$ in pipe or channel flow). Note: the drag reduction by surfactants in this thesis is not investigated, but it is to show that the potential of drag reduction by surfactants may be higher than polymers even though concentration for surfactants in the drag-reducing flow is higher than the one of polymers, which may increase the cost of drag reduction. The drag reduction started to happen from the onset point of turbulent flow (the Reynolds number 4000 for pipe and channel flow). With a higher Reynolds number, the friction factor will be decreased further until the optimum Reynolds number appears under a given concentration. Under the optimum Reynolds number, the drag reduction reaches its maximum value. If the Reynolds number is further increased, the drag reduction will be smaller, which is explained in our work (Zhang et al., 2018), and also will be shown in Chapter 3.

$$f = \frac{16}{Re} \tag{2-2}$$

$$f = 0.079Re^{-0.25} \tag{2-3}$$

$$f = 0.59Re^{-0.58} \tag{2-4}$$

$$f = 0.32Re^{-0.55} \tag{2-5}$$

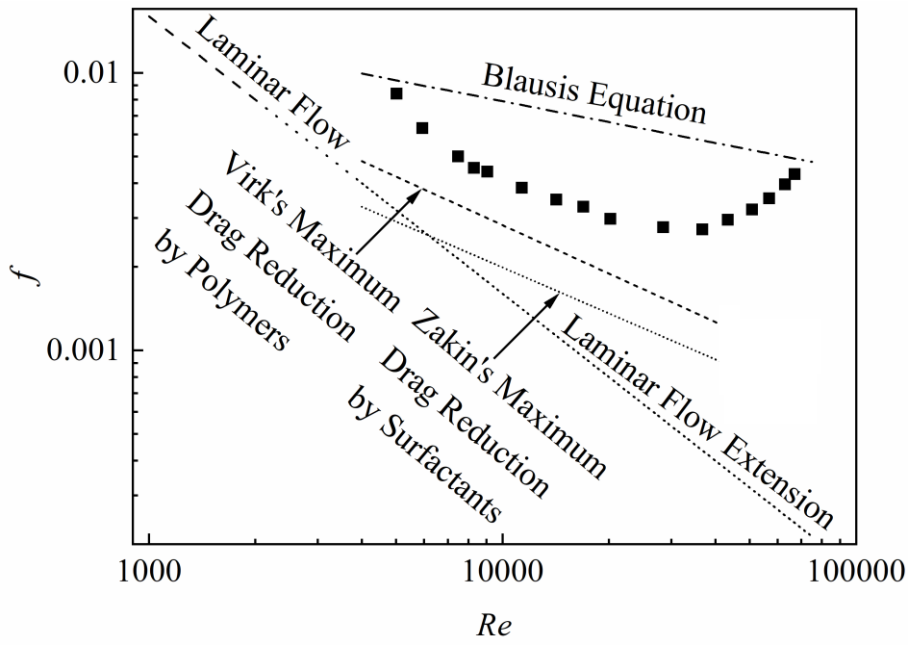

Figure 2-1 A typical result of drag reduction by polymers (data from Savins (1967))

2.1.2 Modelling of Drag Reduction

From the 1970s, researchers started to modify the Reynolds stress model (Hassid, 1979), turbulent energy dissipation (ε-k) model (Hassid & Poreh, 1975 and 1978) to investigate the drag reduction by polymers. Others used similar models, focusing on the modified boundary layer by polymers (Anderson & Wu, 1971; Test, 1974). One of the main results in these studies is the velocity profile in the drag-reducing turbulent flow, validated by several experimental results (Eskin 2017; Yang 2009; Yang & Ding, 2013 and 2014; Yang & Dou, 2008), where the velocity profile data were measured by PIV (particle imaging velocimetry).

Nowadays, these models are no longer used. In most papers, only one model is used, i.e., the FENE-P model (Finitely Extensible Nonlinear Elastic and P for the Peterlin equation). In this model, the traditional Naiver-Stokes equation is modified with consideration of the effects of polymers in the turbulent flow. The drag-reducing polymer is regarded as a dumbbell. The key in

this model is the relaxation time of polymers in the flow, which will be shown later. Several studies tried to use experimental data to verify this model. Den Toonder (1997) and Ptasinski et al. (2003) used the velocity profile measured by PIV to validate the velocity profile in the numerical simulation. The model can be validated by some experimental results, but this model cannot predict all the drag reduction data. Researchers still need empirical correlations to predict the drag reduction. In the following section, a summary of empirical drag reduction prediction equations is shown.

2.1.3 Scale-Up Effect and Correlations

As mentioned above, researchers cannot fully understand the drag reduction phenomenon and further propose a mechanism which is accepted universally, so the focus has been on predicting the drag reduction in experimental conditions. In the prediction of drag reduction by polymers, the most critical problem is the scale-up effect: most drag reduction studies are performed in small diameter pipes, i.e. the lab scale. However, the diameter in the application of oil and gas transportation is much larger than the lab-scale one. Thus, it is necessary to use some methods to predict the drag reduction in the large scale from data obtained in a small scale. Researchers have introduced several criteria for this scale-up effect.

Hoyt in his series of works (Hoyt, 1991; Hoyt and Sellin, 1993) proposed a similarity law to predict the friction factor in the drag-reducing flow in Eq. 2-6. From this similarity law, drag reduction data from a small diameter pipe can be used to predict the drag reduction in a large diameter pipe.

$$Re_2 = Re_1 \sqrt{\frac{f_2}{f_1}} \frac{d_2}{d_1} \tag{2-6}$$

If this equation is rearranged, Eq. 2-7 can be obtained.

$$\frac{Re_1\sqrt{f_1}}{d_1} = \frac{Re_2\sqrt{f_2}}{d_2} \tag{2-7}$$

From this equation, the $Re\sqrt{f}/d$ can be treated as a constant. The Reynolds number is a function of pipe diameter, bulk velocity, fluid density and viscosity. So, it can be further rewritten as:

$$\frac{Re\sqrt{f}}{d} = Const \tag{2-8}$$

From this equation, if the ratio of *Re*/*d* in the drag-reducing flow is the same, the friction factor can be the same. But this criterion is not widely adopted since only limited data (Hoyt, 1991; Hoyt and Sellin, 1993) could validate it.

The previous similarity law only considered fluid properties (Reynolds number and pressure drop) but did not consider the drag-reducing polymers since no parameters related to polymers are involved in them. Instead, Virk & Baher (1970) proposed another similarity law that combined the friction velocity and properties of the polymer solution, shown in Eq. 2-9. μ_S is the viscosity of the solvent and R_G is the radius of gyration of polymers in the coiled state. u_τ is the friction velocity, a function of shear stress at the wall, defined in Eq. 2-10. Shear stress is a function of friction factor, defined in Eq. 2-11.

$$\frac{u_\tau}{\mu_S} R_G = Const \tag{2-9}$$

$$u_\tau = \sqrt{\frac{\tau_W}{\rho}} \tag{2-10}$$

$$\tau_W = f\frac{\rho {U_b}^2}{2} \tag{2-11}$$

Although no other work followed this criteria, it is still valuable since it points out that the configuration of polymers - the gyration of radius of polymers, R_G, is involved in drag

reduction. This important parameter of polymer inspires future work, which considers the relaxation time, another critical parameter in drag reduction.

Relaxation process refers to the polymer's behavior from the stretched state to the coiled state, and the relaxation time describes the time from the stretched state back to the coiled state. This property is very critical in drag reduction since it is the key to understand the mechanism of drag reduction suggested by De Gennes (1986). The mechanism suspension will be discussed in the following section.

The definition of relaxation time of polymer, λ, is clear and it is related to two dimensionless numbers related to correlation to predict the drag reduction, Deborah number (*De*) and Weissenberg number (*Wi*), defined below (Dealy, 2010; Poole, 2012). t_P is the residence time of polymers in the flow and $\dot{r}$ is the shear rate at the wall.

$$De = \frac{\lambda}{t_P} = \frac{\lambda}{\frac{l}{U_b}} \tag{2-12}$$

$$Wi = \lambda\dot{r} = \lambda\frac{8U_b}{d} \tag{2-13}$$

The definition of these two dimensionless variables has been discussed for many years in many articles. Roriguez et al. (1969) introduced a "dimensional Deborah number" (not dimensionless one) to correlate the drag reduction and this "dimensional Deborah number", and detailed information of this dimensional Deborah number can be found in this work. Different from this method, the dimensionless Deborah number in several works (Darby & Chang, 1984; Darby & Pivsa-Art, 1991; Gordon, 1970; Sever & Metzner, 1967) was a function of the relaxation time, shear rate, Reynolds number and many other fluid property variables, which definition did not follow the original one. Since the Deborah number is critical to predict the drag reduction, Gordon (1971) compared several definitions, but he failed to provide a

conclusive definition. Recently, this confusing dimensionless number is clarified in one paper (Zhang et al., 2019): the diameter of the pipe is related to the Weissenberg number and the length of the pipe is related to the Deborah number.

Several similarity laws exist, but none of them can be applied in all drag reduction studies. Thus, most studies still used experimental data to establish many empirical correlations to predict drag reduction. There are two types of empirical correlations, dimensional and dimensionless.

Many empirical correlation methods, such as artificial intelligence approach and response surface methodology, were used for the prediction of drag reduction (Karami et al., 2016; Zabihi et al., 2019). Correlations by these methods have a good agreement between the prediction and experimental data, but these methods are not very useful since these two methods can be regarded as a complete black box, and are not helpful to manifest the mechanism. Besides, many dimensional variables are involved in these correlations. As known to all, dimensionless numbers are preferred in the classic fluid dynamics theory, so correlations by these methods are not very good even though they can predict the data well. Similar drawbacks can also be found in other works, which also use dimensional variables (Kamel and Shah, 2009; Zhao et al., 2018).

As shown above, since there are two types of scale-up effect criteria, there are also two types of correlations, one based on the Reynolds number, and the other based on the Weissenberg or Deborah number.

Dodge & Metzner (1959) first proposed a friction factor in the drag-reducing fluid. In this equation, the generalised Reynolds number was employed, and two coefficients were functions of the flow behaviour index, n'. Savins (1964) further expanded this equation. He argued that two coefficients were more complicated than what Dodge & Metzner (1959) expected: these two

coefficients were functions, but they could not be represented in a simple method as Dodge & Metzner (1959) suggested. In fact, they were dependent on the polymer type and concentration.

Some researchers used another type of Reynolds number in the correlation. Shah et al. (2002) introduced another correlation based on the solvent-based Reynolds number to predict the friction factor in the drag-reducing flow (detailed information of two coefficients were not listed). Following this idea, Shah & Kamel (2010) and Shah and Vyas (2011) used two polynomials to predict the drag reduction or friction factor in the drag-reducing fluids. Similar to Savins's (1964) conclusion, they also agreed that the concentration was involved in the drag reduction prediction correlation. The Reynolds number in these correlations were based on the solvent, Re_S, not generalized Re_G based on the polymer solution. A summary of these correlations and their application range is shown in Table 2-1.

These models could only explain the data in their own work, and could not be validated by others. Thus, researchers started to use another method to develop correlations based on the Weissenberg number or Deborah number, *Wi* or *De*, whose idea may be from the scale-up effect view based on the relaxation process of the polymer as mentioned above.

Owolabi et al. (2017) provided their different view on the relaxation time. They used the CaBER (Capillary Breakup Extensional Rheometer) to measure the relaxation time, not from the rheology equation, as shown by Owolabi et al. (2017). The model was applied for their data in a semi-dilute polymer solution. The definition of their Weissenberg number is shown in Eq. 2-13. This thesis will use another method, i.e., the Zimm's theory, to estimate the relaxation time for the dilute polymer solution (see Chapter 4). The new correlation from this method can predict data in our experiments and other studies. Thus, there are three methods to obtain the relaxation

time of polymers in the solution: rheology equation, CaBER measurement and Zimm's theory. The summary of these equations is shown in Table 2-2.

2.1.4 Experimental Methods

Most drag reduction experiments are performed in a flow loop aiming to simulate the industrial applications. Some are in a rotating disk apparatus or similar devices (Choi et al., 1999; Kim et al., 1997 and 2002; Yang et al., 1994), whose importance is less than the one of the flow loop experiment since this type of experiment cannot simulate the industrial application, thus the publication number is also limited. In flow-loop experiments, there are two methods in the drag reduction experiment: homogeneous and heterogeneous method (Bewersdorff et al., 1993; Frings, 1988; Zhang et al., 2019). The homogeneous method means that polymers are premixed with solvents and this polymer solution under a given concentration is transported into the pipeline by a pump, centrifugal pump (non-positive displacement pump) in most cases. The heterogeneous method means that polymers are not premixed in solvents; instead, solvents are transported by a centrifugal pump and polymer solutions are injected by a positive displacement pump, diaphragm pump in most cases. Unlike the centrifugal pump, diaphragm pump does not have a rotational blade that causes polymer degradation. Instead, in a diaphragm pump, by a reciprocating diaphragm pushing liquid, concentrated polymer solution in drag reduction study is injected into the pipeline, so this pump does not cause the degradation of polymers. The degradation of polymers is shown in the next section.

Table 2-1 Summary of drag reduction correlation based on the Reynolds number

Author	Year	Correlation	Reynolds number	Note
Dodge and Metzner	1959	$\frac{1}{\sqrt{f}} = \frac{4}{(n')^{0.75}} \log\left(Re_G f^{1-\frac{n'}{2}}\right) - \frac{1.2}{(n')^{1.2}}$	Generalized Reynolds number for power-law fluids: $Re_G = \frac{d^{n'} \rho U_b^{2-n'}}{K' 8^{n'-1} \left(\frac{3n'+1}{4n'}\right)^{n'-1}}$ Power-law fluids: $\tau_w = K' \left(\frac{8U_b}{d}\right)^{n'}$	Polymer: Polyacrylic acid Concentration: 2000-5000 ppm Reynolds number: 5000-36000
Savins	1964	$\frac{1}{\sqrt{f}} = A(n') \log\left(Re_G f^{1-\frac{n'}{2}}\right) - B(n')$		Polymer: Cellulose, vinyl polymer and gum Concentration: 180-2800 ppm Reynolds number: 2000-50000
Shah et al.	2002	$f_P = A + \frac{B}{Re_S^C}$	Reynolds number based-on solvent: $Re_S = \frac{d\rho U_b}{\mu_S}$	Polymer: PHPA and XCD Concentration: 1100-1200 ppm Reynolds number: 1000-7000 Three coefficients, *A*, *B* and *C* are not shown in the original paper.
Shah and Kamel	2010	$f_P = 6.19 \times 10^{-3} + 9.68 \times 10^{-22} Re^3 + 3.88 \frac{\ln(Re_S)}{Re_S}$		Polymer: ASP 700 and ASP 820 Concentration: 1100-1200 ppm Reynolds number: 22000-150000
Shah and Vyas	2011	$DR = A + \frac{B}{\ln Re_S} + \frac{C}{(\ln Re_S)^2} + \frac{D}{(\ln Re_S)^3}$		For coiled pipe: $A = -1740C_P - 216$ $B = 54743C_P + 7413$ $C = -558708C_P - 84342$ $D = 1830200C_P + 320414$ Polymer: ASP 700 and ASP 820 Concentration: 300-700 ppm

				Reynolds number: 12000-130000
				For straight pipe: $A = 1436C_P - 174$ $B = -52475C_P + 5968$ $C = 640160C_P - 67898$ $D = -2610021C_P + 257873$ Polymer: ASP 700 and ASP 820 Concentration: 300-700 ppm Reynolds number: 12000-130000

Note: PHPA, ASP-700 and ASP-800 for partially hydrolyzed polyacrylamide and XCD for polysaccharide gum

2.2 Degradation of Drag Reduction

When polymers experience turbulent flow for a long-time, the polymer chain scissions happen by shear and the molecular weight decreases. This causes the degradation of drag reduction by polymers in the drag-reducing flow. Polymers with a low molecular weight have a lower efficiency of drag reduction ability and the drag reduction ability decreases with time. There are two types of degradation studies, in rotational flow or pipe flow. In rotational flow, the polymer solution is added in a rotating disk apparatus or a similar device (Choi et al., 2000; Dai et al., 2018; Kim et al., 2000). It seems that this type of degradation is not related to the degradation in the pipe flow since the geometries of rotational flow and pipe flow are completely different. So, researchers also use pipe flow to test the degradation of drag reduction by polymers, which aims to simulate the degradation in real oil and gas pipelines (Motta et al., 2019; Soares et al., 2019). However, these studies did not achieve the goal. Because most experiments are conducted in a closed flow loop, meaning that the polymers experience the degradation caused by the centrifugal pump as mentioned before. The degradation happens at two sections, in the pump and pipe. Thus, these two degradations cannot be differentiated. Overall, it is argued these two methods are essentially the same, indicating that the degradation test in the flow loop cannot simulate the degradation in long-distance pipe flow in the industry. If anyone wants to do the degradation test and hopes to use these data for industrial usages, the researcher must have a long-enough open flow loop (long-distance non-closed flow line to avoid repetitive degradation by centrifugal pumps). One work (Jouenne et al., 2015) almost fits these requirements. However, the pipeline is not straight, and several corners are involved, thus it is not helpful to predict the drag reduction in straight pipelines.

Table 2-2 Summary of drag reduction correlation based on the Deborah number or Weissenberg number

Author	Year	Correlation	Weissenberg or Deborah number	Note
Darby and Chang	1984	$f_P = \frac{f_S}{\sqrt{1+De^2}}$	$De = \frac{0.0166(8u\lambda/d)Re_S^{0.375}(\mu_S/\mu_0)^{0.5}}{[1+(8u\lambda/d)^2]^{0.25}}$	Polymer: AP-30 Concentration: 100-500 ppm Reynolds number: 4000-100000 Method for obtaining relaxation time and μ_0: Jeffrey model
Darby, and Pivsa-Art	1991		$De = \frac{0.0163(8u\lambda/d)Re_S^{0.338}(\mu_S/\mu_0)^{0.5}}{[1/Re_S^{0.75}+0.00476(8u\lambda/d)^2(\mu_S/\mu_0)^{0.75}]^{0.318}}$	Polymer: PEO, PAM E198, Rhodopol 23 (Xantham Gum) Concentration: 100-500 ppm Reynolds number: 10000-100000 Method for obtaining relaxation time and μ_0: Jeffrey model
Gallego, and Shah	2009		$De = \frac{1.186(f_S Re_S)^{0.322}(8u\lambda/d)}{[1+(8u\lambda/d)^2]^{0.703}}\left(\frac{\rho_P\mu_S}{\rho_S\mu_0}\right)^{0.192}$	For straight tubing Polymer: ASP-700 and ASP-820 Concentration: 300-1000 ppm Reynolds number: 12000-100000 Method for obtaining relaxation time and μ_0: Jeffrey model

			$De = \frac{1.67 \times 10^{-3}(f_P Re_S)^{1.408}(8u\lambda/d)}{[1 + 1.097(8f_P Re_S u\lambda/d)^2]^{1.423}}\left(\frac{\rho_P \mu_S}{\rho_S \mu_0}\right)^{0.113}$	For coiled tubing Polymer: ASP-700 and ASP-820 Concentration: 300-1000 ppm Reynolds number: 12000-100000 Method for obtaining relaxation time and μ_0: Jeffrey model
Owolabi et al.	2017	$DR\% = 128\left(\frac{1}{1 + e^{0.5 - Wi}} - 0.5\right)$	$Wi = \frac{8u}{d}$	Polymer: PAA Concentration: 150-200 ppm Reynolds number: 6000-10000 Method for obtaining relaxation time: CaBER

Note: AP-30 for partially hydrolyzed polyacrylamide; PAM E198 for Polyacrylamide; PAA for Polycarylamide; Rhodopol 23 for Xantham Gum; PAA for Polyacrylic acid; PEO for Polyethylene oxide.

There are two types of widely accepted correlations for the degradation of drag reduction by polymers.

$$DR(t) = DR(0)e^{-kt} \tag{2-14}$$

$$\frac{DR(t)}{DR(0)} = \frac{1}{1 + W(1 - e^{-ht})} \tag{2-15}$$

Eq. 2-15 is developed from an assumption, Eq. 2-16.

$$\frac{DR(t)}{DR(0)} = \frac{M(t)}{M(0)} \tag{2-16}$$

In these equations, $DR(0)$ is the drag reduction value at the initial state, and $DR(t)$ is the degradation value at any time during the degradation process; $M(0)$ is the average molecular weight at the initial state, and $M(t)$ is the average molecular weight at any time during the degradation process. W, h and k are constants. Both correlations can be used for prediction of degradation of drag reduction by polymers in many works in both rotational flow and pipe flow (Brostow et al., 2007; Choi et al., 2000; Hong et al., 2008; Le Brun et al., 2016). However, a problem in these two equations is that the physical meaning of parameters is not clear. In this thesis, Eq. 2-14 to Eq. 2-16 will be combined to develop a correlation to predict the drag reduction degradation. The degradation of drag reduction is regarded as a first-order chemical reaction since the polymer chain scission is involved in the degradation process (the original long chain polymers disappear and new shot chain polymers form). Further analysis with experimental data will show that Eq. 2-16 is not correct, because this assumption only considers the single-distribution polymer (DNA as an example) and neglects the possible aggregate of polymer in the turbulent drag-reducing flow.

2.3 Mechanism of Drag Reduction by Polymers

2.3.1 Introduction

Drag reduction by linear polymers and its degradation in turbulent flows have been investigated for many years, but the exact mechanism of these processes is still not clear. Some existing theories are summarized as follows. Lumley (1973) proposed a mechanism from a viscosity view: polymers enter the boundary layer of turbulent flow and increase the viscosity in this region, which damps the small eddies so that less turbulent energy is dissipated, and pressure drop decreases. De Gennes (1986) suggested a mechanism from the elastic view: polymers in turbulent flow experience extension; elasticity in this extension transition damps eddies in the turbulent flow, so the pressure drop decreases. Brostow et al. (1999) provided a mechanism from flow domain theory: polymers form flow domains surrounding the solvents and suppressing eddies formation; eddies disappear and drag reduction happens. Camail et al. (2009) offered a mechanism from polymer stretching: drag reduction happens at two consecutive stretching steps, from aggregates to isolated coils and from isolated coils to stretched coils. A common problem with these proposed mechanisms is that aggregates of polymers are neglected. Besides, the critical energy introduced by Camail et al. (2009) was not very clear.

2.3.2 Unresolved Problems in the Proposed Drag Reduction Mechanism

There are several proposed mechanisms of drag reduction by polymers. However, most of these are not validated with experimental data. Currently, the most promising mechanism is the elasticity theory by De Gennes. He thinks that the polymer phase change process (from the coiled state to the stretched state) could absorb the turbulent energy sot that more energy could be used in the main direction of pipe flow and the conformation of polymers remains in the stretched state (De Gennes, 1986; Tabor & De Gennes, 1986). But he did not observe this stretch

process then, because the first direct observation of polymer in a flow was done in 1992 (Smith et al., 1992). Does the observation validate this theory? No. Several independent works reported that the conformation of polymers (real-time length of polymers) observed by fluorescent microscope was time-dependent, not a constant after stretching (Bakajin et al., 1998; Lueth & Shaqfeh, 2009; Sachdev et al., 2016; Teixeira et al., 2005).

The other factor that makes the drag reduction hard to understand is the "molecular individualism", first introduced by De Gennes (1997). He claimed that the behaviour of a single Macromolecule (DNA as an example) in flow was hard to predict – the macromolecule could stretch, relax and even tumble, the last behavior indicating that polymers may have a rigid feature even thought it is flexible. Current models cannot handle all these features. Thus, researchers cannot have a good understanding of this phenomenon.

The huge difference between the simulation and experimental conditions also causes a difficulty in understanding the mechanism. Experimental data were used to validate the FENE-P model and a semi-empirical correlation to predict the drag reduction was proposed, but there is still a concern about the gap between experiment and simulation: the Weissenberg number, *Wi*, in these two types of study is very different. In most numerical studies, the order of magnitude of the Weissenberg number is $O(10^2)$, and *Wi* between 10 and 100 (Kim et al., 2007; Li & Graham, 2007; Tesauro et al., 2007; Thais et al., 2010; Zhu et a., 2018); while in experimental studies, the order of magnitude will be $O(10^1)$, usually less than 10 (Owolabi et al., 2017). This huge gap causes the concern that maybe a new model should be developed, instead of the FENE-F model, for the numerical simulation study.

The existence of aggregate in the dilute polymer solution is still in debate (Devanand & Selser, 1990). If aggregates are also involved, the drag reduction by polymers will be more

complicated: the relaxation time of free polymers and aggregates are different. So, one should not use just one parameter to consider the effects of a polymer with a given molecular weight and molecular weight distribution.

The molecular weight distribution of drag-reducing polymers should be taken into considerations (Hunston, 1974; Little & Ting, 1976). In most cases, drag-reducing polymers are synthetic, so polymers have a wide distribution of molecule weight. Either the number-averaged, weight-averaged or viscosity-averaged molecular weight is used to describe the overall property of these drag-reducing polymers. But can these average molecular weights represent the true property of the polymer in drag reduction analysis? No. A profile of molecular weight exists, and the same molecular weight could represent totally different polymers. Let's take the weight-averaged molecular weight (most used in the literature) as an example. Imagine that there are two polymers with the same type and weight-averaged molecular weight, while their molecular weight distribution is different, one being narrow and the other broad. These two polymers have different drag reduction abilities under the same flow condition. It is well known that there is a critical molecular weight, and polymers that have a molecular weight less than the critical one have no drag reduction ability in a certain condition. The polymer with a narrow molecular weight distribution has more "useful" polymers while the polymer with a board profile has less. More useful polymers can contribute more to the relaxation time, and with a better drag reduction ability. Thus, it is not appropriate to use one single molecular weight to represent the overall property of the drag-reducing polymer.

The method of preparing a polymer solution is another factor that may cause different results in the drag reduction study. Any difference in the preparation method may cause the difference of the polymer solution, i.e. mechanical or magnetic mixing, low or high temperature,

low or high rotation speed (shear rate which may cause the degradation discussed above), long or short mixing time, type of mixing blade, etc. All these differences could affect the polymer solution. Rowin et al. (2018) provided several clues about the optimal preparation methods, but few studies about this specific question in the drag reduction are available.

2.4 Summary

This chapter presents a literature review on flow drag reduction and degradation. Some general conclusions, models, and correlations, and the scale-up criteria are summarized. Several proposed drag reduction and degradation mechanisms are discussed, along with the reasons why there is no universally accepted mechanism in the literature. In the next chapter, a semi-analytical solution of the drag reduction using the FENE-P model for drag-reducing flow will be provided to show the upper limit of drag reduction with polymer additives.

Chapter 3 A Semi-Analytical Model for the Upper Limit of Drag Reduction with Polymer Additives

In Chapter 3, a semi-analytical solution for drag reduction prediction is proposed based on the FENE-P model. This solution is tuned by previous experimental results and able to predict the upper limit of drag reduction with polymer additives. The main content of this chapter has been published as a journal paper (Zhang, X., Duan, X., & Muzychka, Y. (2018). "Analytical upper limit of drag reduction with polymer additives in turbulent pipe flow". Journal of Fluids Engineering, 140(5), 051204). The author of this thesis is the first author of this paper. The first author developed the model, analyzed the data, prepared the manuscript, and made the revisions. Prof. Duan and Prof. Muzychka as the second and third authors provided their suggestions on the model development and helped in the revision of the manuscript.

3.1 Model Formulation

In this study, the classic FENE-P model is used to obtain a stress tensor $\vec{T}$, shown in Eq. 3-1, induced by polymer drag reduction agents (DRAs). This is the basis for drag reduction analysis of polymeric flows and this stress tensor is the key property of the polymer related to drag reduction. Zhang et al. (2013) summarized all equations of the FENE-P model so only a brief review will be provided here. Also note that all the equations in this model are dimensionless.

$$\vec{T} = \frac{1}{Wi}\left[\frac{\vec{c}}{1 - \frac{trace(\vec{c})}{L^2}} - \vec{I}\right] \tag{3-1}$$

In Eq. 3-1, $\vec{c}$ is the conformation tensor of the polymers, defined as $\vec{c} = \langle \vec{Q}\vec{Q} \rangle$, where $\vec{Q}$ is the end-to-end vector of the polymer and the bracket indicates the average in the flow field. *L* is

the dimensionless maximum length of the polymer in the solution, estimated in the simulation process; $\vec{I}$ is a unit tensor; Wi is the Weissenberg number, defined as:

$$Wi = \lambda \dot{r} \tag{3-2}$$

where λ is the relaxation time of the drag-reducing agent and $\dot{r}$ is the shear rate in the turbulent flow.

The governing equation for drag reduction is a modified Naiver-Stokes equation as follows:

$$\frac{\partial \vec{u}}{\partial t} + \vec{u} \cdot \nabla \vec{u} = -\nabla \vec{p} + \frac{\beta}{Re_b} \nabla^2 \vec{u} + \frac{1-\beta}{Re_b} \nabla \cdot \vec{T} \tag{3-3}$$

where $\vec{u}$ is the dimensionless velocity vector of the turbulent flow with the bulk velocity U_b as a reference; $\nabla \vec{p}$ is the dimensionless pressure gradient with a reference pressure, ρU_b^2; length is nondimensionalized by the diameter of the pipeline, *d*; time is nondimensionalized by a characteristic time, d/U_b; β is the ratio of the viscosity of the solvent to the viscosity of liquid after the polymer is added at the zero shear rate, defined as follows:

$$\beta = \frac{\mu_S}{\mu_S + \mu_{P,0}} \tag{3-4}$$

where μ_S and $\mu_{P,0}$ represent the viscosity of solvent and polymers added in at zero shear rate. For tensor $\vec{c}$, the governing equation is as follows:

$$\frac{\partial \vec{c}}{\partial t} + (\vec{u} \cdot \nabla)\vec{c} = \vec{c} \cdot (\nabla \vec{u}) + (\nabla \vec{u})^T \cdot \vec{c} - \vec{T} \tag{3-5}$$

The governing equations are analyzed with the following assumptions and simplifications.

Assumption 1**:** Previous publications have proved that DRAs can reduce the fluctuation velocity or Reynolds stress (Amarouchene & Kellay, 2002; Iwamoto et al., 2005; Samanta et al.,

2009; Warholic et al., 2001). If all the fluctuation velocities disappear, and with a constant flow rate (basic condition for drag reduction studies), a steady flow is achieved, with $\partial\vec{u}/\partial t = 0$, and consequently $\partial\vec{c}/\partial t = 0$. If all turbulent structures disappear, turbulent flow becomes laminar flow, which is supported by Kostic (1994), who found that there was a laminarization trend of turbulent flow after DRA was added. Furthermore, this assumption has been partially proved by experiments. Many results (Bizhani et al., 2015; Li et al., 2005; Paschkewitz et al., 2005; Shao et al., 2002; Tamano & Itoh, 2011;) were published with PIV data to show that fluctuating velocity (Reynolds stress) decreases when DRAs are added. The extreme situation is that all the turbulent structures disappear, and the upper limit of drag reduction is achieved.

Assumption 2: u_y is negligible as u_x is more important in pipelines, which was also assumed by Barenblatt (2008). The turbulent flow in pipelines is assumed to be fully developed, therefore $\partial u_x/\partial x = 0$. Under this circumstance, the only direction in which polymers can stretch is the x direction. The component of $\vec{Q}$ in the x direction, $Q_x \neq 0$, and the component in the y direction, $Q_y \neq 0$. For simplification, Q is used to replace Q_x in the following text. Similarly, $c_y = 0$, $c_x = trace(\vec{c})$, and c is used to replace $trace(\vec{c})$. T is used to replace the component of $\vec{T}$ in the x direction.

These simplifications make the problem one-dimensional, and Eq. 1-1, Eq. 1-3, and Eq. 1-5 are reduced to the following,

$$\frac{dp}{dx} = \frac{\beta}{Re_b}\frac{d^2u_x}{dy^2} + \frac{1-\beta}{Re_b}\frac{dT}{dx} \tag{3-6}$$

$$u_x\frac{dc}{dx} = -T = -\frac{1}{Wi}\left(\frac{c}{1-\frac{c}{L^2}} - 1\right) \tag{3-7}$$

With complete laminarization of turbulent flow explained earlier, the velocity profile is assumed to be a second order polynomial (all the parameters used, i. e., velocity and distance, are still dimensionless) (here the Cartesian coordinates is used since all governing equations use the Cartesian coordinates):

$$u_x = a_0 y^2 + a_1 y + a_2 \tag{3-8}$$

In the pipeline, the following three boundary conditions can be used to obtain the coefficients in Eq. 3-8.

$$u_x(1) = u_x(0) = 0 \tag{3-9}$$

$$1 = \int_0^1 u_x \, dy \tag{3-10}$$

This leads to the following velocity profile:

$$u_x = -6y^2 + 6y \tag{3-11}$$

which is similar to the results by Japper-Jaafar et al. (2010)

According to Eq. 3-6, the pressure gradient without polymers can be represented in Eq. 3-12 as β =1 when no drag-reducing agents are added.

$$\left(\frac{dp}{dx}\right)_{without} = \frac{1}{Re_b}\frac{d^2u_x}{dy^2} \tag{3-12}$$

The definition of drag reduction (*DR*%) is given in Eq. 3-13.

$$DR\% = \frac{\left(\frac{dp}{dx}\right)_{without} - \left(\frac{dp}{dx}\right)_{with}}{\left(\frac{dp}{dx}\right)_{without}} \times 100\% \tag{3-13}$$

$(dp/dx)_{with}$ and $(dp/dx)_{without}$ represent pressure drop with and without polymers, respectively. After Eq. 3-6 and Eq. 3-12 are introduced, Eq. 3-13 can be transformed to:

$$DR\% = (1-\beta)\left(1-\frac{\frac{dT}{dx}}{\frac{d^2u_x}{dy^2}}\right) \tag{3-14}$$

The term dT/dx, according to chain rule of derivation, can be written as:

$$\frac{dT}{dx} = \frac{dT}{dc}\frac{dc}{dx} = \frac{1}{u_x Wi^2}\frac{1-c-\frac{c}{L^2}}{\left(1-\frac{c}{L^2}\right)^3} \tag{3-15}$$

One method of establishing an average drag reduction in the pipeline is to use the dimensionless bulk velocity (1) to replace u_x. Thus, the equation for average drag reduction (*DR*%) can be shown as:

$$R\% = (1-\beta)\left(1+\frac{1}{12Wi^2}\right)\frac{1-c-\frac{c}{L^2}}{\left(1-\frac{c}{L^2}\right)^3} \tag{3-16}$$

Eq. 3-16 gives the upper limit of drag reduction with polymer additives when complete laminarization happens in a turbulent pipe flow.

It is impossible to measure the conformation tensor and maximum length of the polymer in the flow. To validate this model and make it useful in practical engineering applications, a special case of $c = 0$ is considered to yield the following,

$$DR\% = (1-\beta)\left(1+\frac{1}{12Wi^2}\right) \tag{3-17}$$

This represents an extreme condition with lowest drag reduction ability of the polymers when the polymers are in a completely coiled state therefore the end-to-end vector is 0, which was proved by Procaccia et al. (2008). In any other conditions when the polymers are stretched, i.e., $c \neq 0$, the drag reduction will be higher than what is predicted by Eq. 3-17.

The remaining polymer properties in Eq. 3-17, β and *Wi*, can be easily measured in a pipe flow or in a rheometer. Then the model can be validated and further analyzed. One should

also note that the difference between Eq. 3-16 and Eq. 3-17. $(1 - c - c/L^2)/(1 - c/L^2)^3$, represents the effects of polymer length and conformation tensor, which are both related to viscosity and elasticity properties of the fluid. These viscoelastic effects can also be investigated alternatively with the remaining properties in Eq. 3-17. These aspects will be discussed in the following section.

3.2 Model Tuning and Discussions

Since we establish an upper limit model of drag reduction by polymers, experimental data from Japper-Jaafar et al. (2009) are used to tune the model developed in this work. Eq. 3-17 will be tuned against these data. Based on its definition, the Weissenberg number can be expressed by the polymer relaxation time and the shear rate:

$$Wi = \lambda \dot{r} = \lambda \frac{8U_b}{d} \tag{3-18}$$

where *d* is the diameter of the pipeline. Relaxation time can be obtained from the definition (Malkin & Isayev, 2017):

$$\lambda = \frac{\mu}{G} \tag{3-19}$$

G is the elasticity and μ is the viscosity measured from rheometers.

The viscosity at a certain shear rate can be calculated by the Carreau–Yasuda model as:

$$\frac{\mu - \mu_0}{\mu - \mu_\infty} = \frac{1}{[1 + (\lambda_{CY}\dot{r})^{a_{CY}}]^{\frac{n_{CY}}{a_{CY}}}} \tag{3-20}$$

where μ_0 and μ_∞ represent the viscosity at zero shear rate and infinite shear rate; λ_{CY}, n_{CY} and a_{CY} are three constants correlated from experimental data. Note that λ_{CY} is not relaxation time but a time parameter in the Carreau–Yasuda model. The other parameter, β, can also be calculated when shear rate (velocity) is known.

In the experimental data, drag reduction values were measured with concentration of 0.075% and less, while the modulus to calculate the Weissenberg number was measured with concentration of more than 0.075%. So, the modulus found for concentrations of less than 0.075% with high shear rate (100 s^{-1}) will be used in all calculations as it is impossible to estimate the modulus for concentrations of less than 0.075%. The loss and storage modulus, *G*' and *G*", under shear rate are 0.2 and 0.4 Pa by estimation from the original paper. Thus, the modulus based on definition in Eq. 3-21 is 0.45 Pa, which will be used in all the following calculation.

$$G = \sqrt{(G')^2 + (G'')^2} \tag{3-21}$$

Since the current model predicts upper limit of drag reduction (with complete laminarization), the predicted drag reduction (with polymeric fluid properties measured from rheometer), DR_{Cal}, should always be larger than the one reported for pipelines, DR_{Exp}. This can be clearly seen in Figure 3-1, providing the desired tuning.

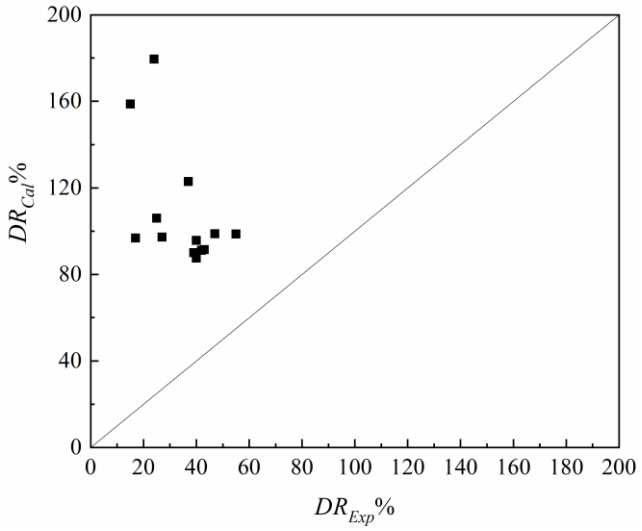

Figure 3-1 Comparison of experimental data with calculated drag reduction from the upper limit model (data from Japper-Jaafar et al. (2009))

In Figure 3-1, the straight line represents $DR_{Cal} = DR_{Exp}$. All data points are above the straight line, which shows that DR_{Cal} is indeed greater than DR_{Exp} over the entire range of data. One may notice that although most DR_{Cal} values in Figure 3-1 are in the range of 0 – 1, some are larger than 1. Real drag reduction (percentage) should always be less than 1. Those values larger than 1 are due to the experimental data issue explained earlier. The reference by Japper-Jaafar et al. (2009) did not provide modulus values for data conditions of concentrations less than 0.075%. For those conditions, estimation was made using the modulus for concentration of 0.075% (higher than their true values). The trend of data by Japper-Jaafar et al. (2009) suggests that higher concentration leads to higher modulus. So for those conditions, the modulus used in prediction was higher than the true values. This subsequently makes the calculated drag reduction larger. This is evident in Eq. 3-22, which is an expansion of Eq. 3-17.

$$DR\% = (1-\beta)\left(1+\frac{1}{12\left(\frac{\mu}{G}\dot{r}\right)^2}\right) = (1-\beta)\left(1+\frac{G^2}{12(\mu\dot{r})^2}\right) \tag{3-22}$$

If complete data were available, those points for lower concentrations would have lower modulus values, making the calculated drag reduction lower than 1. From this perspective, these results actually verify that the developed model works well in drag reduction prediction with fluid and polymer properties.

A new parameter for the ratio of DR_{Cal} and DR_{Exp} can be introduced,

$$\alpha = \frac{DR_{Exp}}{DR_{Cal}} \tag{3-23}$$

Since DR_{Cal} is larger than DR_{Exp} in all experimental conditions, α is less than 1. The relationship between α and DR_{Exp} is shown in Figure 3-2.

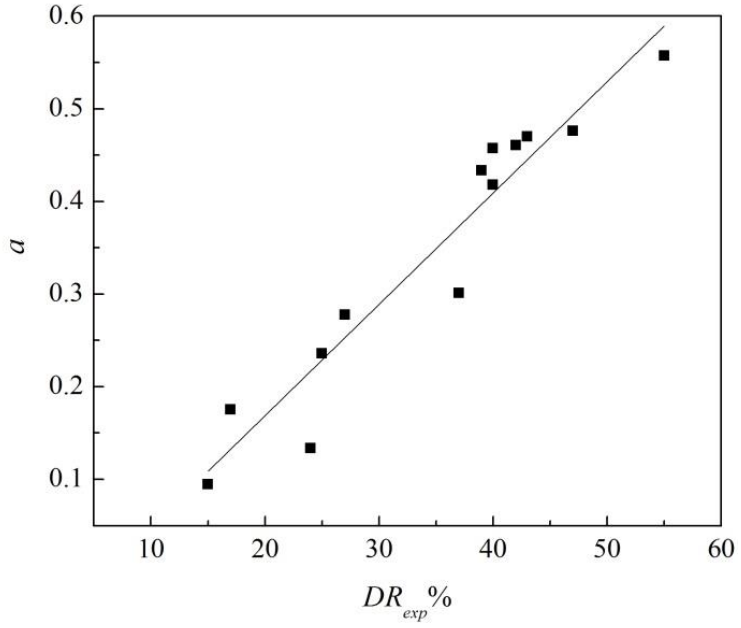

Figure 3-2 The linear relationship between α and DR_{Exp}

Figure 3-2 shows an interesting linear relationship between the drag reduction ratio α and DR_{Exp},

$$\alpha = 0.0120DR_{Exp} - 0.0712 \tag{3-24}$$

Combining Eq. 3-23 and Eq. 3-24 then rearrangement leads to an explicit relationship between the calculated upper limit of drag reduction and estimated drag reduction in pipe flow, as shown in Eq. 3-25.

$$DR_{Exp} = \frac{0.0712DR_{Cal}}{0.012DR_{Cal} - 1} \tag{3-25}$$

It is often costly and time-consuming to build a flow loop to test the drag reduction in pipelines, and even harder to monitor drag reduction performance in real pipelines. In this case, Eq. 3-25 provides a convenient way to estimate drag reduction in pipeline (DR_{Exp}) from the upper limit of drag reduction (DR_{Cal}) calculated using the analytical model and fluid properties,

i.e., modulus and viscosity, measured in rheometer. These relationships are depicted in Figure 3-3.

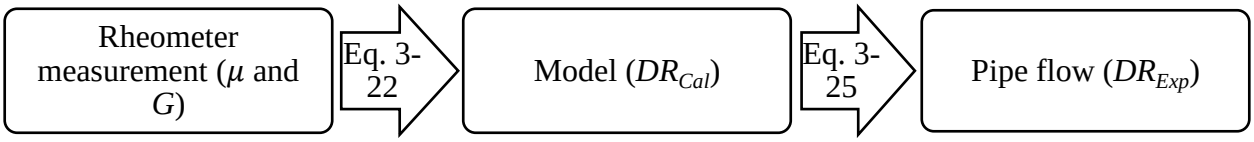

Figure 3-3 Relationships between measured fluid properties in rheometer, calculated upper limit of drag reduction (DR_{Cal}), and estimated drag reduction in pipe flow (DR_{Exp})

It should be noted that this correlation may be dependent on the types of chemical additives, but a similar method can be used for other DRAs, which may result in a different coefficient for the linear relationship in Eq. 3-24. This study will not attempt to develop a universal correlation. However, if more studies combining rheometer and flow loop measurements can be completed, the coefficients in Eq. 3-24 can be refined, making this correlation applicable to a wider range of conditions of drag reduction in pipelines.

In this method, a relaxation time of polymer is needed to predict the drag reduction. However, when the polymer concentration is extremely low, it may be impossible to measure the relaxation time (Lim et al., 2003). In this case, one method to predict the Deborah number, a dimensionless number regarding relaxation time, can be used (Hong et al., 2015).

Further examination of the model in Eq. 3-17 leads to useful insights to understand the drag reduction mechanism, particularly the effects of elasticity and viscosity. Expanding Eq. 3-17 also gives the following:

$$DR\% = \frac{1}{1+\frac{\mu_{P,0}}{\mu_S}}\left(1+\frac{G^2d^2}{768U_b^2\mu^2}\right) \tag{3-26}$$

Many factors are involved in Eq. 3-26, i.e., viscosity, modulus, velocity, and concentration and they are all interrelated. It is unreasonable to evaluate the elasticity and viscosity effects separately as both can contribute to drag reduction. Here a new explanation of viscoelasticity effects in drag reduction is shown.

Assume that a polymer solution with a constant concentration can reduce the friction in pipelines and the concentration varies in different conditions. At an initial state, the velocity of flow is low then gradually increases. The total value $G^2/U_b^2\mu^2$ starts to increase, since the growth momentum of G^2 is greater than that of $U_b^2\mu^2$. Thus, drag reduction increases until the maximum drag reduction is achieved. In this period, elasticity plays a positive role since it offsets the growth momentum of $U_b^2\mu^2$, which results in a drag reduction increase. But this trend will stop when G^2 starts to grow slower than $U_b^2\mu^2$. Now, $G^2/U_b^2\mu^2$ starts to decrease, which leads to a decrease in drag reduction. In this period, modulus plays a negative role in drag reduction. Even though elasticity still increases, it cannot offset the growth of viscosity. Overall, this phenomenon can be summarized as follows. At a critical concentration, drag reduction will reach its maximum value when velocity increases to a certain point, after which, drag reduction starts to decrease. This theory can be supported by many previous results (Gasljevic et al., 1999; Zhang et al., 2005; Kamel & Shah, 2009; Dosunmu & Shah, 2014) shown in Figure 3-4.

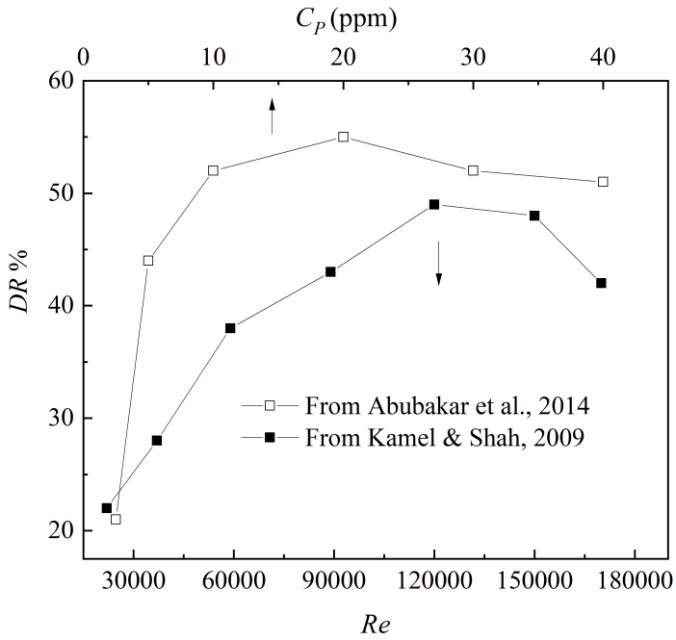

Figure 3-4 Drag reduction performance of two DRAs ability at the same velocity originally from Abubakar et al. (2014) and at the same concentration from Kamel & Shah (2009)

It is also important to consider the other situation: drag reduction with a constant velocity and varying concentrations. With increasing concentration, $\mu_{P,0}$ increases and the term $1 - \mu_S/(\mu_S + \mu_{P,0})$ increases. And increasing concentration will also increase the modulus, which can increase the drag reduction. When the concentration reaches a certain point, the drag reduction also reaches its maximum, after which, drag reduction starts to decrease even though elasticity still increases with increasing velocity. The increasing momentum of modulus cannot offset the momentum of the viscosity, so drag reduction starts to decrease. This phenomenon has also been observed by previous studies (Abubakar et al., 2014; Guersoni et al., 2015) as shown in Figure 3-4.

3.3 Summary

In Chapter 3, a new model for drag reduction by polymer is proposed and tuned with previous experimental data. This model assumes complete laminarization in the flow and predicts the upper limitation of drag reduction in pipe flows. Comparison of predicted and measured data also leads to a correlation between drag reduction in pipe flow and predicted upper limit of drag reduction using fluid properties measured in a rheometer. The correlation provides a convenient and useful way for estimation of pipeline drag reduction with low cost. This model is also used to explain the mechanism of drag reduction by DRAs. Both viscosity and elasticity of the polymeric fluid affect the drag reduction. With a constant concentration, drag reduction increases with increasing velocity as the growth of modulus is limited. After maximum drag reduction occurs, drag reduction starts to decrease as the growth of velocity and viscosity is larger than that of the modulus. With a constant velocity, increasing concentration increases the drag reduction due to positive effects from the modulus. Once a maximum drag reduction occurs, drag reduction decreases because the growth of modulus is greater than that of the viscosity.

Chapter 4 Experimental Correlation for Pipe Flow Drag Reduction Using Relaxation Time

A semi-analytical model was presented in the earlier chapter for the drag reduction prediction by polymers. However, it is difficult to measure the relaxation time of the polymer in the dilute solution. In this chapter, the concept of relaxation time of the polymers is further examined and an experimental study on drag reduction in a pipe flow is conducted to develop a correlation for drag reduction by polymers. The main content of this chapter has been published (Zhang, X., Duan, X., Muzychka, Y., & Wang, Z. (2020). "Experimental correlation for pipe flow drag reduction using relaxation time of linear flexible polymers in a dilute solution". The Canadian Journal of Chemical Engineering, 98(3), 792-803.). The author of this thesis is the first author of this paper. The first author conducted the experiments, analyzed the data, developed the correlation and prepared the manuscript. Prof. Duan and Prof. Muzychka as the second and third authors provided their suggestions on the correlation development and revisions of this paper. Prof. Wang as the fourth author helped me in the construction of the flow loop.

4.1 Theories and Correlation Formulation

4.1.1 Clarification of the Relaxation Time, Deborah Number, and Weissenberg Number

As discussed earlier, the relaxation time of a DRA is a key property in determining its drag reduction efficiency. It refers to the transition time of a DRA from the stretched state to the coiled state. Figure 4-1 illustrates the coiled state and stretched state of a long chain linear flexible polymer in a dilute solution. In the coiled state, its radius of gyration, R_G, refers to the radius of an imaginary sphere enclosing the coiled polymer. This definition of relaxation was not followed by previous works (Ghajar & Azar, 1988; Kwack & Hartnett, 1983).

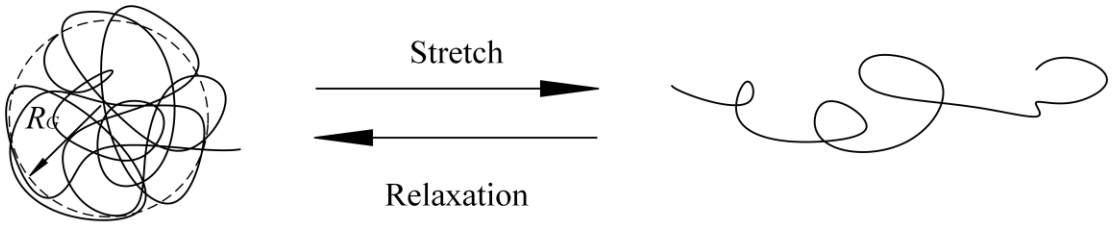

Figure 4-1 Polymer behaviors in a dilute solution

The relaxation time could be measured by rheometers, defined as the ratio of viscosity over the modulus. In previous studies, the relaxation time of surfactants was measured by this method. However, this method cannot be used in dilute polymer solutions because the rheometer cannot measure the modulus of the dilute polymer solution (Campo-Deano & Clasen, 2010). One previous study showed that the relaxation time could be measured by a filament method using a commercial capillary breakup extensional rheometer (CaBER) (Owolabi et al., 2017). However, the method is still limited to relatively high concentrations, at least semi-dilute solutions (several hundred ppm), and cannot be used for dilute solutions (<100 ppm).

Therefore, another method to investigate the relaxation time of polymers is needed in dilute solutions. In this study, the theory of Zimm, a theory to determine the relaxation process of linear flexible polymers, is used for this estimation and shown in Eq. 4-1 and Eq. 4-2 (Zimm, 1956). This theory appeared in many classic reviews on drag reduction (Sreenivasan, K. R., & White, 2008; Sreenivasan & White, 2000):

$$R_G = aN^{0.6} \tag{4-1}$$

$$\lambda = \frac{\mu_S R_G^3}{k_B T} \tag{4-2}$$

where R_G is the radius of gyration of the polymers in a dilute solution (m); k_B is the Boltzmann constant, 1.38×10^{-23} J · K $^{-1}$; T is the temperature (K); a is the length of monomer of polymer

(m); and N is the degree of polymerization. The radius of gyration is defined as the average distance from the centre of the polymer to the edge of an imaginary sphere covering the outer edge of the coiled polymer, as shown on the left side of Figure 4-1.

In this chapter, the concentration effect on the relaxation time of the dilute polymer solution is not considered as it was in a previous work (Muthukumar, 1984). This concentration dependency is due to the viscosity variation of the polymer solution. It was reported by Ebagninin et al. (2009) that for a 4×10^6 g/mol PEO solution at a concentration of 2500 ppm, the viscosity remains almost the same as water. In the current work, the concentration of polymer is so low (from 5 ppm to 20 ppm) that the viscosity of the dilute polymer solution is assumed the same as the solvent, water.

The original definition of Deborah number by Reiner (1964) was based on the ratio of relaxation time over observation time, shown in Equation (3) (Dealy, 2010; Poole, 2012):

$$De = \frac{\lambda}{t_P} = \frac{\lambda}{\frac{l}{U_b}} \tag{4-3}$$

where λ is the relaxation time (s); and t_P is the observation time (s), calculated from the length of the pipe, l (m), and the average velocity, U_b (m/s). The current study considers this as the only correct definition of this dimensionless number. Compared with the other complex definitions of Deborah number in the literature, the definition in Eq. 4-3 has a clear physical meaning and is easy to use.

An alternative dimensionless number involving the relaxation time is the Weissenberg number, defined in Eq. 4-4 (Dealy, 2010; Poole, 2012):

$$Wi = \lambda\dot{r} = \lambda\frac{8U_b}{d} \tag{4-4}$$

where $\dot{r}$ is the shear rate at the wall of the pipe in turbulent flow (s^{-1}) as suggested by Metzner and Park (1964). The shear rate in the near wall region is used because the vortex structure in this region is modified by the polymers added in the turbulent flow (White et al., 2004). In Eq. 4-4, U_b is the average velocity (m/s) and d is the diameter of the pipeline (m). As discussed earlier, the viscosity of a dilute polymer solution remains the same as the solvent (water). This solution shows Newtonian fluid characteristics, which explains the shear rate expression in Eq. 4-4. The Weissenberg number describes the ratio of elastic force over viscous force in the flow.

These definitions of the Deborah number and the Weissenberg number, and the difference between the two, have been discussed by Dealy (2010) and Poole (2012). Many previous studies did not follow these definitions, and the Deborah and Weissenberg numbers are often misused. In a pipe flow, the Deborah number (*De*) and Weissenberg number (*Wi*) are related to the length and the diameter of the pipe, respectively. In this study, the Weissenberg number is used since shear rate, related to the pipe diameter, is important in the drag reduction.

4.1.2 Correlation Formulation

When a polymer is used as a DRA in a turbulent pipe flow, the drag reduction efficiency, *DR%*, can be defined as the relative decrease of pressure drop:

$$DR\% = \frac{\Delta P_S - \Delta P_P}{\Delta P_S} \times 100\% \tag{4-5}$$

where ΔP_S (Pa) is the pressure drop without the polymer DRA; and ΔP_P (Pa) is the pressure drop with the DRA. In this definition, *DR%* is a dimensionless number. As discussed earlier, it is determined by several parameters. With a constant temperature, the drag reduction efficiency is a function of the pipe diameter (d), bulk velocity (U_b), viscosity of the solvent (μ_S), and the characteristic length of the turbulent flow with polymers. This length is a function of the polymer type, molecular weight, and concentration (Gasljevic et al., 1999). In this study, only water is

used as the solvent and its density is ~1000 kg/m^3; therefore, the density is not added as a variable. In this experiment, only one type of polymer (PEO) is used, and therefore the degree of polymerization (N) is used to replace the average molecular weight, M. The polymer concentration (C_P) is essentially a dimensionless number (weight-based, ppm). With these considerations, the drag reduction can be expressed in Eq. 4-6:

$$DR\% = f(d, U_b, \mu_S, C_P, N) \tag{4-6}$$

Eq. 4-6 has six factors and three dimensions (length, time, and mass). To make Eq. 4-6 dimensionless, three dimensionless groups using these variables should be prepared. Two dimensionless numbers already exist, $DR\%$ and C_P. The remaining question is how to combine the other four variables, d, U_b, N, and μ_S to make one dimensionless number, the details of which can be found in Appendix I. Examining the definition of the Weissenberg number in Eq. 4-4, and the relaxation time estimation from Eq. 4-1 and Eq. 4-2, one can find that the diameter d, velocity U_b, dynamic viscosity μ_S, and polymerization degree N can all be incorporated in the Weissenberg number. Thus, Eq. 4-6 becomes the following:

$$DR\% = f(Wi, C_P) \tag{4-7}$$

Many formats exist for the drag reduction correlation (Koskinen et al., 2004; Shah & Vyas, 2011; White, 1970), with different degrees of acceptance in the literature. In this work, the findings in previous studies are followed to develop the format of Eq. 4-8 for the prediction of drag reduction from a viscoelastic perspective. In Eq. 4-8, the viscoelastic prosperity is separated into two parts, viscous part and elastic part. The elastic part is the square of the Weissenberg number, Wi^2, suggested in our previous work (see appendix II for further explanations about why Wi^2 is used instead of Wi) (Zhang et al., 2018); the viscous part is the polymer concentration, C_P, based on work by Kim et al. (1997) and Yang et al. (1994). With substantial experimental data,

these researchers showed that in a dilute polymer solution the drag reduction was approximately proportional to the polymer concentration, i.e., $\partial DR/\partial C_P \approx const$. The other experimental conditions incorporate molecular weight, velocity, and geometry in the drag reduction flow, which are combined as the Weissenberg number mentioned above. Without polymer, $C_P = Wi = 0$, there will be no drag reduction, i.e., $DR\% = 0$. The two constants, A and B, in Eq. 4-8 are to be determined from experimental data:

$$DR\% = AC_P + BWi^2 \tag{4-8}$$

4.1.3 Concentration Range for Correlation

This correlation, Eq. 4-8, works for drag reduction in dilute polymer solutions as mentioned. Under this condition, there is no interaction between two polymer chains, as illustrated in Figure 4-2a, and the only interaction is the one between the solvent and the polymer. Here it is helpful to understand the concept of overlap concentration for polymer solutions. Figure 4-2 illustrates relationships between polymer chains (in coiled state and shown as imaginary spheres) in solutions of three different concentrations. In the dilute solution, the concentration C_P is low and there is no overlap or interaction between the polymers, shown in Figure 4-2a. At a critical concentration, C^*, the imaginary spheres of polymers are tangent to each other, as shown in Figure 4-2b; there will be interactions between them once the concentration increases slightly. This critical concentration is called the overlap concentration (Cotton et al., 1976; Graessley, 1980; Ying & Chu, 1987). If the concentration continues to increase, there will be significant interactions between the polymer chains and the solution is called a semi-dilute polymer solution, shown in Figure 4-2c.

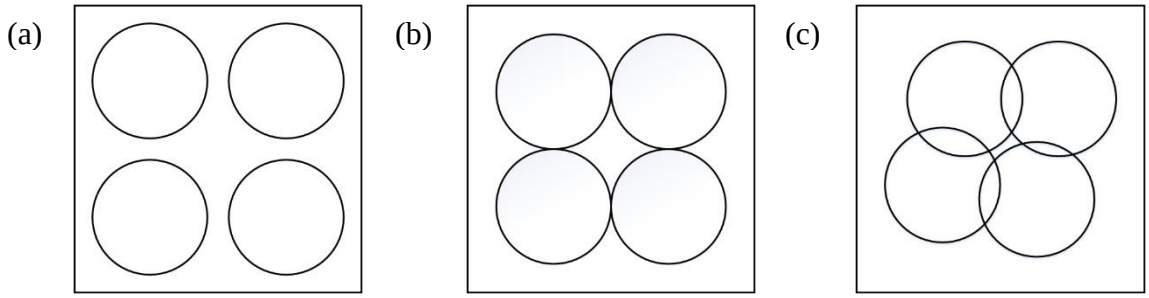

Figure 4-2 (a) Dilute polymer solution when c is less than C^*, (b) Critical state when c is equal to C^*, (c) Semi-dilute solution when c is greater than C^*

This overlap concentration concept has been discussed in many publications (Graessley, 1980; Ying & Chu, 1987), and many equations have been proposed to calculate the overlap concentration. In this study, one classic equation by Broseta et al. (1986) and Cotton et al. (1980) is used, as shown in Eq. 4-9:

$$C^* = \frac{M}{\frac{4}{3}\pi N_A R_G^3} \tag{4-9}$$

where M is the average molecular weight, g·mol^{-1}; and N_A is the Avogadro constant, 6.02×10^{23} mol^{-1}. Note that there are other methods to calculate the overlap concentration, such as those based on the sudden change of viscosity versus the polymer concentration (Ebagninin et al., 2009). The definition in Eq. 4-9 is better since it has clear physical meaning and is widely accepted.

In this study, PEO (from Sigma-Aldrich Canada) as the drag-reducing polymer is used, with three viscosity-average molecular weights, 10^6, 2×10^6, and 4×10^6 g/mol. The viscosity-average molecular weight to calculate the degree of polymerization (N) is used because it is the only available molecular weight from the supplier of these polymers. The monomer length to calculate the radius of gyration of relaxation time of PEO is 0.278 nm (Oesterhelt et al., 1999).

The overlap concentration is shown in Table 1. The profile of the molecular weights is not considered since this study intends to use the average molecular weight to predict the drag reduction via relaxation time.

Table 4-1 Overlap concentration (C^*) at different molecular weights

M (10^6 g/mol)	N	R_G ($\times 10^7$ m)	C^* (g/m^3 $\approx$ ppm)
1	22727	1.14	266
2	45455	1.73	153
4	90909	2.63	88

The Flory interaction (or solubility) parameter is also an important parameter of polymers in drag reduction, as suggested by Choi et al. (1999) and Lim et al. (2007). However, the current correlation of Eq. 4-6 does not include this parameter. It is not a variable in our study since only one type of drag reducing polymer (PEO) is used and it has a fixed solubility parameter. This variable will be considered in future research that involves other polymer types. Since the PEO concentration is low, it is assumed that the density of the dilute solution remains the same as the water density, ~10^3 kg/m^3 in experimental conditions. Thus, g/m^3 is treated as g/10^6 g, the latter being equal to ppm (here ppm is dimensionless). Thus, the concentration in this study should be less than 88 ppm. Even lower concentrations are used in the experiments to ensure dilute solutions.

4.2 Experimental Setup and Procedure

The schematic of the flow loop for the drag reduction investigation is illustrated in Figure 4-3. Water is transported to the pipeline via a self-prime pump (6050 Series Bronze AC Motor

Pump Unit, Xylem USA) from a 0.22 m^3 tank. To regulate the flow rate in the experiment, two globe valves are installed in the main pipeline with bypass. A high-accuracy flowmeter (FTB691A-NPT from Omega, USA) measures the flow rate in the experiment. The uncertainty of flow rate measurement is as follows: 3% of reading for flow rate from 3.8 L/min-38 L/min (litre per minute), and 5% when the flow rate is less than 3.8 L/min. The nominal pipe diameter from the outlet of the pump to the polymer injection point is 0.0254 m.

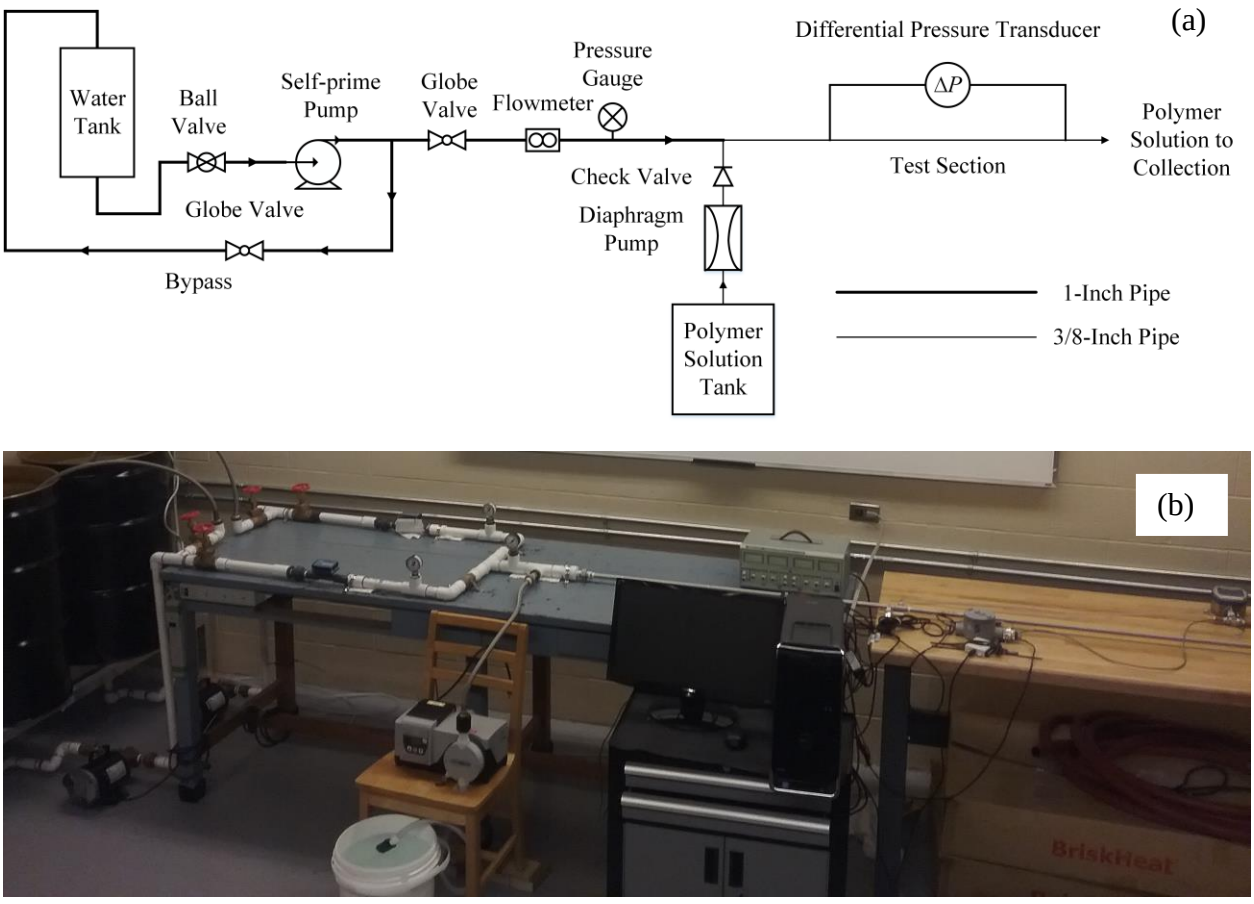

Figure 4-3 Schematic diagram (a) and photo (b) of the flow loop

The concentrated PEO solution in the polymer solution tank is prepared in a mild condition. Tap water and PEO are mixed with a magnetic stirring device in a low rotational

speed for 24 hours until no cluster or aggregate can be observed. This concentrated PEO solution is settled for another 24 hours to be homogenized and it will be used up in one day. The concentrated polymer solution is injected into the pipe flow by a diaphragm metering pump (PHP-804M, Omega, USA). Previous studies showed that this heterogeneous injection method with a diaphragm pump prevented mechanical degradation of the DRAs and led to optimal drag reduction performance (Hoyer & Gyr, 1998; Hoyt & Sellin, 1988; Vleggaar & Tels, 1973; Wells Jr & Spangler, 1967). Also, the master solutions are injected at the wall (rather than centre) of the pipe as suggested by previous studies for better drag reduction efficiency (Hoyt & Sellin, 1988; Kim & Sirviente, 2007). The concentration of all PEO concentrated solutions (with PEOs of three molecular weights) is 750 ppm, and the concentration in the pipeline is 5, 10, 15, and 20 ppm with four different flow rates.

After the injection point, a stainless-steel pipe with an inner diameter of 1.27 cm is used as the test section. To eliminate the entrance effect in drag-reducing pipe flow, the entrance length before the test section is 1.3 m (~102d), as suggested by previous studies (Omrani et al., 2012; Seyer & Catania 1972; Tuan & Mizunuma, 2013). The pressure drop in the test section (2.02 m long, ~159d) is measured by a differential pressure transducer (DPGM409-350HDWU, Omega, USA). The measurement uncertainty for the pressure drop is 28 Pa. The polymer solutions are collected at the outlet of the test section for treatment and disposal to avoid environmental problems. Temperature is measured in all experiments for the calculation of the Weissenberg number.

The Fanning friction factor can then be calculated from the experimental data using Eq. 4-10:

$$f = \frac{d\Delta P}{2l\rho u^2} \tag{4-10}$$

where d is the diameter of the pipe; l is the length; ρ is density of the dilute polymer flow (as explained earlier); ΔP is the measured pressure drop; and u is the mean velocity calculated from the measured flow rate from Eq. 4-11:

$$u = \frac{4Q}{\pi d^2} \tag{4-11}$$

Using the methods of Kline and McClintock (1953) the uncertainty of the friction factor can be estimated with Eq. 4-12:

$$\delta f = \sqrt{\left(\frac{\partial f}{\partial(\Delta P)}\delta(\Delta P)\right)^2 + \left(\frac{\partial f}{\partial u}\delta u\right)^2 + \left(\frac{\partial f}{\partial d}\delta d\right)^2 + \left(\frac{\partial f}{\partial l}\delta l\right)^2} \tag{4-12}$$

where $\delta(\Delta P)$ is the uncertainty of the differential pressure sensor; δd and δl are 0.1 mm and 1 mm, respectively; and δu is the uncertainty the measured mean flow velocity, which can also be estimated using the same Kline and McClintock method:

$$\delta u = \sqrt{\left(\frac{\partial u}{\partial Q}\delta Q\right)^2 + \left(\frac{\partial u}{\partial d}\delta d\right)^2} \tag{4-13}$$

where δQ is the uncertainty of flow rate measurement as discussed earlier. Similarly, the uncertainty of drag reduction efficiency (DR%) can be estimated with Eq. 4-14:

$$\delta(DR\%) = \sqrt{\left(\frac{\partial(DR\%)}{\partial(\Delta P_S)}\delta(\Delta P_S)\right)^2 + \left(\frac{\partial(DR\%)}{\partial(\Delta P_P)}\delta(\Delta P_P)\right)^2} \tag{4-14}$$

A series of experiments were conducted with water but without polymer additives in the test section to verify the experimental setup. For verification purposes, the measured Fanning friction factors are compared with the classic Colebrook–White correlation in Eq. 4-15:

$$\frac{1}{\sqrt{f}} = -2\log\left(\frac{2.51}{Re\sqrt{f}} + \frac{\varepsilon}{3.7d}\right) \tag{4-15}$$

where $\mathcal{E}$ is the absolute roughness of the pipe, equal to 0.015 mm in this study. The results in Figure 4-4 show a good agreement between the measurements and the results from the classic correlation: all predicted value are covered by the error bars from the uncertainty analysis. This demonstrates the reliability of the experimental setup and data analysis method, and guarantees the data repeatability due to the small error. Note that error bars are shown in Figure 4-4 yet not shown in the figures of the next sections, for the purpose of clean presentations.

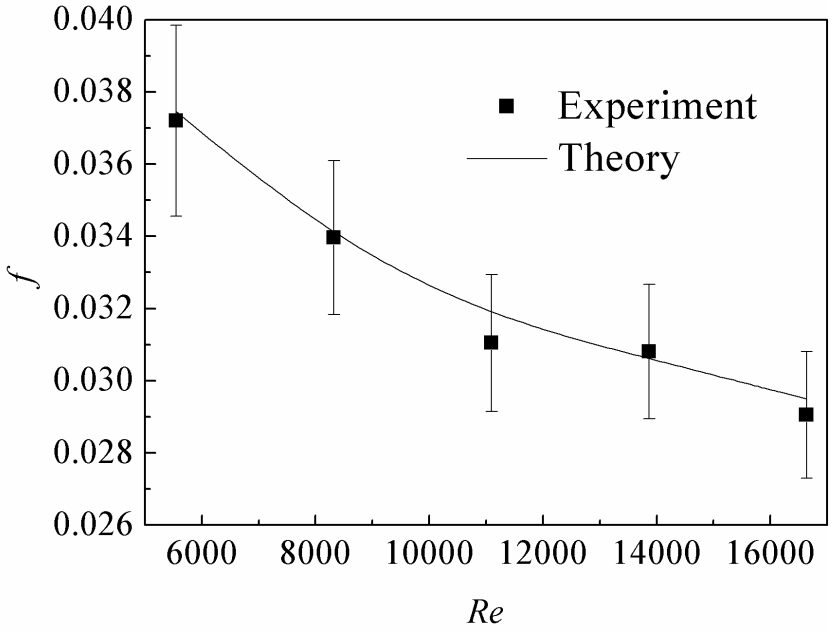

Figure 4-4 Benchmark test for the flow loop

4.3 Experimental Results

4.3.1 Drag Reduction Experimental Data and Analysis

Figure 4-5 shows the measured Fanning friction factor at different Reynolds numbers of the drag-reducing flow. As clarified earlier, the solvent viscosity is used to calculate the

Reynolds number since in the dilute polymer solution (several ppm levels), the polymers will not significantly change the viscosity (Burshtein et al., 2017). As expected, the friction factors with polymers are less than the friction factors predicted by the Blasius equation ($4000 \leq Re \leq 4\times10^4$ in pipe flows) with no drag reduction, i.e., Eq. 4-16 and the dash-dotted lines in Figure 4-5. Also, the friction factors of flow with polymers are higher than the friction factors predicted by Virk's asymptote (Virk, 1975; Virk et al., 1970, $4000 \leq Re \leq 4\times10^4$ in pipe flows), i.e., Eq. 4-17 and the dotted lines in Figure 4-5, which represents the minimum friction factor by polymers. The laminar flow and laminar flow extension lines from the Hagen–Poiseuille equation, i.e., Eq. 4-18 ($Re \leq 2300$ in pipe flows) and solid and dash lines in Figure 4-5, are used as a reference to indicate that whatever polymer is added to reduce the friction, it is always greater than the ones in a laminar flow:

$$f = 0.079Re^{-0.25} \tag{4-16}$$

$$f = 0.59Re^{-0.58} \tag{4-17}$$

$$f = \frac{16}{Re} \tag{4-18}$$

These qualitative analyses further verify that experimental data are correct and also show that the drag reduction is influenced by polymer concentration.

(a)

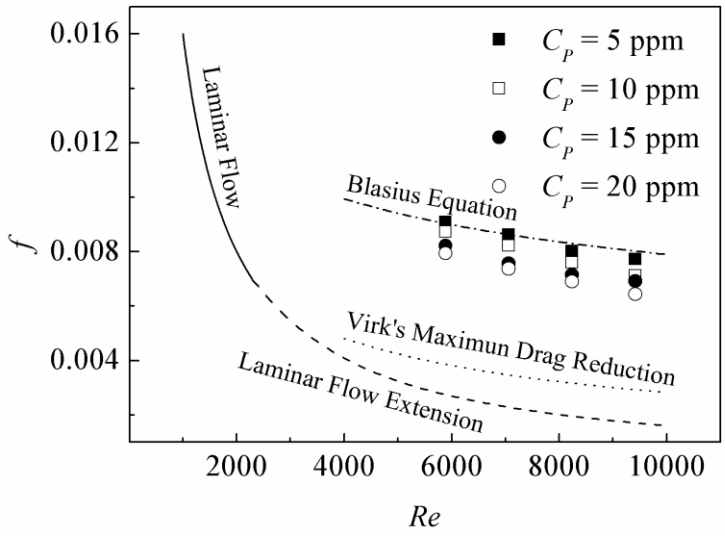
0.016
0.012
0.008
0.004
f
2000
4000
6000
8000
10000
Re
C_P = 5 ppm
C_P = 10 ppm
C_P = 15 ppm
C_P = 20 ppm
Laminar Flow
Blasius Equation
Virk's Maximun Drag Reduction
Laminar Flow Extension

(b)

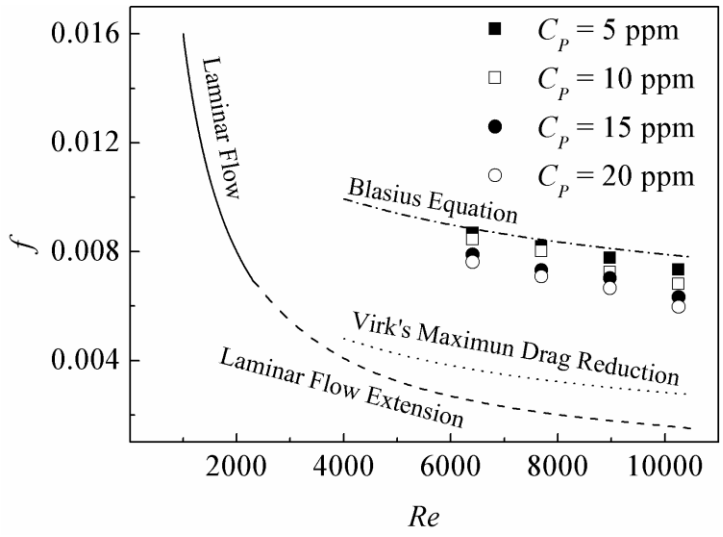
0.016
0.012
0.008
0.004
f
2000
4000
6000
8000
10000
Re
C_P = 5 ppm
C_P = 10 ppm
C_P = 15 ppm
C_P = 20 ppm
Laminar Flow
Blasius Equation
Virk's Maximun Drag Reduction
Laminar Flow Extension

(c)

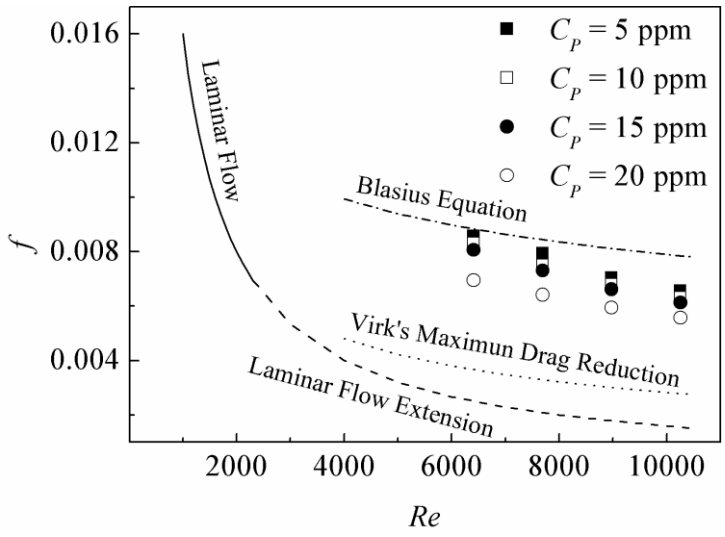
0.016
0.012
0.008
0.004
f
2000
4000
6000
8000
10000
Re
C_P = 5 ppm
C_P = 10 ppm
C_P = 15 ppm
C_P = 20 ppm
Laminar Flow
Blasius Equation
Virk's Maximun Drag Reduction
Laminar Flow Extension

Figure 4-5 The relationship between friction factor and Reynolds number at different concentrations. (a) When $M = 10^6$ g/mol, (b) When $M = 2\times10^6$ g/mol, (c) When $M = 4\times10^6$ g/mol

Figure 4-6 shows the relationship between the drag reduction and polymer concentration. With the same polymer, a higher concentration can increase the drag reduction. In a polymer solution with a higher concentration, more polymers are available to dampen the turbulent structures. The energy dissipated by these turbulent structures can be reused for flow in the stream-wise direction. In this case, the turbulent flow needs less extra energy (pressure drop) to sustain. This is how the drag reduction is defined (Benzi & Ching, 2018).

(a)

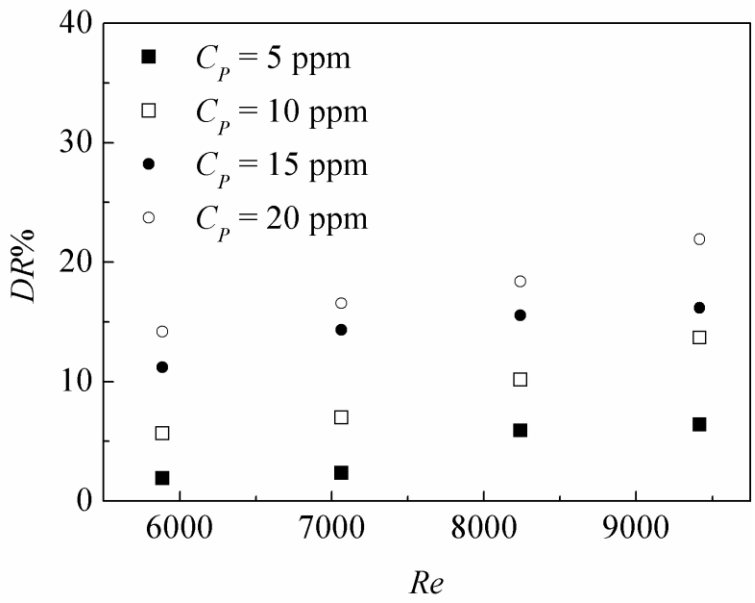

(b)

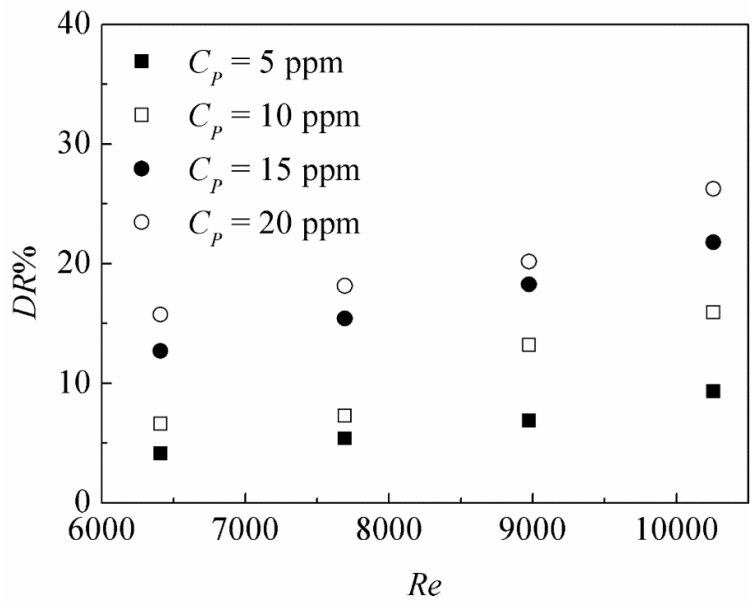

(c)

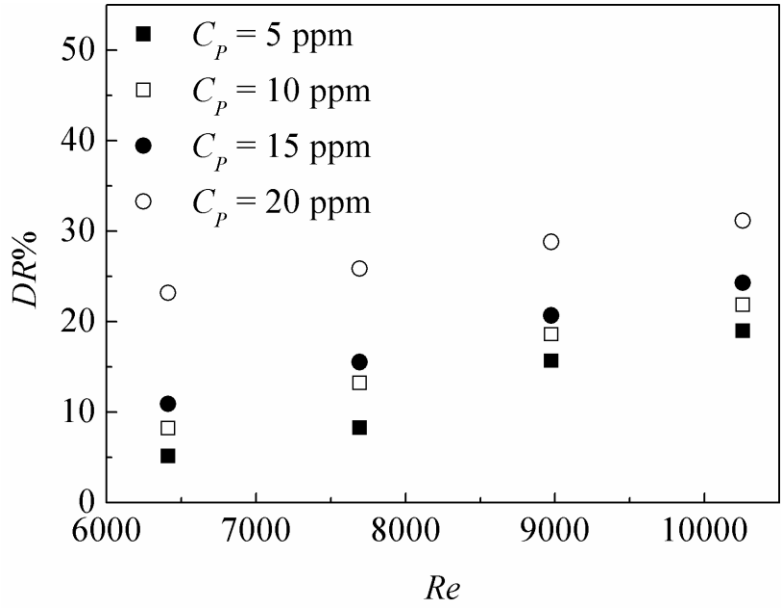

Figure 4-6 The relationship between drag reduction and Reynolds number at different concentrations. (a) When $M = 10^6$ g/mol, (b) When $M = 2\times10^6$ g/mol, (c) When $M = 4\times10^6$ g/mol

Figure 4-7 shows the relationship between the Weissenberg number and drag reduction. The sloid straight lines in Figure 4-7 represent the linear relationship between the drag reduction, *DR*%, and the square of the Weissenberg number, Wi^2, as suggested in a previous work (Zhang

et al., 2018). Under a given molecular weight, the drag reduction increases with an increasing Weissenberg number. As discussed earlier, a higher Weissenberg number means a higher elasticity in the solution, which is better in dampening the vortex structure in the flow so the energy can be used for flow in the streamwise direction (De Gennes, 1986; Tabor & De Gennes, 1986).

(a)

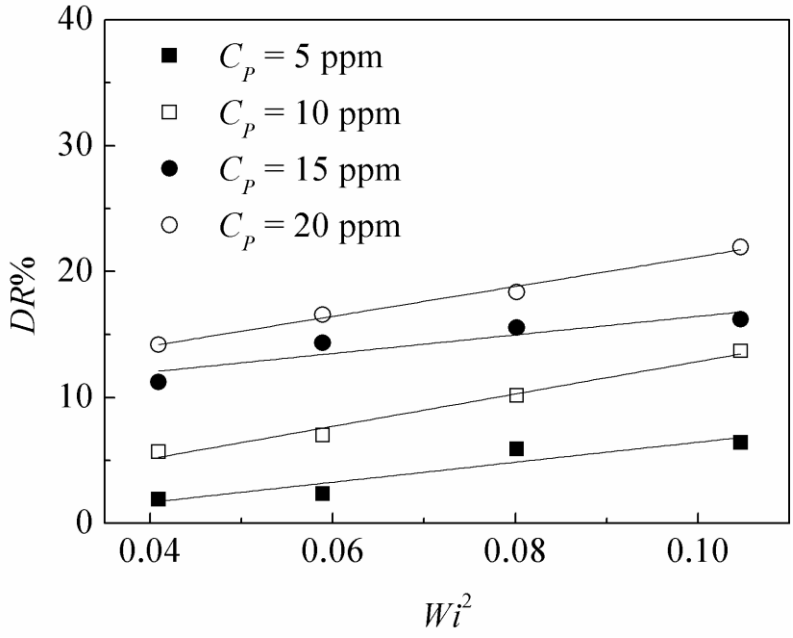

(b)

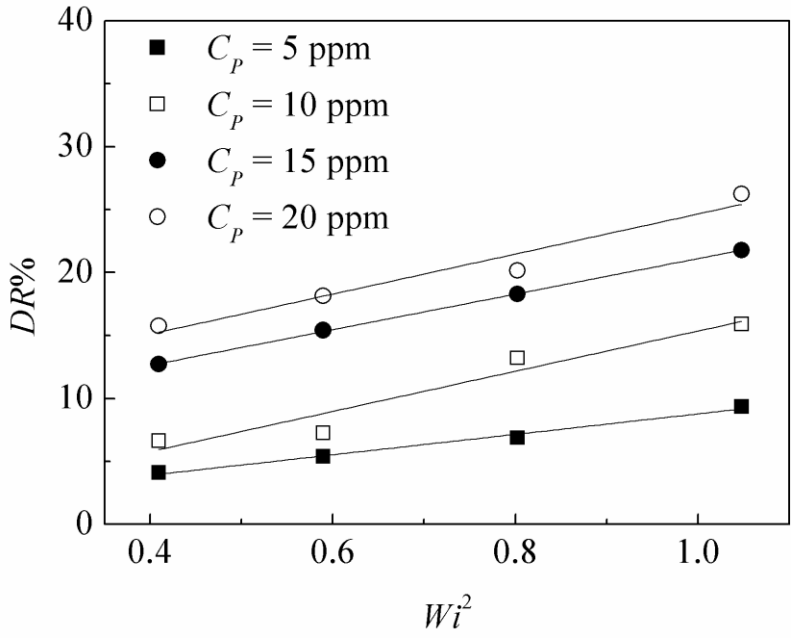

(c)

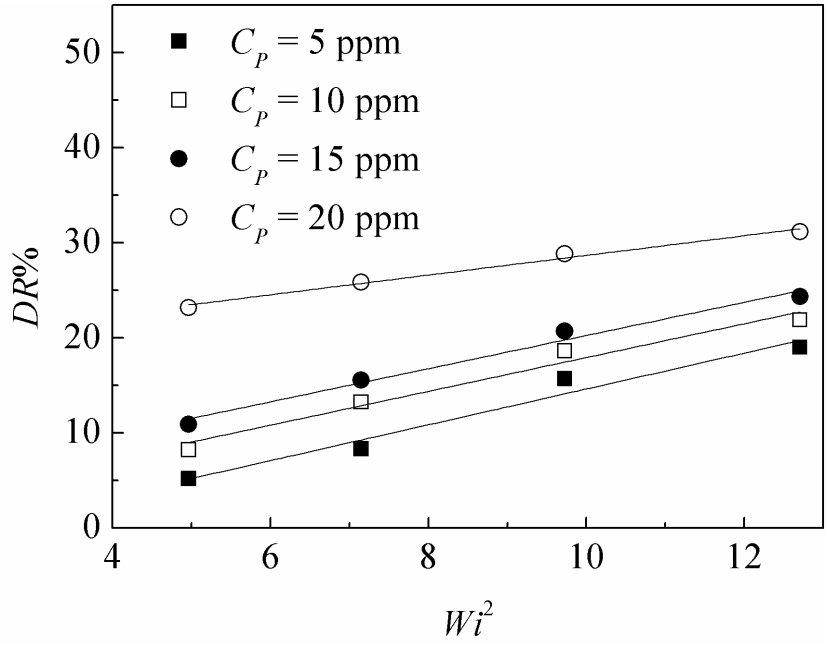

Figure 4-7 Drag reduction at different Weissenberg numbers: (a) when M = 10^6 g/mol; (b) when M = 2 × 10^6 g/mol; (c) when M = 4 × 10^6 g/mol

4.3.2 Correlation and Validation

All experimental data are analyzed in Excel and a regression is conducted following the format in Eq. 4-8, leading to the following final correlation:

$$DR\% = 0.935C_P + 0.858Wi^2 \quad (4\text{-}19)$$

The coefficient of determination of Eq. 4-19, R^2, is 0.96, indicating a good correlation for the experimental data. As shown in Figure 4-8, most data are adequately covered within a +/- 30% relative error range.

To further validate the correlation and demonstrate its wider range of applications, other drag reduction data by PEO from previous works are added in the analysis and shown in Figure 4-8 (Goren & Norbury, 1967; Inge et al., 1979; Interthal & Wilski, 1985; Kim et al., 2009; Paterson & Abernathy, 1970). These additional data are obtained in other conditions, i.e.,

different molecular weight, concentration, flow velocity, and diameter, as summarized in Table 4-2. All experiments were conducted at room temperature, ~17 °C.

Table 4-2 Summary of previous experimental data and conditions for correlation validation

Reference	M (10^6 g/mol)	C_P (ppm)	u (m/s)	d (cm)
Goren & Norbury (1967)	4	5-20	0.73-1.11	5.1
Inge et al. (1979)	4	0.4-1.6	1.44-2.17	1
Interthal & Wilski (1985)	4	50	0.74-2.04	15.2-20.3
Kim et al. (2009)	0.2-4	1-20	2-3.3	1.71
Paterson & Abernathy (1970)	0.5	5-10	2.67-4.15	0.63

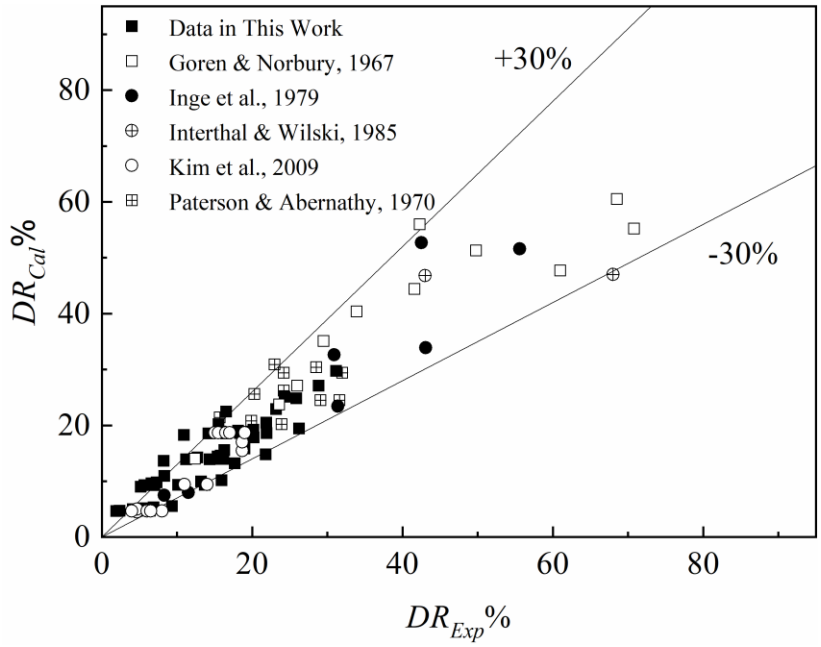

Figure 4-8 Comparison of drag reduction data from experiments and predictions by the developed correlation in Eq. 4-19

As shown in Figure 4-8, these extra data are also in the +/- 30% range of predictions from Eq. 4-19. These results show that the new correlation has a wide range of applications and is not limited to conditions in this study. In these additional validations, the most convincing one is from the work of Interthal and Wilski (1985). In this work, the test was conducted in a pipe system with 15.2 and 20.3 cm diameters, the latter being the largest diameter in the drag reduction tests by PEO until the current study, which is very close to pipes in real liquid transportation systems.

4.4 Discussions

The theory and correlation developed in this work can explain an interesting phenomenon previously discovered by Peyser & Little (1971). They mentioned that an increasing viscosity of the solvent led to an increase in the drag reduction. If the definitions of Weissenberg number in Eq. 4-4 and relaxation time in Eq. 4-2 are combined, one can see that a higher viscosity leads to higher relaxation time and Weissenberg number. From the new correlation in Eq. 4-19, a higher Weissenberg number leads to higher drag reduction.

The correlation developed in this study provides a promising tool for predicting drag reduction with lower concentration polymer additives. One advantage of this new correlation over the previous ones is that it includes the key property of relaxation time in a non-dimensional form; therefore, the polymer type and molecular weight are considered. Many earlier drag reduction studies used another method, the power law of drag-reducing flows, to correlate experimental data (Bogue & Metzner, 1963; Dodge & Metzner, 1959; Malin, 1997). That method does not require an understanding of the relaxation process. Instead, it only requires information about the flow consistency index and flow behaviour index. There is an obvious flaw in this method. If the polymer concentration is so low that these two factors are the same as

those for a Newtonian fluid, this method will no longer work. The new method of using the relaxation time in the current study overcomes this problem. Even in a dilute polymer solution, the relaxation time can still be estimated by the Zimm's theory.

An additional advantage is that there is no need to build a large-scale flow device or use a high flow velocity by this new correlation. In most previous correlations for the drag reduction estimation, the friction factor was a function of Reynolds number (Hoyt & Sellin, 1993; Liang et al., 2017). In the Reynolds number definition, the diameter and velocity are the numerators. Most industrial drag reduction applications involve large pipes and higher flow velocity. To achieve these large Reynolds numbers with a small pipe in the lab, the velocity must be increased dramatically. The high velocity and large pressure drop requires expensive instruments and can cause many safety problems. The new correlation in this study does not use the Reynolds number and uses the Weissenberg number instead to predict the drag reduction. In the Weissenberg number definition, the pipe diameter is the denominator and the velocity is the numerator. To predict the flow drag reduction in a pipe with a large diameter, one can calculate the ratio of velocity and diameter, and use this ratio in a flow loop with a small diameter to predict the reduced friction. Thus, this method can predict the drag reduction based on the industrial needs and avoid the lab safety and cost problems mentioned above. As shown in the correlation validation, previous data are used to validate the correlation. The diameters in these tests are different from the one used in our experiments, which range from 0.63 cm-20.3 cm. The validation result is acceptable, within a +/- 30% relative error, confirming that one can use a small flow loop for the prediction of the reduced friction at a larger scale. To further validate our model, future drag reduction tests can be conducted in smaller diameter pipes (< 1 mm) as suggested by Ushida et al (2012, 2016 & 2018).

When this new correlation is used for long-distance fluid transportation systems, the degradation issue needs to be considered. In these long-distance systems, the polymers tend to degrade over time under a high shear rate. Nesyn et al. (2018) showed that in a long-distance oil transportation system, when a proper drag-reducing polymer was selected, the ratio of drag reduction at the 500^{th} km and 50^{th} km is ~0.56. This empirical ratio may be useful in the design of drag reduction for long pipeline transportation. The study of the degradation of DRAs is another important research topic, and it will be discussed in the next chapter.

4.5 Summary

In Chapter 4, a semi-empirical correlation based on two dimensionless numbers, the Weissenberg number and polymer concentration, is developed for the estimation of the drag reduction in turbulent pipe flow in dilute polymer solutions. The Weissenberg number in the correlation is based on Zimm's theory regarding the polymer relaxation process, and the polymer concentration is lower than the overlap concentration. Experimental data from the flow loop shows that the drag reduction efficiency increases with the Weissenberg number and polymer concentration. These data are used to develop the correlation, and the relative error between experimental data and predicted values is within +/- 30%. Previous experimental data in laboratory and industrial systems are used to further validate the correlation with similar good agreement. The application and advantages of this new correlation is discussed. One of the key benefits is that one can use a lab-scale flow loop in relatively low velocities and small diameters to achieve the prediction of the drag reduction in a large industrial scale system.

Chapter 5 Mechanism and Correlation for Degradation of Drag Reduction by Polymers in Rotational Flows

In this chapter, the degradation of drag reduction is investigated and a mechanism of the degradation is proposed. The main content of this chapter has been published (Zhang, X., Duan, X., & Muzychka, Y. (2018). "New mechanism and correlation for degradation of drag-reducing agents in turbulent flow with measured data from a double-gap rheometer". Colloid and Polymer Science, 296(4), 829-834). The author of this thesis is the first author of this paper. The first author conducted the experiments, analyzed the data, and prepared the manuscript. Prof. Duan and Prof. Muzychka as the second and third authors provided their suggestions on correlation development and revision of this paper.

5.1 Experiment

The DRA used in this study is a water-soluble polymer - PEO (from Sigma-Aldrich Canada) with three molecular weights, 10^6, 2×10^6, 4×10^6 g/mol. First the polymers are mixed with deionized water under a mild rotation speed, 60 rpm, for 5 hours until all the polymers are dissolved. Then, the solution is left to stand still for 24 hours to ensure homogeneous concentration. No clustering or crystallization was observed in the polymer solution before each experiment. The concentration of polymer used in the experiment is 20, 35 and 50 ppm.

The modified RDA used in this study is based on a MCR301 rheometer (Physica, Anton Paar Ltd, United Kingdom) with a high torque resolution, 10^{-6} N·m. The temperatures in experiments were maintained at constant levels of 25, 45 and 65 ^{o}C with a high-resolution temperature-control system. The geometry used in our experiments is a double gap (DG) shown in Figure 5-1. There are two advantages with this geometry. First, it can reduce the evaporation of the liquids under relatively high temperatures. This helps to avoid measurement error due to change of

concentration of the polymer solution, since a fixed concentration is required in each experiment. Therefore, this DG design is more suitable than the other geometries, such as parallel plate (PP) and cone plate (CP). Second, this geometry can also prevent samples splashing out. In the test of drag reduction and degradation, a high shear rate (rotation speed) is needed (Andrade et al., 2016). If the CP or PP were used in the test, the sample could splash out resulting in a measurement error. It is believed that a DG device is the best choice for the drag reduction and degradation test (Pereira et al., 2013).

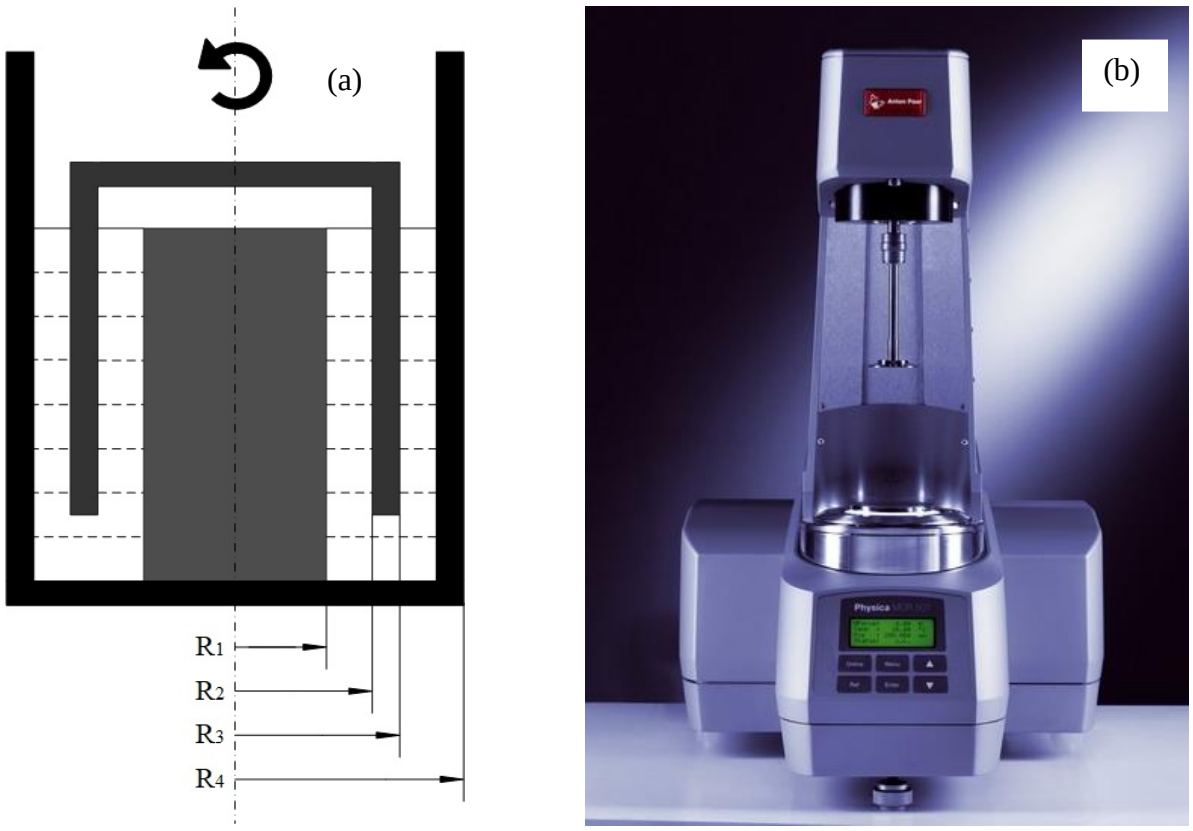

Figure 5-1 (a) Geometry of a double gap (DG) rheometer, R_1 = 11.909 mm, R_2 = 12.328 mm, R_3 = 13.332 mm, R_4 = 13.797 mm; (b) photo of the rheometer (The copyright of this photo belongs to the Anton-Paar website)

Drag reduction is measured by the torque with (T_P) and without DRAs (T_S) under the same rotation speed, temperature, and concentration of the polymer, as the follow:

$$DR = \frac{T_S - T_P}{T_S} \tag{5-1}$$

The uncertainty analysis is carried out based on the Kline & Mcclintocks's theory (1953), shown in Eq. 5-2.

$$\delta(DR) = \sqrt{\left[\frac{\partial(DR)}{\partial T_S}\delta T_S\right]^2 + \left[\frac{\partial(DR)}{\partial T_P}\delta T_P\right]^2} \tag{5-2}$$

In Eq. 5-2, $\delta(DR)$, δT_S and δT_P are the uncertainty of drag reduction, torque without polymer solutions and with polymer solutions. The latter two terms, δT_s and δT_p are equal to 0.001 mN·m. These two terms can be replaced by δT. Eq. 5-2 can be simplified to Eq. 5-3

$$\delta(DR) = \frac{\delta T}{T_S}\sqrt{1 + \left(\frac{T_P}{T_S}\right)^2} \tag{5-3}$$

Because T_P is always smaller than T_S in drag reduction experiments, the ratio of T_P/T_S is less than 1. In these experiments, the minimum value of T_S is approximately 1 mN·m and the uncertainty, δT, in this rheometer is 0.001 mN·m. The maximum uncertainty of drag reduction $\delta(DR)$ is 0.0014, which is far less than the drag reduction range in the experiment. So, the uncertainty in the following experiments can be neglected and error bars are not shown in the figures of results.

5.2 A New Theory of Degradation Mechanism by Polymers

As discussed in the introduction, the current theory cannot explain the mechanism of drag reduction degradation since the physical meanings of many factors are still not clear. Here a new theory is proposed by analyzing the degradation of DRA from a chemistry dynamics perspective. Bizotto & Sabadini (2008) used the rate of DRA concentration change, with a unit of

mol·m^{-3}·s^{-1}, to represent the degradation of DRA in a rotating disk apparatus experiment. This is a unit of chemical reaction. Inspired by this unit, it is proposed that DRA degradation is treated as a chemical reaction. The original polymer concentration decreases due to the turbulent flow. It means that original polymers with a high molecular weight are cut into smaller entities and new polymers with low molecular weights form. ($r_p = k\, dC_p/dt$, k is the chemical reaction constant and dC_p/dt is the change rate of polymer concentration). However, DRA degradation is not only related to its concentration, but also the molecular weight. Several previous non-drag-reduction studies (Madras & Chattopadhyay, 2001; Sung et al., 2004) used the change of polymer's molecular weight to represent the degradation rate of polymers. This view, which uses molecular weight to indicate the degradation and drag reduction to study polymer degradation in the drag reduction, is used. Following this practice, the present work considers DRA degradation as a chemical reaction with a reaction rate represented by the change of molecular weight, shown in Eq. 5-4,

$$r_P = k[M]^{\alpha} \tag{5-4}$$

where r_P is the reaction rate, i.e., DRA degradation rate, with a unit of g·mol^{-1}·s^{-1} ; [M] is the molecular weight of DRA, with a unit of g mol^{-1}; and α is the order of degradation rate; k is the reaction constant. In chemistry, the reaction rate by definition is

$$r_P = -\frac{d[M]}{dt} \tag{5-5}$$

Combining Eq. 5-4 and Eq. 5-5 leads to

$$-\frac{d[M]}{dt} = k[M]^{\alpha} \tag{5-6}$$

Rearranging and integration leads to Eq. 5-6:

$$-\int_{M(0)}^{M(t)} \frac{d[M]}{dt} = \int_0^t k dt \tag{5-7}$$

$M(0)$ and $M(t)$ are the molecular weight at initial state ($t = 0$) and any time, t, during the degradation.

A widely-accepted assumption proposed by Brostow and his colleagues (1983 & 1990) is shown in Eq. 5-8, i.e., the ability of drag reduction is proportional to the molecular weight of DRA. Here $DR(0)$ and $DR(t)$ is the drag reduction at the initial state ($t = 0$) and any time, t, in the degradation process. Essentially it assumes that the degradation rate of drag reduction is equal to the degradation rate of DRA:

$$\frac{DR(t)}{DR(0)} = \frac{M(t)}{M(0)} \tag{5-8}$$

Combining Eq. 5-8 with the degradation correlation of Eq. 5-9 leads to Eq. 5-10.

$$DR(t) = DR(0)e^{-kt} \tag{5-9}$$

$$M(t) = M(0)e^{-kt} \tag{5-10}$$

It can be seen that Eq. 5-10 is a solution of Eq. 5-7 if $\alpha = 1$. However, it is still necessary to determine that if α equals to 1 in the drag reduction degradation case.

Drag reduction (degradation) induced by DRAs happens when the concentration of DRAs is very low, often in ppm (weight based). So, the interaction between different polymer chains can be neglected (Andrade et al., 2014), and the only possible interaction in the polymer solution is that between the solvent and the DRAs. The chemical reaction rate can be described in Eq. 5-11.

$$r_P = k'[S][M] \tag{5-11}$$

In Eq. 5-11, $[S]$ represents the molecular weight of the solvent, water in this case. Since the water structure cannot be destroyed in turbulent flow, it is reasonable to combine k' and $[S]$,

which can be rewritten as *k*. This indicates that the degradation of DRAs can be treated as a first-order chemical reaction, i.e., $r_P = k[M]$, or α = 1 in earlier equations.

With this theoretical analysis, the physical meaning of *k* and the mechanism of degradation of DRAs can be explained in a new way: the degradation is a first-order chemical reaction based on the molecular weight, and *k* is the constant of the chemical reaction rate. The final correlation for drag reduction degradation still bears the same format as in Eq. 5-9 but several extensions can be made based on this new theory. The results and discussions are shown in the next section.

5.3 Results and Discussions

The degradation of DRAs is a function of time, temperature, rotation speed (shear rate), the concentration of DRAs and molecular weight. This phenomenon can be shown in Figure 5-2. In this figure, the torque of DI water remains as a constant over time. However, torques for the PEO solution show a time-dependent characteristic. There is a large initial torque difference between the dilute polymer solution and water. At this initial state, the polymer structure has high integrity. The lower torque with the polymer solution indicates its effectiveness of flow drag reduction. After a period of time under high shear rates, the long chain polymers can be cut and the interaction between the solvent, water and polymer starts to change. At this point, the increase of torque represents the degradation of drag reduction caused by degradation of the polymers. A series of experiments with different experimental conditions are performed, and one result is shown in Figure 5-2 because all the experimental data in other conditions have similar trend shown in Figure 5-2.

The same time-dependent performance of the drag reduction is shown in Figure 5-3. At the initial state, drag reduction is large because the polymer is not destroyed by the high shear

rate. Note that drag reduction value at the initial state, $DR(0)$, is not measured in the experimental setup since it is not possible to measure a torque at the initial state ($t = 0$). That value can be deducted from the trend with Eq. 5-9, as did in previous studies (Deshmukh et al., 1991). Similar to Figure 5-2, there is no need to show more results in drag reduction and degradation since this result is similar to those from many previous studies (Lim et al., 2005 & 2007; Zhang et al., 2011). Results in Figure 5-3 further shows that the previous correlation format shown in Eq. 5-9 can indeed provide reasonable prediction of the experimental data from this rheometer geometry.

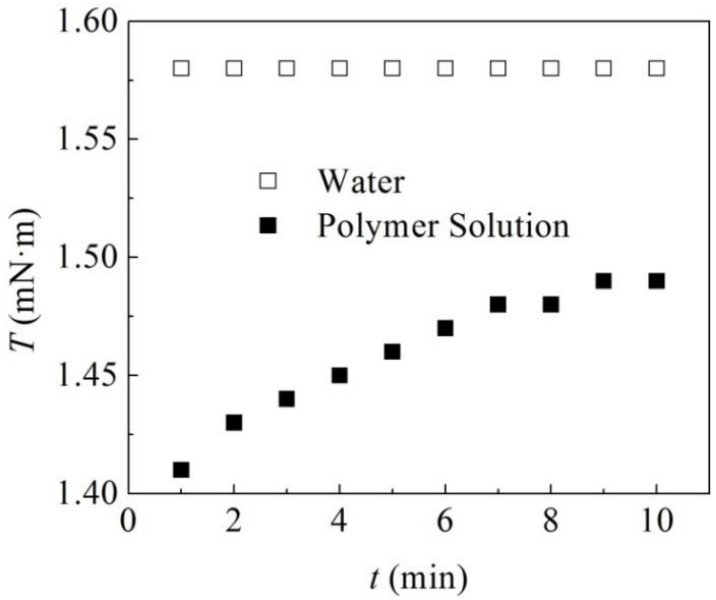

Figure 5-2 Torque of DI water and polymer solution (C_P = 20 ppm, T = 318 K, $\dot{r}$ = 8000 s^{-1}, M = 2×10^6 g/mol)

Correlation development in this study will stay with the format of Eq. 5-9 but extend it to include detailed correlation of $DR(0)$ and k which now has a clear physical meaning. Based on analysis in the previous section, k is the first-order chemical reaction rate. From this perspective,

the Arrhenius equation, Eq. 5-12, can be used for k, where k_0 is the pre-exponential factor and E_a is the activation energy of reaction.

$$k = k_0 e^{-\frac{E_a}{RT}} \tag{5-12}$$

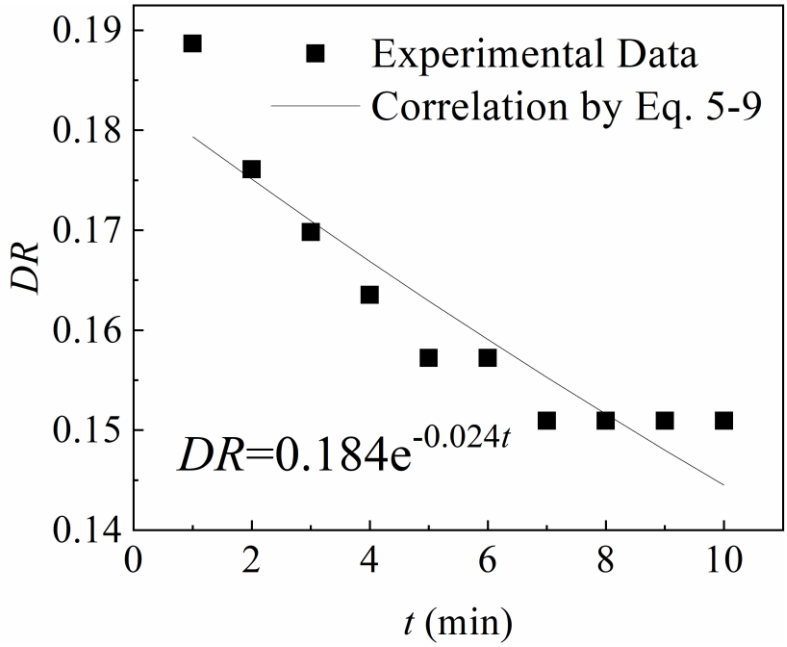

Figure 5-3 Experiment data and correlation by Eq. 5-9 (C_P = 35 ppm, T = 318 k, $\dot{r}$ = 7000 s^{-1}, M = 4×10^6 g/mol)

In the current experiments for degradation of drag reduction polymers, the degradation rate is affected by many factors including temperature, concentration of the polymers and the rotation speed (shear rate). To account for all these factors, the classic Arrhenius equation in Eq. 5-12 are extended by correlating the pre-exponential factor (k_0) with polymer concentration (C_P) and shear rate ($\dot{r}$). The effect of temperature is already considered in the classic equation. The correlation of k_0 was done with a polynomial method in Eq. 5-13, similar to previous works (Kalashnikov, 2002; Pereira & Soares, 2012) in predicting polymer degradation.

$$k_0 = a_0 + a_1\dot{r} + a_2 C_P + a_3\dot{r}^2 + a_4 C_P^2 + a_5 C_P\dot{r} \tag{5-13}$$

After combining the new pre-exponential factor in Eq. 5-13 and the classical Arrhenius equation in Eq. 5-12, the format of reaction constant for the DRA degradation is shown in Eq. 5-14.

$$k = (a_0 + a_1\dot{r} + a_2 C_P + a_3\dot{r}^2 + a_4 C_P^2 + a_5 C_P\dot{r})e^{-\frac{\dot{E_a}}{RT}} \tag{5-14}$$

By correlating all the experimental data in the double gap rheometer setup in three temperatures, 298, 318 and 338 K, the final correlation for the chemical reaction constant is

$$k = (5.376 \times 10^6 + 1.027 \times 10^4\dot{r} - 1556C_P - 822.9\dot{r}^2 + 0.0983C_P^2 + 6.71cr)e^{-\frac{\dot{37480}}{RT}} \tag{5-15}$$

In Eq. 5-15, the activation energy, E_a is 37.48 kJ/mol. This positive activation energy shows that increasing temperature can accelerate the degradation rate of DRAs, which is supported by previous work (Zhang et al., 2016).

Drag reduction at the initial state, *DR*(0) is also affected by many factors including polymer concentration and molecular weight, shear rate, and temperature. *DR*(0) is correlated with these factors using the experimental data with a product type of correlation in Eq. 5-16:

$$DR(0) = 9.46 \times 10^{-3} C_P^{0.265} \left(\frac{\dot{r}}{1000}\right)^{0.420} \left(\frac{T}{T_t}\right)^{-2.657} \left(\frac{M}{M_0}\right)^{0.616} \tag{5-16}$$

where T is the Kelvin temperature at experiment conditions, k; T_t is the Kelvin temperature of transition temperature of PEO, 338 k; M_0 is a reference molecular weight, 10^6 g/mol; 1000 s^{-1} is a reference shear rate. Putting Eq. 5-16 and Eq. 5-17 into Eq. 5-9 gives the final correlation to predict the drag reduction at any time during the degradation.

Figure 5-4 shows three sample results of *DR* prediction with this new correlation. An average relative error (*ARE*) (Ng et al., 2002), shown in Eq. 5-17, is introduced to indicate the

accuracy of the predictions. DR_{Cal} and DR_{Exp} represent the prediction and the experimental data, respectively.

$$ARE = \frac{1}{N}\sum\left|\frac{DR_{Cal} - DR_{Exp}}{DR_{Exp}}\right| \tag{5-17}$$

These results show that the proposed correlation can predict the data reasonably well, almost within 15% accuracy on average. This is better than some previous correlations such as those by Bizotto & Sabadini (2005) (with ±50% accuracy) and Zhang's et al. (2016) (whose results showed a relatively larger error but not given directly). More importantly, this correlation scheme provides a new mechanism of degradation as a first-order chemical reaction. All the parameters in this new correlation have clear physical meanings. These results demonstrate the validity of the proposed new degradation theory.

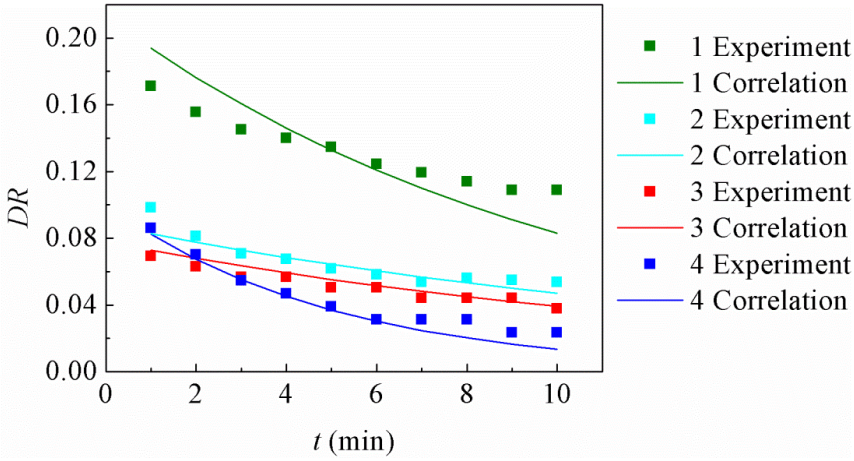

Figure 5-4 Comparison between experimental data and prediction by Eq. 5-15 and Eq. 5-16 at different fluid and flow conditions: (1) $M = 4\times10^6$ g/mol, $C_P = 50$ ppm, $T = 298$ K, $\dot{r} = 8000$ s^{-1}, $ARE = 11.7\%$; (2) $M = 2\times10^6$ g/mol, $C_P = 50$ ppm, $T = 338$ K, $\dot{r} = 6000$ s^{-1}, $ARE = 6.43\%$; (3) $M = 10^6$ g/mol, $C_P = 35$ ppm, $T = 298$ K, $\dot{r} = 7000$ s^{-1}, $ARE = 6.27\%$; (4) $M = 2\times10^6$ g/mol, $C_P = 35$ ppm, $T = 318$ K, $\dot{r} = 7000$ s^{-1}, $ARE = 14.8\%$

Another observation from these results is that the accuracy of this correlation varies between different experimental conditions. This indicates that there are probably other factors that are not accounted. For example, in developing the new theory of degradation mechanism and the new correlation, only the "overall" property of the polymer solution during degradation is considered, i.e., the molecular weight and concentration, but the molecular weight distribution of the polymers is neglected. In this experiment, the profile of molecular weight is not analyzed so this profile is unknown. In drag reduction, the contribution by each molecule group (with a molecular weight) is different, so the degradation of polymers under different molecular weight is suspected to be different. An overall property of polymer solution can not include this difference.

Furthermore, the fundamental assumption in Eq. 5-9, i.e., the degradation of drag reduction is equal to the degradation of polymer may need further investigation. Although this assumption has been applied in many previous studies, it is still based on observations, not any rigorous chemical or physical analysis, nor is it validated by experimental results. The ratio $[(DR(t)/DR(0)]/[M(t)/M(0)]$ might not equal to 1. It is suspected that this ratio is a time-dependent parameter or one dependent on fluids/flow conditions. Based on discussions above, further experiments are needed to investigate how the molecular weight distribution affects the drag reduction and degradation. These issues will be addressed in the next chapter.

5.4 Summary

In Chapter 5, drag reduction and degradation by polymers in a double-gap rheometer are investigated. A new theory based on Brostow's assumption is proposed that the degradation of the polymer in the turbulent drag reduction is a first-order chemical reaction. Based on this theory and measured drag reduction data in the double-gap rotating apparatus, a correlation with

a modified Arrhenius equation is developed to predict the drag reduction effectiveness at any time during the degradation. The relative error of this correlation is ±15%.

Chapter 6 A New Molecular View of Polymer Degradation in Drag-Reducing Flow

Research presented in the earlier chapter indicate that the Brostow's assumption might be incorrect. In this chapter, experimental data are used to show that this important assumption is indeed incorrect in many cases. An improved mechanism is then proposed to explain the degradation of drag reduction. The main content of this chapter has been published as a journal paper (Zhang, X., Duan, X., & Muzychka, Y. (2019). "Degradation of flow drag reduction with polymer additives - a new molecular view". Journal of Molecular Liquids, 292, 111360). The author of this thesis is the first author of this paper. The first author analyzed the data and prepared the manuscript. Prof. Duan and Prof. Muzychka as the second and third authors provided their suggestions on the analysis and revisions of this paper.

6.1 Examination of Brostow's Assumption

To examine Brostow's assumption, one would need to measure the degradation of drag reduction, $DR(t)/DR(0)$ and the degradation of the molecular weight of the drag-reducing polymer, $M(t)/M(0)$. The former can be measured by a differential pressure sensor in pipe flow (Zhang et al., 2018) or a torque sensor in rotational flow (Zhang et al., 2011); the latter can be measured by a size exclusion chromatography (SEC). The degradations of drag reduction and molecular weight have been measured in two studies, i.e., by Lee et al. (2002) in a rotational flow and Vanapalli et al. (2005) in a pipe flow. Their data are reorganized and presented in Figure 6-1. These data suggest that Brostow's hypothesis in Eq. 6-1 is incorrect – the degradation rate of drag reduction is very different than that of the molecular weight decrease.

$$\frac{DR(t)}{DR(0)} = \frac{M(t)}{M(0)} \tag{6-1}$$

(a)

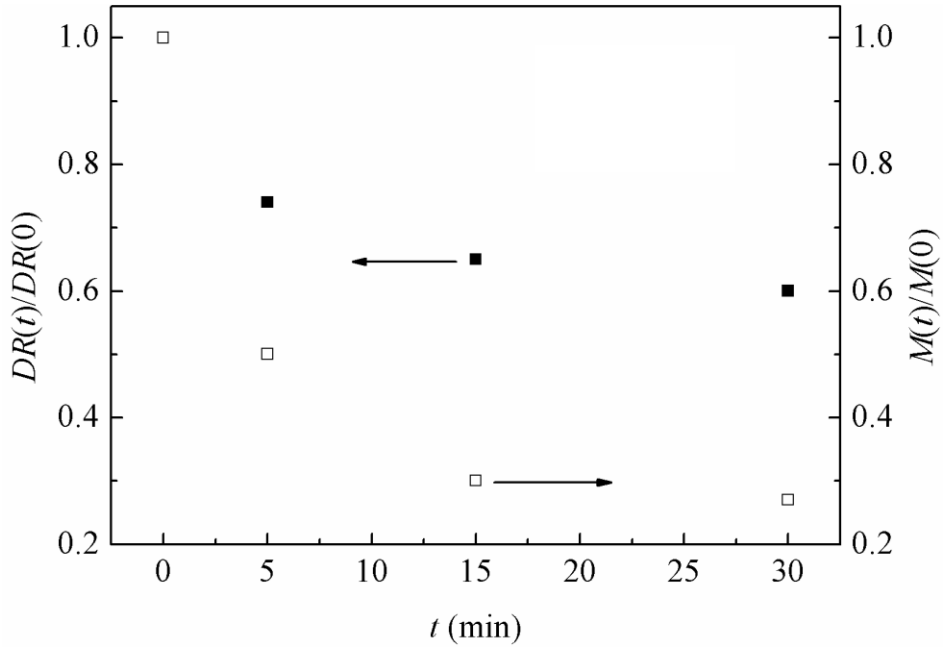

(b)

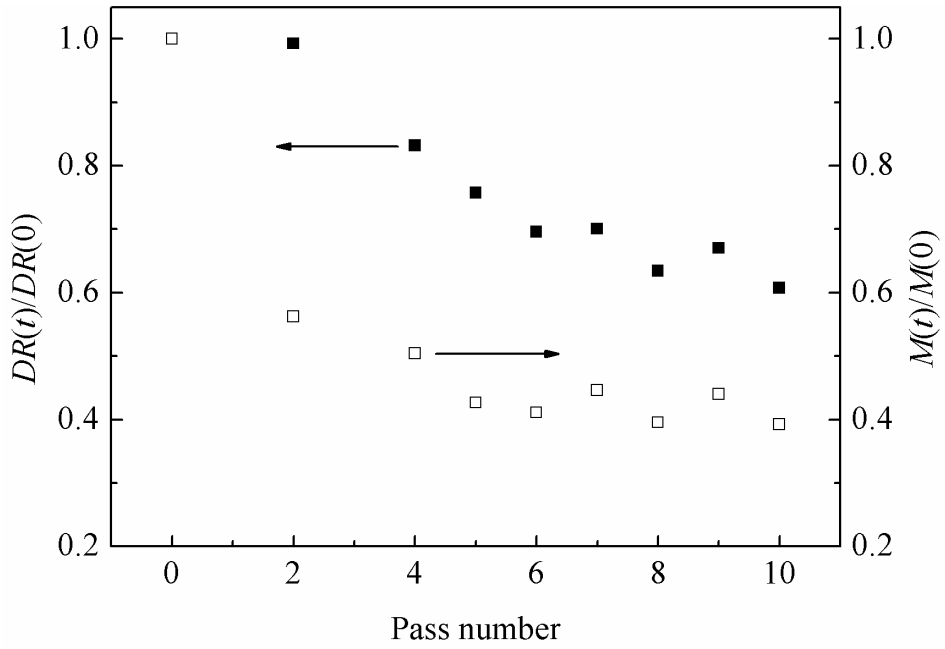

Figure 6-1 The relationship of $DR(t)/DR(0)$ and $M(t)/M(0)$: (a) revised from Lee et al. (2002) and (b) from Vanapalli et al. (2005)

Brostow's assumption (Eq. 6-1) provides a useful way to study the degradation of flow drag reduction with time. It also attempts to relate the drag reduction degradation to the

degradation of the drag reducing polymers, which gives a correct direction of finding the mechanisms of drag reduction and its degradation from a molecular point of view. However, the strong relationship that Eq. 6-1 has never been rigorously derived from physical or chemical principles, nor has it been supported by experimental data. Most of the later research work only followed the idea or format of the correlation induced by this assumption, i.e., drag reduction degradation is a function of molecular weight decrease, but not the exact relationship that the two rates are identical. Brostow obtained the assumption from the following statement, "At low concentrations the changes in molecular weight can only be followed by measuring changes in drag reduction" (Brostow, 1983; Brostow et al., 1990). The assumption was from limited observations of experiments of drag-reducing flows, making it not suitable for all experimental conditions, i.e., rotational flow, pipe flow, different polymer types, concentrations and flow velocities, etc. On another important point, this assumption is based on monodisperse polymers. While, it is well known that most drag-reducing polymers are synthetic polymers, which usually have a wide distribution of molecular weight (Vanapalli et al., 2005). The key problem in Brostow's hypothesis is that it only considers the molecular weight of the free polymer but neglects another important structure, the aggregate of polymers in the drag-reducing flow.

There are strong evidences in the literature that aggregate degradation is involved in the drag-reducing flow. Van Dam & Wegdam (1993) investigated the degradation of drag reduction by polyethylene oxide (PEO) with a 3.8×10^6 g/mol molecular weight and a 20 ppm concentration (dilute solution). They also measured the hydrodynamic radius of the degraded polymers, $R_H(t)$, with a dynamic light scattering (DLS) method. This radius describes the size of polymers in the coiled state or aggregates that contain several free polymers. Unlike SEC that filters the aggregates in the polymer solution and only measures the molecular weight of free polymers,

DLS measures the hydrodynamic radius and it does not differentiate free polymers and aggregates in the polymer solution. If there are no aggregates in the polymer solution, the hydrodynamics radius represents the size of a free polymer; if both free polymers and aggregate are in the solution, the radius of hydrodynamics provided by DLS is the average value of these two. The hydrodynamics radius of a free polymer, $R_H'(t)$, is proportional to $M(t)^{\alpha}$ (α is a constant between 0.5 – 0.6 for linear flexible polymers, PEO included); a free polymer with a higher molecular weight has a larger hydrodynamic radius (Selser, 1981). Data from Van Dam & Wegdam (1993) are analyzed and shown in Figure 6-2. The ratio of $DR(t)$ over $DR(0)$ is shown as solid squares and ratio of $R_H(t)$ over $R_H(0)$ (the hydrodynamics radius at the initial state without degradation) is shown in hollow squares. It is not surprising to see the rate of drag reduction degradation is different than that of the hydrodynamic radiuses decrease. It is more interesting to analyze why the hydrodynamic radius at the three early times (less than 50 s, as shown in the doted box) remains nearly unchanged (or even slight increase). The similar hydrodynamic radius means the average size of free polymers or aggregates is almost the same. As shown and discussed earlier, the linear flexible PEO degrades with time in the turbulent flow. If Brostow's assumption were valid and there were no aggregates, then the molecular weight and the hydrodynamic radius would continuously decrease. However, the data suggest otherwise. The non-decreasing hydrodynamic radius is due to the aggregates in the solution. The larger hydrodynamic radius of the newly formed aggregates makes the average hydrodynamic radius of the degraded polymers larger. This effect disappears when the aggregates becomes much smaller with longer residence time in the turbulent flow. Degradation of the aggregates will be discussed in the next section.

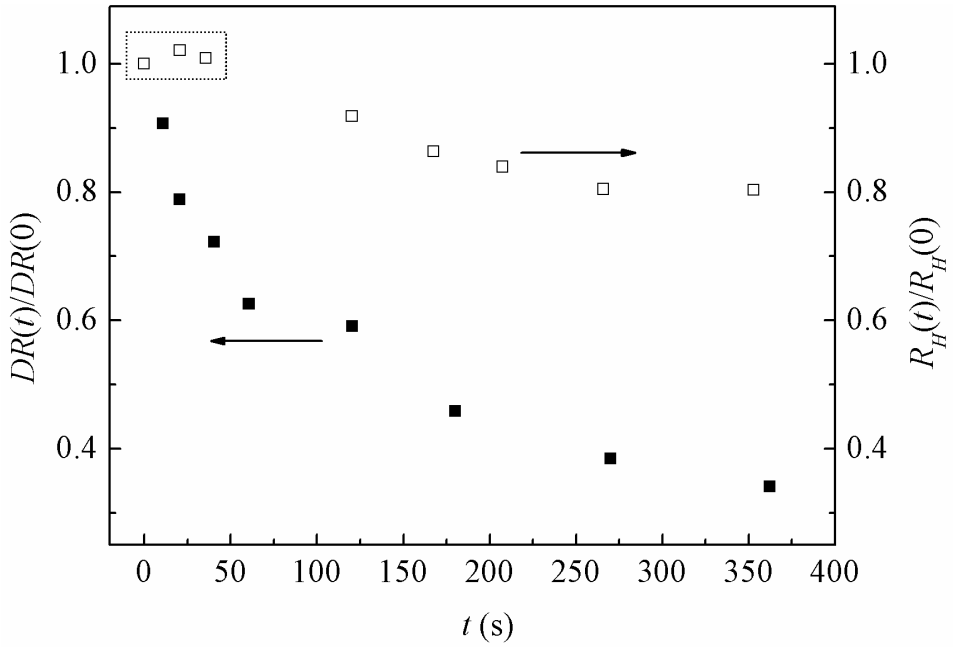

Figure 6-2 The relationship between drag reduction and radius of hydrodynamics from Van Dam & Wegdam's paper (1993)

6.2 Aggregate Degradation in Drag-Reducing Flow

Aggregates of polymers commonly exist in polymer solutions, even in a dilute polymer solution (Peyser & Little, 1971). Shetty & Solomon (2009) used the DLS method to confirm that aggregate structures existed in drag-reducing flows. Their results indicate that the dilute polymer solution in the drag reducing flow is not as simple as it seems. Another evidence for the existence of the aggregate structure is from the activation energy of the degradation process. Dunlop & Cox (1977) showed that if the drag degradation was caused by the degradation of the free polymer, i.e., the chain scission process, the activation energy should range from 125 to 420 kJ/mol. While, if it was caused by the aggregate decomposition, the activation energy should range from 8 to 20 kJ/mol. A previous study (Zhang et al., 2018) showed that the activation energy of degradation of turbulent water flow with PEO is approximately 40 kJ/mol, which is

between the lower and higher ranges mentioned above. This result indicates that aggregates exist in the dilute polymer solution and the degradation of drag reduction is caused by both chain scission and aggregate decomposition.

Formation of aggregate structures is due to the hydrophobic/hydrophilic effect between the polymer and the solvent (Polverari & van de Ven, 1996). The common drag-reducing polymer PEO in water are used as an example. PEO has two types of groups, CH_2, a hydrophobic group and O, OH, hydrophilic groups. PEO is a water-soluble polymer, but the hydrophobic effect still exists due to the CH_2 group. In a dilute PEO solution, the CH_2 structures from one polymer chain may attract the CH_2 structures from another chain; meanwhile, OH and O have similar behaviours. Thus, the aggregate forms in the dilute solution.

The aggregate structure is shown in Figure 6-3 as suggested by Hammouda et al. (2004). Note that this structure is not scaled to real proportion but only an illustrative schematic. Each colour represents one polymer chain with a given molecular weight. The dashed line between O and OH represents the hydrogen bond, and the dashed line between CH_2 and CH_2 represents the hydrophobic effect. Based on the structure of aggregate, two possible polymer degradation mechanisms exist: (1) the decomposition of interaction between polymers, i.e., only the hydrogen bond and hydrophobic effect are destroyed but the polymer chain remains integral, as shown in Figure 6-3a; or (2) the decomposition of polymer chain, i.e., the chain scission happens at the polymer chain of aggregate, as shown in Figure 6-3b.

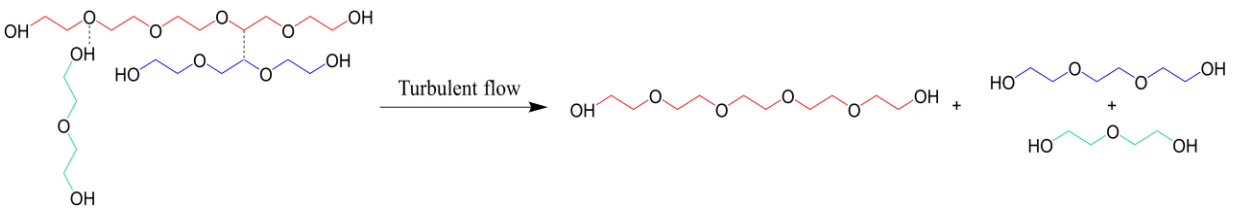

(a)

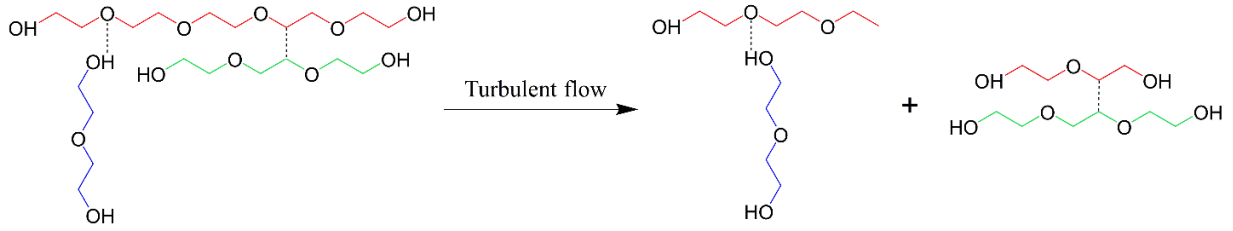

(b)

Figure 6-3 Possible aggregate degradation mechanism in drag-reducing flow

Additional experimental studies were conducted to investigate the behaviors of polymer aggregates during turbulent flow drag reduction. The details of the experimental setup and materials can be found in my previous paper (Zhang et al., 2018). Figure 6-4 shows two types of degradation tests of PEO in water: (1) continuous degradation, where polymers experience 6-min degradation continuously; (2) the batch degradation, where polymers experience a 2-min degradation, followed by a 10 min break (without flow movement); then more cycles of the degradation are repeated until the polymers experience a 6-min degradation test in total.

The results show that the two types of degradation tests give almost the same results (with only 2% offset due to the minor difference of the initial torque at the beginning of the tests). These results indicate that a standing time does not help the polymer aggregate recovery to regain the drag reducing ability. This phenomenon happens because the behavior of polymer aggregates in drag-reducing flows follows the mechanism shown in Figure 6-3b. If the

mechanism was the one shown in Figure 6-3a, the standing time should help the polymer aggregates to reform (Polverari & van de Ven, 1996; Duval & Gross, 2013) and their drag reduction ability should recover. However, it does not happen. Thus, the mechanism in Figure 6-3b is the correct one to describe the degradation of aggregates in the drag-reducing flow. Here it is not intended to show that the interaction between two polymer chains cannot be interrupted by the turbulent flow. In fact, this interaction can be interrupted but can reform due to the recovery after degradation.

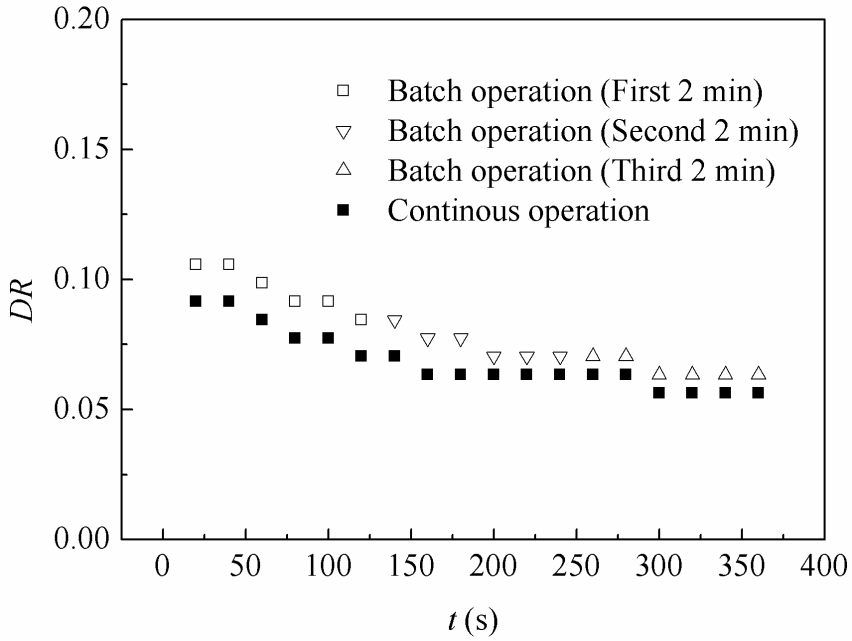

Figure 6-4 Continuous and batch degradation test of PEO (molecular weight 4 $\times 10^6$ g/mol, concentration 20 ppm, temperature 20 °C and shear rate 6500 s^{-1})

Note that the polymer degradation behavior in the drag reducing flow is different than the behavior of surfactants. For surfactants, the recombination of surfactant micelle can recover the drag-reducing ability of surfactants. The high shear rate can only cause the degradation of the

micelle, not the surfactant itself, so the drag-reducing ability can recover after degradation (Liu et al., 2018).

6.3 Molecular Weight Distribution Shift in Drag-Reducing Flow

The other issue in the degradation of drag reduction is the molecular weight distribution after the degradation. The polymer chain is cut into small pieces after experiencing a high shear rate in the turbulent flow. So, the molecular weight should decrease, but it is still not clear if the molecular weight distribution after degradation is broader or narrower or remains the same. In dilute polymer solutions, the degradation of polymers is a random process, but it is possible that the chain scission happens in the middle of the chain, which is supported by Bueche (1960) from theory, and Horn & Merrill (1984) in experiments with Polystyrene and Choi et al. (2002) & Lim et al. (2005) in experiments with DNA. Buchholz et al. (2004) further proved that polymers with a higher molecular weight are more likely to degrade than that with a lower molecular weight.

One example is used to manifest the shift of molecular weight distribution after the degradation in a drag-reducing flow. Assume that one drag-reducing polymer has an average molecular weight of M, with a distribution profile, $M/2$, M and $2M$, shown in Figure 6-5. At a given time in the drag-reducing flow, polymers with a molecular weight M may experience the chain scission once, and the molecular weight becomes $M/2$; polymers with a molecular weight $2M$ may experience the chain scission twice due to the higher molecular weight, and their molecular weight also becomes $M/2$; polymers with a molecular weight $M/2$ may not experience the chain scission at all due to its low molecular weight, and their molecular weight remains the same, $M/2$. After this degradation process, the average molecular weight becomes $M/2$, therefore the molecular weight distribution becomes much narrower. Some other studies showed different results. For example, Liberatore et al. (2004) reported that the average molecular weight and

distribution remained the same after degradation of drag reduction in the flow. This is due to the high polymer concentration (approximately 1000 ppm in these studies) that is much higher than the dilute solution mentioned above. In high concentration (semi-dilute) solutions, aggregates are more likely to form and affect the drag reduction, so less free polymers are involved in the drag reduction and degradation. In this case, the free polymers could remain integral. Before the SEC test, the aggregates are filtered, and the integral polymers after the degradation are injected into the SEC, so the measured molecular weight and its profile remain the same as in the original condition.

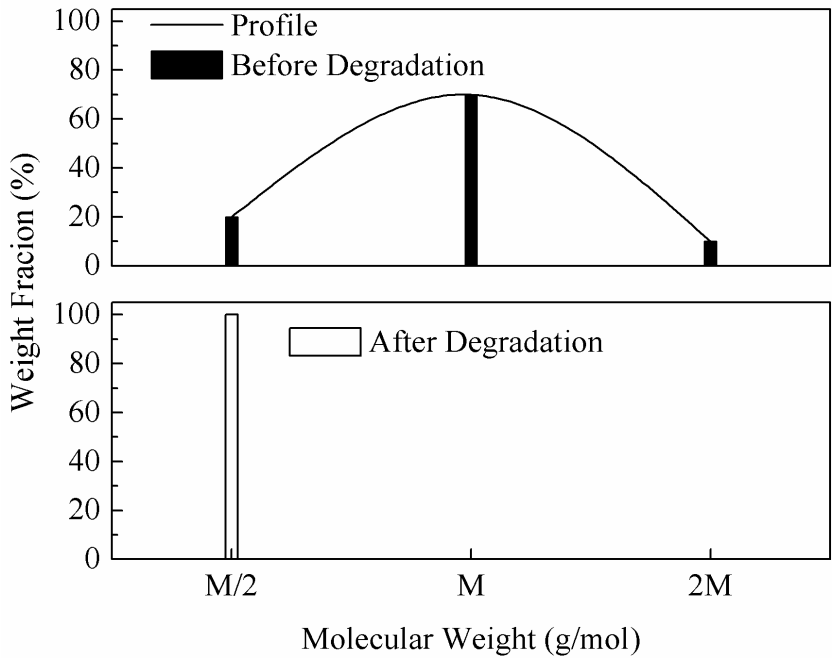

Figure 6-5 The molecular weight distribution before and after degradation

Besides what is shown above, another drag reduction test can validate our view of the distribution shift, as shown in Figure 6-6. It shows that the profile indeed becomes narrower after more passes (longer degradation time).

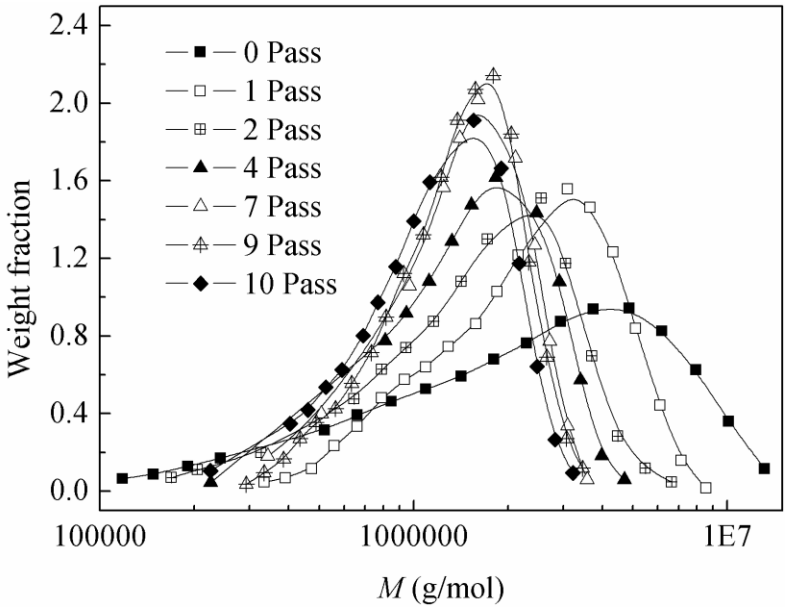

Figure 6-6 Molecular weight distribution of degraded polymer in drag reduction (data from Vanapalli et al. (2005))

6.4 Summary

In Chapter 6, the degradation of flow drag reduction and the degradation of the drag-reducing polymers are investigated. The critical assumption of Brostow that the rate of drag reduction degradation is identical to the rate of molecular weight decrease of the drag-reducing polymer is shown to be not correct in rotational flows and pipe flows. This is mainly due to the existence of polymer aggregates. Experimental results show that the molecular weight of the degraded polymer in the dilute solution becomes lower and the molecular weight distribution becomes narrower. Finally, the degradation mechanism of polymer aggregates in the drag-reducing flow is proposed: the turbulent flow causes the chain scission of the aggregate and the degraded aggregate losses its drag-reducing ability.

Chapter 7 Mechanism of Drag Reduction and Degradation from Chemical Thermodynamics and Kinetics

In previous chapters, it is seen that drag reduction is related to the polymer relaxation process and degradation is related to the chain scission. In this chapter, these two major conclusions are combined, and a new explanation of drag reduction by polymers from the chemical thermodynamics and kinetics is proposed. The main content of this chapter has been published as a journal paper (Zhang, X., Duan, X., & Muzychka, Y. (2020). "Drag reduction by linear flexible polymers and its degradation in turbulent flow: a phenomenological explanation from chemical thermodynamics and kinetics". Physics of Fluids, 32(1), 013101). I am the first author of this paper. I analyzed the data, prepared the draft paper, and made the revisions. Prof. Duan and Prof. Muzychka as the second and third authors provided their suggestions on the analysis and revisions of this paper.

7.1 Explanation of Drag Reduction by Polymers

The polymers' behavior in the flow can be treated as a conformational phase change process between the coiled state and the stretched state (Fidalgo et al., 2017), further regarded as a chemical reaction (Ferguson et al., 1987), so the chemical thermodynamics and kinetics are used to analyze this process.

Figure 7-1 shows the schematic of this transition, i.e., polymer configuration changes from the coiled state to the stretched state in a dilute solution of certain concentration in flow under a constant temperature. Here, this transition can be treated as a reversible process within a given time, which is supported by experimental results (Fidalgo et al., 2017) shown in Figure 7-1. In this experiment, a special polymer, i.e., DNA, is used. It has a uniform molecular weight distribution. In Figure 7-1 x/L is the ratio of the real-time length of DNA to the maximum length

measured by a fluorescence microscope. Figure 7-1 shows two processes, i.e., relaxation (from the stretched state to coiled state) and stretching (from the coiled state to stretched state, also regarded as elongation). The time-dependent length can be approximated by a cosine function, as shown by the solid curve in Figure 7-1. Besides, the order of magnitude of the length ratio of stretched-state polymer over the coiled-state polymer is 10, validated by Virk (1976). This periodic function indicates that our view of the polymer configuration is correct: a transition between the coiled and stretched states exists and this transition is reversible within a limited time. The limited time is emphasized since degradation happens – to be discussed later.

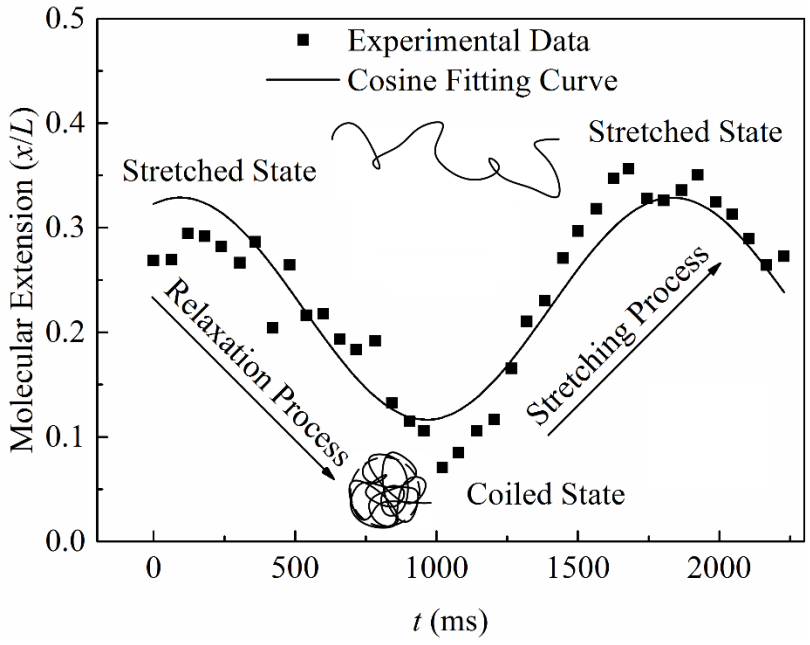

Figure 7-1 Polymer transition between the coiled state and the stretched state (data from Fidalgo et al. (2017))

Next, the equilibrium constant *K* of this reversible transition process is defined below. In traditional chemical thermodynamics, the reactant and product concentrations at the equilibrium

state are involved in the equilibrium constant. In this case, the exact number of polymers in the coiled and stretched states should be employed, however, current measurement technology cannot achieve that. To propose a phenomenological explanation, the microscopic feature of the polymers in the coiled and stretched state are used, ΔP_S (pressure drop when polymers are in the coiled state, equal to the one of pure solvent, which will be explained below) and ΔP_P (pressure drop when polymers are in the stretched state) under the same flow rate. Here the viscosity difference of pure solvent and polymer solutions is not considered since polymers at ppm level have negligible influence on the viscosity (Zhang et al., 2019).

$$K = \frac{\Delta P_P}{\Delta P_S} \tag{7-1}$$

Usually, the pressure drops with and without polymers are compared to identify if the drag reduction happens. Slightly different from this approach, the pressure drops with polymers in coiled states and the one with polymers in stretched states are compared. Here it is assumed that the pressure drop in the pure solvent without polymers is equal to the pressure drop when the polymer is in the coiled state, and further, the pressure drop when polymers in the coiled state and stretched state are compared to determine if the drag reduction occurs. This assumption is based on the fact that the polymer in the coiled state can be regarded as a small particle (Virk, 1976) and it has no drag reduction ability in a low concentration: many independent works found that the minimum concentration of micro or nano-particles to reduce the flow friction is several hundred ppm (Pirih & Swanson, 1972; Pouranfard et al., 2014; Radin et al., 1975), much higher than the polymer concentration of the dilute solution, usually less than 100 ppm. Thus, it is assumed that polymers in the coiled state in the dilute solution cannot induce drag reduction.

The Gibbs free energy of this reaction ΔG is shown in Eq. 7-2. ΔG_S and ΔG_P represent the Gibbs free energy of the polymers in the coiled state and stretched state in the turbulent flow.

The physical meaning of these terms will be explained below. R is the ideal gas constant, 8.314 $J \cdot mol^{-1} \cdot K^{-1}$; T is the Kelvin temperature (K). When the drag reduction happens, ΔP_S is larger than ΔP_P and the equilibrium constant (K) is less than 1.

$$\Delta G = \Delta G_P - \Delta G_S = -RT \ln K \tag{7-2}$$

From Eq. 7-2, it can be seen that the ΔG of this reaction is greater than 0 when the drag reduction happens, so this reaction (drag reduction) is non-spontaneous at a given concentration. In drag reduction by polymers, an onset point exists at a given concentration (Virk, 1975). The drag reduction phenomenon only happens in turbulent flow (based on the Reynolds number, 4000 for pipe flow) even though there are some counterexamples (Choueiri et al., 2018). At a given concentration, only a high enough velocity that can induce the stretching of the polymer chain can cause drag reduction. This onset point explains the physical meaning of the critical energy in Camail et al.'s work (2009).

The Gibbs free energy of polymers in the stretched state is higher than that of the polymer in the coiled state from Eq. 7-2. This higher potential means that the stretched polymer has a higher chemical potential thermodynamically, so the stretched polymer has higher reactive activity. This higher activity causes the stretched polymers to interact with turbulent structures, and the energy in the vortex is reused in the stream-wise direction (laminarization). Finally, drag reduction happens, and the purely viscous turbulent flow (when no polymers are added) is laminarized and becomes elongational turbulent flow (Zhang et al., 2018 & 2019). Here the physical meaning of the Gibbs energy of polymer is clear: it represents the energy stored in the polymer. A longer polymer chain means a high Gibbs energy which can interact with the turbulent flow structures, and this interaction leads to a better drag reduction. This explains why a higher molecular weight has a better effect on drag reduction (Zhang et al., 2019).

Turbulent flow provides an unstable environment for polymers in the coiled state thermodynamically so that free polymers can be stretched, and the drag reduction happens in this elongational turbulent flow. However, this elongational turbulent flow also causes the polymers to become unstable kinetically. Because the Gibbs free energy of the stretched polymer is higher than the one in the coiled state, it has more potential to interact with the turbulent structure. In turn, the turbulent structure also interacts with the free polymer, which means that the polymers experience the chain scission, also known as the degradation (Zhang et al., 2018). Recent work showed that polymer degradation truly happened in both rotational and pipe flows (Zhang et al., 2019). Molecular weight measured by size exclusion chromatograph decreased with time, indicating that the chain scission happens.

The free polymer behavior in drag reduction are discussed. While in the polymer solution, another structure coexists with the free polymer - the polymer aggregate, which contains several polymer chains. The behavior of polymer aggregates is similar to free polymers, which can interact with turbulent structure (Kalashnikov & Kudin, 1973) and be degraded by the chain scission, detailed information provided in ref. by Zhang et al. (2019).

In summary, an explanation of the drag reduction by polymers is proposed in Figure 7-2, and this explanation is divided into three stages.

(1) Dissolution. The solid polymer is dissolved in the solvent, and two types of polymer form in the solution, free (single) polymers and the polymer aggregates.

(2) Unstable thermodynamics for polymer chain stretching. When the turbulent flow overcomes the onset point to stretch the free polymer and polymer aggregate, the drag reduction happens due to the unstable thermodynamic environment. This process is reversible.

(3) Unstable kinetics for polymer chain scission. After the free polymer and polymer aggregates experience long-time turbulent flow, the chain scission happens, and it causes the degradation of drag reduction due to the unstable kinetic environment. This process is irreversible.

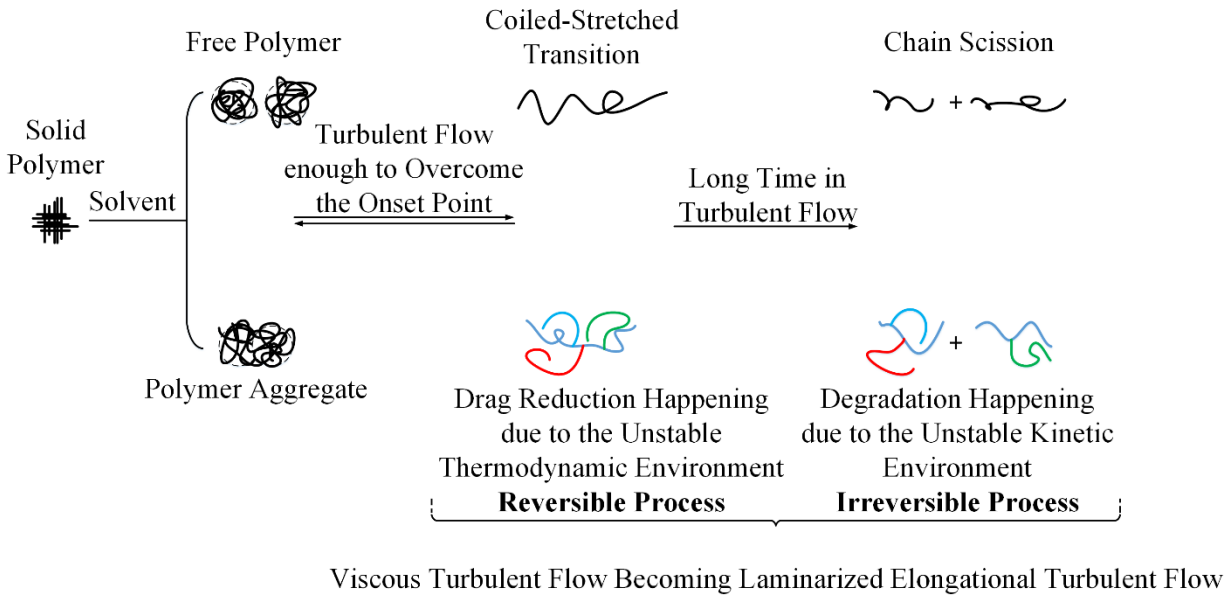

Figure 7-2 The proposed explanation of the drag reduction and degradation by linear flexible polymers

7.2 Discussions

One advantage of this theory is that it can explain why polymers cannot reduce the friction completely - friction not being equal to zero. Theoretically, if there were enough polymers in a turbulent flow and all the polymer elasticity potential was used to damp the turbulent structures, the flow friction could be eliminated entirely. But this never happens, which is due to our proposed explanation from the Gibbs free energy view. The Gibbs free energy describes the “maximum non-expansion reversible” work in a thermodynamic system under

constant temperature. Please note that maximum work only happens in a reversible process, not for an irreversible process. As discussed above, both reversible (chain stretch) and irreversible (chain scission) processes are involved in drag reduction by polymers. Thus, the whole drag reduction process is an irreversible process. Therefore, the friction in turbulent flow cannot be reduced to 0.

In the proposed explanation, the polymer chain has two features, coiled-stretched transition and chain scission, the former being a periodic process (reversible) and the latter one a non-periodic process (irreversible). Overall, it can be treated as a damped oscillation process (damped for chain scission and oscillation for coiled-stretched transition).

The statement above about damped oscillation is the behaviour of drag-reducing polymer in turbulent flow from the microscopic view, which is also reflected in the drag reduction from a macroscopic view. Bewersdorff & Petersmann (1987) and McComb & Rabie (1978) measured the drag reduction in different locations of a straight pipeline independently: in Figure 7-3a (from ref. by McComb & Rabie, 1978) and 7-3b (from ref. Bewersdorff & Petersmann, 1987), x is the length from the polymer injector to the measuring point, m. There is a "quasi-cyclic" (introduced by McComb & Rabie (1978) originally) drag reduction at different locations in Figure 3a: near the polymer injector, the drag reduction is small due to the entrance length effect; at far-enough locations from the polymer injector, the drag reduction oscillation happens. The quasi-cyclic behavior of drag reduction further supports our explanation from a molecular behaviour view: in the coiled-stretched transition, the length of the polymer in the coiled state is short, whose extreme condition can be regarded as a small particle and in general can be regarded as a polymer with a low molecular weight, so the drag reduction is low; the length of the polymer in the stretched state is long, which can be regarded as a polymer with a high molecular weight, so

the drag reduction is high. Besides, the transition of the polymer between the coiled-stretched states from the microscopic view is reflected in the drag reduction oscillation from the macroscopic view.

Does the oscillation truly happen or is it from the uncertainty of the measurement? McComb & Rabie (1978) repeated the same experiment, also shown in Figure 7-3a. The results show that data repeatability is good at least for the data in the marked box, which are measured at far-enough locations from the polymer solution injector. These two almost-identical experimental results with repeatable trends indicate that the oscillation truly happens. Bewersdorff & Petersmann's results (1987) in Figure 7-3b further validate the existence of this drag reduction oscillation.

However, it seems that there is no degradation of drag reduction in these results, which do not agree with the proposed explanation. This is due to the short distance from the polymer injector to the last measuring point: in Figure 7-3a, x/d is 200 approximately, which means that the distance of measured drag reduction data is very short in a lab-scale experiment. Besides, the Reynolds number in these experiments is 45,000, indicating a high velocity. Short distance and high velocity (short residence time) show that the polymer residence time in the drag-reducing pipe flow is small (in Figure 7-3b, the maximum residence time in the flow is 3.5 s) so that the degradation is not obvious. If the residence time is long enough, the degradation can be observed. Camail et al. (1998) tested the polyacrylamide in a rotational flow for more than three days and the results are shown in Figure 3c. In this test, a peak of the drag reduction appeared, which can be viewed as the drag reduction fluctuation (oscillation); after that the degradation of drag reduction started to happen until it almost disappeared in 2.5 days. More data from oil transportation pipeline support the ideas. The article by Strelnikova & Yushchenko (2019)

provides many drag reduction data from field tests with polymers in several oil & gas transpiration systems. Figure 7-3d shows one of those tests where the damped oscillation trend of drag reduction by polymers versus distance.

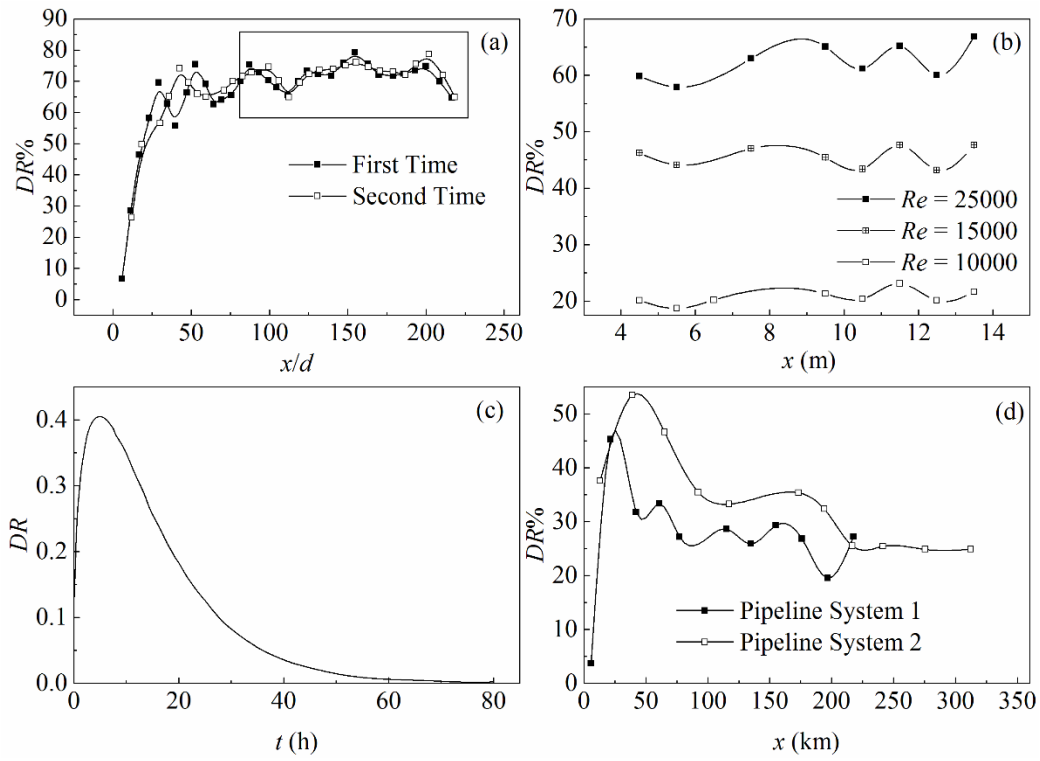

Figure 7-3 Drag reduction oscillation versus distance or time (a: data from McComb & Rabie (1978); b: data from Bewersdorff & Petersmann (1987); c: data from Camail et al. (1998); d: data from Strelnikova & Yushchenko (2019))

More data from ref. by Strelnikova & Yushchenko (2019) are shown in Figures 7-4a and 7-4c. The damped ossification feature of the drag reduction along the pipeline distance is similar to a wave. This inspires us to use the Fourier series, a method for wave study, to analyze the characteristic of the drag reduction versus distance. In Fourier series, a wave can be separated by a constant and the sum of several simple harmonic waves with different frequencies. Strictly

speaking, Fourier series is for the periodic function, not for non-periodic function such as the damped oscillation of the drag reduction. But this method is still extended here since it is helpful to explain the contribution of drag reduction by the molecular weight distribution.

The Fourier series is shown in Eq. 7-3.

$$DR(x) = a_0 + \sum_{k=1}^{n} a_k \cos(k\omega x) + b_k \sin(k\omega x) \tag{7-3}$$

In Eq. 7-3, a_k and b_k are fitting parameters. Eq. 7-3 can be converted to Eq. 7-4 by combining sine and cosine terms.

$$DR(x) = a_0 + \sum_{k=1}^{n} c_k \cos(k\omega x - \varphi_k) \tag{7-4}$$

c_k (amplitude) and φ_k (phase angle) are defined in Eq. 7-5 and Eq. 7-6. From Eq. 7-5, c_k (amplitude) represents the ability of drag reduction, a higher c_k means a higher drag reduction potential. From Figure 7-1, the polymer (with a given molecular weight) relaxation process can be correlated by a cosine fitting curve and this relaxation process induces the drag reduction as discussed above. So, in Eq. 7-4, each cosine term indicates one polymer with a specific molecular weight.

$$c_k = \sqrt{a_k^2 + b_k^2} \tag{7-5}$$

$$\varphi_k = \tan^{-1} \frac{b_k}{a_k} \tag{7-6}$$

As an example, n is set as 5 in this analysis, indicating that there are 5 types of polymer with different molecular weights. In Figure 7-4b and 7-4d, it is seen that the drag reduction can be predicted by Eq. 7-4, which verifies that our analysis method with the Fourier series is useful. The solid bar, shaded bar and hollow bar from Figure 7-4b and 7-4d represent the absolute value

of a_n/a_0, b_n/a_0 and c_n/a_0. The results show that neither a_n nor b_n is regular, but c_n is: c_n decreases with the increasing n, which means that the drag reduction ability is large when the frequency is low. This happens because most synthetic drag-reducing polymers have a wide molecular weight distribution (Zhang et al., 2019). This distribution contains high and low molecular weights. The polymer with a high molecular weight has a long relaxation time (a low frequency, also meaning a small n) and a large contribution to the drag reduction.

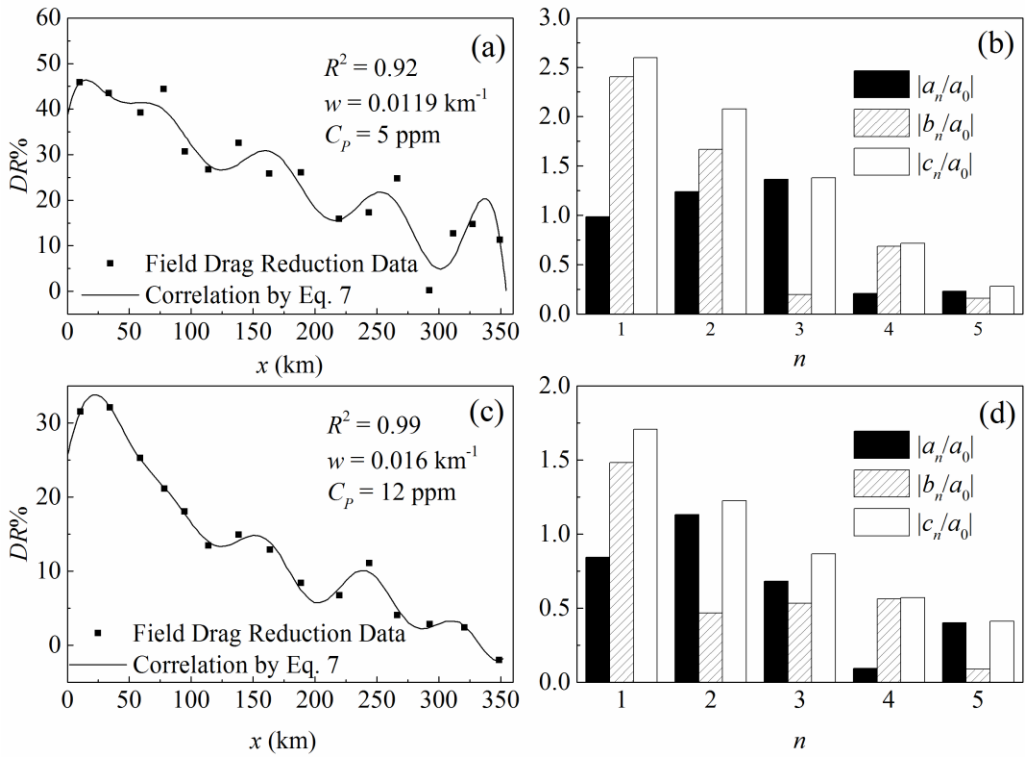

Figure 7-4 Field drag reduction data in an industrial pipeline and their results after Fourier series transformation (data from Ref. by Strelnikova & Yushchenko (2019))

7.3 Summary

In Chapter 7, a new mechanism of the drag reduction and degradation from chemical thermodynamics and kinetics is proposed: the drag reduction phenomenon by linear flexible

polymers can be explained as a non-spontaneous irreversible flow-induced conformational-phase-change process that incorporates both free polymers and aggregates. The entire non-equilibrium process is due to the chain scission of polymers. Drag reduction results from a macroscopic view and polymer behaviours from microscopic views further support this theory. A Fourier series expression indicates that the molecular weight distribution can affect drag reduction.

Chapter 8 Conclusions and Future Work

8.1 Conclusions

In this thesis, flow drag reduction by polymers and its degradation are investigated analytically and experimentally. The main contributions and conclusions from this work are summarized below.

A new model for drag reduction by polymers is proposed and validated by previous experimental data. Based on the FENE-P model, the semi-analytical solution assumes complete laminarization in the turbulent flow and can predict the upper limit of drag reduction in the pipe flow. This model is also used to explain the optimum concentration and velocity at the maximum drag reduction.

A semi-empirical correlation is developed for the estimation of the drag reduction in turbulent pipe flow in dilute polymer solutions, based on the Weissenberg number and polymer concentration. The relaxation time in Weissenberg number is based on Zimm's theory, so the problem that the relaxation time cannot be measured in a low concentration is solved. The definition of low concentration is also clarified. Experimental data from the flow loop are used to develop the correlation, and the relative error between experimental data and predicted values is within +/- 30%. This correlation is further validated by previous experimental data in laboratory and industrial flow systems.

A new theory is proposed that the degradation of polymer in a turbulent drag-reducing flow is a first-order chemical reaction based on the famous Brostow's assumption. According to this theory, a correlation with a modified Arrhenius equation is developed using data from a rotational flow to predict the drag reduction during the degradation with a ±15% relative error.

The Brostow's assumption is shown to be incorrect after it is checked with experimental data from in rotational flows and pipe flows. It is found that the main reason is that this assumption neglects polymer aggregate in the drag-reducing flows. The molecular weight of the polymer decreases, and the molecular weight distribution becomes narrower. An improved mechanism of aggregates in drag-reducing flow is proposed: the polymer aggregate degradation happens due to the chain scission, and degraded aggregates have no drag reduction ability.

Chemical thermodynamics and kinetics are introduced to develop a new theory of the drag reduction and degradation mechanism. Under this frame, the drag reduction phenomenon by linear flexible polymers can be explained as a flow-induced non-spontaneous irreversible (chain scission) conformational-phase-change process (relaxation), which involves both free polymers and aggregates. This is supported by drag reduction data from the macroscopic view and polymer performances from the microscopic tests.

8.2 Future Work

Based on the research work completed in this thesis, the following future research topics seem promising.

8.2.1 Environmental-Friendly Drag-Reducing Agents

The research of environmental-friendly drag-reducing agents was not new. Hoyt and Soli (1965) started to investigate this topic for the first time. There are several different environmental-friendly drag-reducing agents: polymers from algal (Gasljevic et al., 2008; Hoyt, 1970; Hoyt & Soli, 1965; Ramus et al., 1985), from bacteria (Abdulbari et al., 2018; Kenis, 1968; Sar & Rosenberg, 1989) and from plant (Soares et al., 2019). Polymers from these natural resources are considered as non-toxic to the environment which will not cause environmental problems. These agents could reduce the environmental problem introduced by the synthesis

polymers being used nowadays. More research efforts should be spent on the polymers from natural resources.

8.2.2 Anti-Degradation

The other issue about the synthetic drag-reducing polymer is degradation. Future work can target to improve the anti-degradation property of drag-reducing polymers. It is well known that most drag-reducing polymers cannot resist the chain scission by turbulent flow, thus degradation always happens. Several groups have already started to investigate how to synthesize better long chain flexible polymers to resist the chain scission (Camail et al., 2003; Gryte et al., 1980; Ma et al., 2003; Nifant'ev et al., 2018). In these papers, authors show the comparison between the commercially available drag-reducing polymers and synthetic polymers, indicating that many emerging synthetic polymers have better anti-degradation ability. However, few synthetic drag-reducing polymers with degradation resistance ability are available commercially, so more future work in this area is desired.

8.2.3 Oil-Soluble Polymers and Multiphase Flow

Currently, most research on drag reduction by polymers was performed in single-phase water flow, therefore, the research results only have limited industrial applications such as in the oil-gas industry. Thus, more oil-soluble polymers should be involved in the research. Besides, drag reduction in oil flow is still a single-phase flow research, which is not very helpful in the oil and gas industry where multiphase flows are often seen. There are many studies of drag reduction in single-phase flow, with more than 1000 journal papers. While the number of drag reduction studies on multiphase flow is much smaller, with only 70 journal papers published until this thesis is finished. Future researches should focus on the drag reduction by polymers in multiphase flows - a more promising area.

8.2.4 Synergy of Drag Reduction by Polymers and Surface Modification

The synergy effect of drag reduction by polymers and special surfaces should be further studied. Until now, there are limited studies that combine these two strategies of flow drag reduction. If these two methods are combined, the drag reduction could be higher than the one by each method. But the synergy effect is not clear. Mizunuma et al. (1999) mentioned that the V-shape riblet could increase the drag so this surface itself was not a drag-reducing surface, but when drag-reducing polymers were added in the turbulent flow, the drag reduction occurred. Similar observations were reported by Koury & Virk (1995) and Huang & Wei (2017). In another work by Huang et al. (2016), the combined drag reduction by grooved structure and surfactant was shown to be greater than the drag reduction by each method, which is also supported by Abdulbari et al. (2018) and Christodoulou et al. (1991). Anderson et al. (1993) suggested that drag-reducing polymers did not affect the drag reduction induced by a specific-designed surface, meaning that the surface had the drag reduction ability and polymers had no effect on the drag reduction by the surface. In this situation, more work should be completed to investigate the combination of these two methods and make it clear that which combination of surface (with a particular structure) and polymer can lead to a positive synergy effect - a better drag reduction performance.

As mentioned earlier, drag-reducing polymers can also reduce the corrosion to the pipeline inner surface. If the drag reduction by polymers and a certain anti-corrosion surface with drag reduction ability can be combined, the total friction will be reduced significantly and the pipeline can be maintained for a long time due to the anti-corrosion effects by polymers and surfaces.

Reference

Abdulbari, H. A., Ling, F. W., Hassan, Z., & Thin, H. J. (2018). Experimental investigations on biopolymer in enhancing the liquid flow in microchannel. Advances in Polymer Technology.

Abdulbari, H. A., Salleh, M. A. M., Rashed, M. K., & Ismail, M. H. S. (2018). Passive, active, and interactive drag-reduction technique to reduce friction and enhance the mixing intensity in rotating disk apparatus. Chemical Engineering Communications, 205(12), 1623-1640.

Abubakar, A., Al-Hashmi, A. R., Al-Wahaibi, T., Al-Wahaibi, Y., Al-Ajmi, A., & Eshrati, M. (2014). Parameters of drag reducing polymers and drag reduction performance in single-phase water flow. Advances in Mechanical Engineering, 6, 202073.

Aguilar, G., Gasljevic, K., & Matthys, E. F. (2001). Asymptotes of maximum friction and heat transfer reductions for drag-reducing surfactant solutions. International journal of heat and mass transfer, 44(15), 2835-2843.

Amarouchene, Y., & Kellay, H. (2002). Polymers in 2D turbulence: suppression of large scale fluctuations. Physical review letters, 89(10), 104502.

Anderson, G. F., & Wu, Y. K. (1971). Drag reduction by use of MHD boundary-layer control. Journal of Hydronautics, 5(4), 150-152.

Anderson, G. W., Rohr, J. J., & Stanley, S. D. (1993). The combined drag effects of riblets and polymers in pipe flow. Journal of fluids engineering, 115(2), 213-221.

Andrade, R. M., Pereira, A. S., & Soares, E. J. (2014). Drag increase at the very start of drag reducing flows in a rotating cylindrical double gap device. Journal of Non-Newtonian Fluid Mechanics, 212, 73-79.

Andrade, R. M., Pereira, A. S., & Soares, E. J. (2016). Drag reduction in synthetic seawater by flexible and rigid polymer addition into a rotating cylindrical double gap device. Journal of Fluids Engineering, 138(2), 021101.

Bakajin, O. B., Duke, T. A. J., Chou, C. F., Chan, S. S., Austin, R. H., & Cox, E. C. (1998). Electrohydrodynamic stretching of DNA in confined environments. Physical review letters, 80(12), 2737-2740.

Barenblatt, G. I. (2008). A mathematical model of turbulent drag reduction by high-molecular-weight polymeric additives in a shear flow. Physics of Fluids, 20(9), 091702.

Benzi, R., & Ching, E. S. (2018). Polymers in fluid flows. Annual Review of Condensed Matter Physics, 9, 163-181.

Bewersdorff, H. W., & Petersmann, A. (1987). Drag reduction in artificially roughened pipes. Chemical Engineering Communications, 60(1-6), 293-309.

Bewersdorff, H. W., Gyr, A., Hoyer, K., & Tsinober, A. (1993). An investigation of possible mechanisms of heterogeneous drag reduction in pipe and channel flows. Rheologica acta, 32(2), 140-149.

Bizhani, M., Corredor, F. E. R., & Kuru, E. (2015). An Experimental Study of Turbulent Non-Newtonian Fluid Flow in Concentric Annuli Using Particle Image Velocimetry Technique. Flow, Turbulence and Combustion, 94(3), 527-554.

Bizotto, V. C., & Sabadini, E. (2008). Poly (ethylene oxide)× polyacrylamide. Which one is more efficient to promote drag reduction in aqueous solution and less degradable?. Journal of applied polymer science, 110(3), 1844-1850.

Bogue, D. C., & Metzner, A. B. (1963). Velocity profiles in turbulent pipe flow. Newtonian and non-Newtonian fluids. Industrial & Engineering Chemistry Fundamentals, 2(2), 143-149.

Brautlecht, C. A., & Sethi, J. R. (1933). Flow of paper pulps in pipe lines. Industrial & Engineering Chemistry, 25(3), 283-288.

Broseta, D., Leibler, L., Lapp, A., & Strazielle, C. (1986). Universal properties of semi-dilute polymer solutions: a comparison between experiments and theory. EPL (Europhysics Letters), 2(9), 733-737.

Brostow, W. (1983). Drag reduction and mechanical degradation in polymer solutions in flow. Polymer, 24(5), 631-638.

Brostow, W., Ertepinar, H., & Singh, R. P. (1990). Flow of dilute polymer solutions: chain conformations and degradation of drag reducers. Macromolecules, 23(24), 5109-5118.

Brostow, W., Lobland, H. E. H., Reddy, T., Singh, R. P., & White, L. (2007). Lowering mechanical degradation of drag reducers in turbulent flow. Journal of materials research, 22(1), 56-60.

Brostow, W., Majumdar, S., & Singh, R. P. (1999). Drag reduction and solvation in polymer solutions. Macromolecular rapid communications, 20(3), 144-147.

Buchholz, B. A., Zahn, J. M., Kenward, M., Slater, G. W., & Barron, A. E. (2004). Flow-induced chain scission as a physical route to narrowly distributed, high molar mass polymers. Polymer, 45(4), 1223-1234.

Bueche, F. (1960). Mechanical degradation of high polymers. Journal of Applied Polymer Science, 4(10), 101-106.

Burger, E. D., Chorn, L. G., & Perkins, T. K. (1980). Studies of drag reduction conducted over a broad range of pipeline conditions when flowing Prudhoe Bay crude oil. Journal of Rheology, 24(5), 603-626.

Burger, E. D., Munk, W. R., & Wahl, H. A. (1982). Flow increase in the Trans Alaska Pipeline through use of a polymeric drag-reducing additive. Journal of Petroleum Technology, 34(02), 377-386.

Burshtein, N., Zografos, K., Shen, A. Q., Poole, R. J., & Haward, S. J. (2017). Inertioelastic flow instability at a stagnation point. Physical Review X, 7(4), 041039.

Camail, M., Margaillan, A., & Martin, I. (2009). Copolymers of N-alkyl- and N-arylalkylacrylamides with acrylamide: influence of hydrophobic structure on associative properties. Part I: viscometric behaviour in dilute solution and drag reduction performance. Polymer International, 58(2), 149-154.

Camail, M., Margaillan, A., Maesano, J. C., Thuret, S., & Vernet, J. L. (1998). Synthesis and structural study of new copolymers, based on acrylamide and N-acryloyl acids, with persistent drag reduction activity. Polymer, 39(14), 3187-3192.

Camail, M., Margaillan, A., Thuret, S., & Vernet, J. L. (1998). Syntheses of acrylamido acids and copolymerization with acrylamide. Influence of the polymer structure on drag reduction properties. European polymer journal, 34(11), 1683-1688.

Campo-Deano, L., & Clasen, C. (2010). The slow retraction method (SRM) for the determination of ultra-short relaxation times in capillary breakup extensional rheometry experiments. Journal of Non-Newtonian Fluid Mechanics, 165(23-24), 1688-1699.

Cao, D., Li, C., Li, H., & Yang, F. (2018). Effect of dispersing time on the prediction equation of drag reduction rate and its application in the short distance oil pipeline. Petroleum Science and Technology, 36(16), 1312-1318.

Carradine, W. R., Grabois, R. N., Hanna, G. J., & Pace, G. F. (1983). High-performance flow improver for products lines. Oil & Gas Journal, 81(32), 92-96.

Chahine, G. L., Frederick, G. F., & Bateman, R. D. (1993). Propeller tip vortex cavitation suppression using selective polymer injection. Journal of fluids engineering, 115(3), 497-503.

Choi, H. J., Kim, C. A., & Jhon, M. S. (1999). Universal drag reduction characteristics of polyisobutylene in a rotating disk apparatus. Polymer, 40(16), 4527-4530.

Choi, H. J., Kim, C. A., Sohn, J. I., & Jhon, M. S. (2000). An exponential decay function for polymer degradation in turbulent drag reduction. Polymer degradation and stability, 69(3), 341-346.

Choi, H. J., Lim, S. T., Lai, P. Y., & Chan, C. K. (2002). Turbulent drag reduction and degradation of DNA. Physical Review Letters, 89(8), 088302.

Choueiri, G. H., Lopez, J. M., & Hof, B. (2018). Exceeding the asymptotic limit of polymer drag reduction. Physical review letters, 120(12), 124501.

Christodoulou, C., Liu, K. N., & Joseph, D. D. (1991). Combined effects of riblets and polymers on drag reduction in pipes. Physics of Fluids A: Fluid Dynamics, 3(5), 995-996.

Coleman, P. B., Ottenbreit, B. T., & Polimeni, P. I. (1987). Effects of a drag-reducing polyelectrolyte of microscopic linear dimension (Separan AP-273) on rat hemodynamics. Circulation research, 61(6), 787-796.

Cotton, J. P., Nierlich, M., Boue, F., Daoud, M., Farnoux, B., Jannink, G., Duplessix. R., & Picot, C. (1976). Experimental determination of the temperature–concentration diagram of flexible polymer solutions by neutron scattering. The Journal of Chemical Physics, 65(3), 1101-1108.

Dai, X., Li, L., Yin, S., Zhang, G., & Ge, J. (2018). The drag reduction and degradation characteristics of poly α olefin in diesel via rotating disk apparatus. Petroleum Science and Technology, 36(13), 981-986.

Daoudi, M. S., & Dajani, M. S. (1984). The 1967 oil embargo revisited. Journal of Palestine Studies, 13(2), 65-90.

Darby, R., & Chang, H. F. D. (1984). Generalized correlation for friction loss in drag reducing polymer solutions. AIChE journal, 30(2), 274-280.

Darby, R., & Pivsa-Art, S. (1991). An improved correlation for turbulent drag reduction in dilute polymer solutions. The Canadian Journal of Chemical Engineering, 69(6), 1395-1400.

De Gennes, P. G. (1986). Towards a scaling theory of drag reduction. Physica A: Statistical Mechanics and its Applications, 140(1-2), 9-25.

De Gennes, P. G. (1992). Soft matter. Reviews of modern physics, 64(3), 645-648.

De Gennes, P. G. (1997). Molecular individualism. Science, 276(5321), 1999-2000.

Dealy J. M., (2010) Weissenberg and Deborah numbers—Their definition and use. The British Society of Rheology-Rheology Bulletin, 79(2), 14-18.

Den Toonder, J. M. J., Hulsen, M. A., Kuiken, G. D. C., & Nieuwstadt, F. T. M. (1997). Drag reduction by polymer additives in a turbulent pipe flow: numerical and laboratory experiments. Journal of Fluid Mechanics, 337, 193-231.

Deshmukh, S. R., Sudhakar, K., & Singh, R. P. (1991). Drag-reduction efficiency, shear stability, and biodegradation resistance of carboxymethyl cellulose-based and starch-based graft copolymers. Journal of applied polymer science, 43(6), 1091-1101.

Devanand, K., & Selser, J. C. (1990). Polyethylene oxide does not necessarily aggregate in water. Nature, 343(6260), 739-741.

Dodge, D. W., & Metzner, A. B. (1959). Turbulent flow of non-Newtonian systems. AIChE Journal, 5(2), 189-204.

Dosunmu, I. T., & Shah, S. N. (2014). Turbulent flow behavior of surfactant solutions in straight pipes. Journal of Petroleum Science and Engineering, 124, 323-330.

Dunlop, E. H., & Cox, L. R. (1977). Influence of molecular aggregates on drag reduction. The Physics of Fluids, 20(10), S203-S213.

Duval, M., & Gross, E. (2013). Degradation of poly (ethylene oxide) in aqueous solutions by ultrasonic waves. Macromolecules, 46(12), 4972-4977.

Ebagninin, K. W., Benchabane, A., & Bekkour, K. (2009). Rheological characterization of poly (ethylene oxide) solutions of different molecular weights. Journal of colloid and interface science, 336(1), 360-367.

Edomwonyi-Otu, L. C., & Adelakun, D. O. (2018). Effect of heavy molecular weight polymer on quality of drinking water. Materials Today Communications, 15, 337-343.

Eskin, D. (2017). Modeling an effect of pipe diameter on turbulent drag reduction. Chemical Engineering Science, 162, 66-68.

Fabula, A. G. (1971). Fire-fighting benefits of polymeric friction reduction. Journal of Basic Engineering, 93(3), 453-455.

Faruqui, F. I., Otten, M. D., & Polimeni, P. I. (1987). Protection against atherogenesis with the polymer drag-reducing agent Separan AP-30. Circulation, 75(3), 627-635.

Ferguson, J., Hudson, N. E., Warren, B. C. H., & Tomatarian, A. (1987). Phase changes during elongational flow of polymer solutions. Nature, 325(6101), 234-236.

Fidalgo, J., Zografos, K., Casanellas, L., Lindner, A., & Oliveira, M. S. (2017). Customised bifurcating networks for mapping polymer dynamics in shear flows. Biomicrofluidics, 11(6), 064106.

Figueredo, R. C. R., & Sabadini, E. (2003). Firefighting foam stability: the effect of the drag reducer poly (ethylene) oxide. Colloids and Surfaces A: Physicochemical and Engineering Aspects, 215(1), 77-86.

Forrest, F., & Grierson, G. A. (1931). Friction losses in cast iron pipe carrying paper stock. Paper Trade Journal, 92(22), 39-41.

Frings, B. (1988). Heterogeneous drag reduction in turbulent pipe flows using various injection techniques. Rheologica acta, 27(1), 92-110.

Gallego, F., & Shah, S. N. (2009). Friction pressure correlations for turbulent flow of drag reducing polymer solutions in straight and coiled tubing. Journal of Petroleum Science and Engineering, 65(3-4), 147-161.

Gasljevic, K., Aguilar, G., & Matthys, E. F. (1999). An improved diameter scaling correlation for turbulent flow of drag-reducing polymer solutions. Journal of non-Newtonian Fluid Mechanics, 84(2-3), 131-148.

Gasljevic, K., Hall, K., Chapman, D., & Matthys, E. F. (2008). Drag-reducing polysaccharides from marine microalgae: species productivity and drag reduction effectiveness. Journal of applied phycology, 20(3), 299-310.

Ghajar, A. J., & Azar, M. Y. (1988). Empirical correlations for friction factor in drag-reducing turbulent pipe flows. International communications in heat and mass transfer, 15(6), 705-718.

Gordon, R. J. (1970). On the explanation and correlation of turbulent drag reduction in dilute macromolecular solutions. Journal of Applied Polymer Science, 14(8), 2097-2105.

Goren, Y., & Norbury, J. F. (1967). Turbulent flow of dilute aqueous polymer solutions. Journal of Basic Engineering, 89(4), 814-822.

Graessley, W. W. (1980). Polymer chain dimensions and the dependence of viscoelastic properties on concentration, molecular weight and solvent power. Polymer, 21(3), 258-262.

Gryte, C. C., Koroneos, C., Agarwal, A., & Hochberg, A. (1980). Drag reduction characteristics of graft copolymers prepared by the gamma irradiation of poly (oxyethylene) in the presence of acrylic acid. Polymer Engineering & Science, 20(7), 478-484.

Guersoni, V. C. B., Bannwart, A. C., Destefani, T., & Sabadini, E. (2015). Comparative study of drag reducers for light hydrocarbon flow. Petroleum Science and Technology, 33(8), 943-951.

Hammouda, B., Ho, D. L., & Kline, S. (2004). Insight into clustering in poly (ethylene oxide) solutions. Macromolecules, 37(18), 6932-6937.

Hassid, S. (1979). A Reynolds Stress Model for Flows with Drag Reduction. Journal of Fluids Engineering, 101(2), 159-165.

Hassid, S., & Poreh, M. (1975). A turbulent energy model for flows with drag reduction. Journal of Fluids Engineering, 97(2), 234-241.

Hassid, S., & Poreh, M. (1978). A turbulent energy dissipation model for flows with drag reduction. Journal of Fluids Engineering, 100(1), 107-112.

Hawkridge, H. R. J., & Gadd, G. E. (1971). Investigation of drag reduction by certain algae. Nature, 230(5291), 253-255.

Holtmyer, M. D., & Chatterji, J. (1980). Study of oil soluble polymers as drag reducers. Polymer Engineering & Science, 20(7), 473-477.

Hong, C. H., Choi, H. J., & Kim, J. H. (2008). Rotating disk apparatus for polymer-induced turbulent drag reduction. Journal of mechanical science and technology, 22(10), 1908-1913.

Hong, C. H., Jang, C. H., & Choi, H. J. (2015). Turbulent drag reduction with polymers in rotating disk flow. Polymers, 7(7), 1279-1298.

Horn, A. F., & Merrill, E. W. (1984). Midpoint scission of macromolecules in dilute solution in turbulent flow. Nature, 312(5990), 140-141.

Houthakker, H. S. (1983). Whatever happened to the energy crisis?. The Energy Journal, 4(2), 1-8.

Hoyer, K. W., & Gyr, A. (1998). Heterogeneous drag reduction concepts and consequences. Journal of fluids engineering, 120(4), 818-823.

Hoyt, J. W. (1970). High molecular weight algal substances in the sea. Marine Biology, 7(2), 93-99.

Hoyt, J. W. (1991). “Negative roughness” and polymer drag reduction. Experiments in Fluids, 11(2-3), 142-146.

Hoyt, J. W., & Sellin, R. H. J. (1988). Drag reduction by centrally-injected polymer “threads”. Rheologica acta, 27(5), 518-522.

Hoyt, J. W., & Sellin, R. H. J. (1993). Scale effects in polymer solution pipe flow. Experiments in fluids, 15(1), 70-74.

Hoyt, J. W., & Soli, G. (1965). Algal cultures: ability to reduce turbulent friction in flow. Science, 149(3691), 1509-1511.

Huang, C., & Wei, J. (2017). Experimental study on the collaborative drag reduction performance of a surfactant solution in grooved channels. Brazilian Journal of Chemical Engineering, 34(1), 159-170.

Huang, C., Liu, D., & Wei, J. (2016). Experimental study on drag reduction performance of surfactant flow in longitudinal grooved channels. Chemical Engineering Science, 152, 267-279.

Hunston, D. L. (1974). Drag reduction in polymer mixtures and the effect of molecular weight distribution. Nature, 251(5477), 697-698.

Hutchison, K. J., Campbell, J. D., & Karpinski, E. (1989). Decreased poststenotic flow disturbance during drag reduction by polyacrylamide infusion without increased aortic blood flow. Microvascular research, 38(1), 102-109.

Ibrahim, A. F., Nasr-El-Din, H. A., Rabie, A., Lin, G., Zhou, J., & Qu, Q. (2018). A New Friction-Reducing Agent for Slickwater-Fracturing Treatments. SPE Production & Operations, 33(03), 583-595.

Inge, C., Johansson, A. V., & Lindgren, E. R. (1979). Effects of Congo red on the drag reduction properties of polyethylene oxide. The Physics of Fluids, 22(5), 824-829.

Interthal, W., & Wilski, H. (1985). Drag reduction experiments with very large pipes. Colloid and Polymer Science, 263(3), 217-229.

Iwamoto, K., Fukagata, K., Kasagi, N., & Suzuki, Y. (2005). Friction drag reduction achievable by near-wall turbulence manipulation at high Reynolds numbers. Physics of Fluids, 17(1), 011702.

Japper-Jaafar, A., Escudier, M. P., & Poole, R. J. (2009). Turbulent pipe flow of a drag-reducing rigid “rod-like” polymer solution. Journal of Non-Newtonian Fluid Mechanics, 161(1-3), 86-93.

Japper-Jaafar, A., Escudier, M. P., & Poole, R. J. (2010). Laminar, transitional and turbulent annular flow of drag-reducing polymer solutions. Journal of Non-Newtonian Fluid Mechanics, 165(19-20), 1357-1372.

Jouenne, S., Anfray, J., Levitt, D., Souilem, I., Marchal, P., Lemaitre, C., Choplin, L., Nesvik, J. and Waldman, T. (2015). Degradation (or lack thereof) and drag reduction of HPAM solutions during transport in turbulent flow in pipelines. Oil and gas facilities, 4(01), 80-92.

Kalashnikov, V. N. (2002). Degradation accompanying turbulent drag reduction by polymer additives. Journal of Non-Newtonian Fluid Mechanics, 103(2-3), 105-121.

Kalashnikov, V. N., & Kudin, A. M. (1973). Size and Volume Concentration of Aggregates in Drag-reducing Polymer Solution. Nature Physical Science, 242(119), 92-94.

Kamel, A., & Shah, S. N. (2009). Effects of salinity and temperature on drag reduction characteristics of polymers in straight circular pipes. Journal of petroleum Science and Engineering, 67(1-2), 23-33.

Kameneva, M.V., Wu, Z.J., Uraysh, A., Repko, B., Litwak, K.N., Billiar, T.R., Fink, M.P., Simmons, R.L., Griffith, B.P. & Borovetz, H.S. (2004). Blood soluble drag-reducing polymers prevent lethality from hemorrhagic shock in acute animal experiments. Biorheology, 41(1), 53-64.

Karami, H. R., Keyhani, M., & Mowla, D. (2016). Experimental analysis of drag reduction in the pipelines with response surface methodology. Journal of Petroleum Science and Engineering, 138, 104-112.

Kenis, P. R. (1968). Drag reduction by bacterial metabolites. Nature, 217(5132), 940-942.

Khalil, M. F., Kassab, S. Z., Elmiligui, A. A., & Naoum, F. A. (2002). Applications of drag-reducing polymers in sprinkler irrigation systems: Sprinkler head performance. Journal of irrigation and drainage engineering, 128(3), 147-152.

Khomyakov, A., & Elyukhina, I. (2019). Complete dynamic similarity for sea trials and towing tank experiments by means of polymer drag reduction. Ocean Engineering, 178, 31-37.

Kim, C. A., Jo, D. S., Choi, H. J., Kim, C. B., & Jhon, M. S. (2000). A high-precision rotating disk apparatus for drag reduction characterization. Polymer Testing, 20(1), 43-48.

Kim, C. A., Lee, K., Choi, H. J., Kim, C. B., Kim, K. Y., & Jhon, M. S. (1997). Universal characteristics of drag reducing polyisobutylene in kerosene. Journal of Macromolecular Science, Part A: Pure and Applied Chemistry, 34(4), 705-711.

Kim, C. A., Lim, S. T., Choi, H. J., Sohn, J. I., & Jhon, M. S. (2002). Characterization of drag reducing guar gum in a rotating disk flow. Journal of applied polymer science, 83(13), 2938-2944.

Kim, K., & Sirviente, A. I. (2007). Wall versus centerline polymer injection in turbulent channel flows. Flow, turbulence and combustion, 78(1), 69-89.

Kim, K., Li, C. F., Sureshkumar, R., Balachandar, S., & Adrian, R. J. (2007). Effects of polymer stresses on eddy structures in drag-reduced turbulent channel flow. Journal of Fluid Mechanics, 584, 281-299.

Kim, N. J., Kim, S., Lim, S. H., Chen, K., & Chun, W. (2009). Measurement of drag reduction in polymer added turbulent flow. International Communications in Heat and Mass Transfer, 36(10), 1014-1019.

Kline, S. J., & McClintock F. A. (1953). Describing uncertainty in single sample experiments. Mech. Engineering, 75, 3-8.

Koskinen, J., Manninen, M., Pättikangas, T., Alopaeus, V., Keskinen, K. I., & Kolehmainen, E. (2004). Measurements and CFD Modeling of Drag-Reduction Effects. SPE Production & Facilities, 19(03), 142-151.

Kostic, M. (1994). The ultimate asymptotes and possible causes of friction drag and heat transfer reduction phenomena. Journal of Energy Heat Mass Transfer, 16, 1-14.

Kotenko, M., Oskarsson, H., Bojesen, C., & Nielsen, M. P. (2019). An experimental study of the drag reducing surfactant for district heating and cooling. Energy, 78, 72-78.

Koury, E., & Virk, P. S. (1995). Drag reduction by polymer solutions in a riblet-lined pipe. Applied scientific research, 54(4), 323-347.

Kwack, E. Y., & Hartnett, J. P. (1983). New method to determine characteristic time of viscoelastic fluids. International Communications in Heat and Mass Transfer, 10(1), 77-82.

Le Brun, N., Zadrazil, I., Norman, L., Bismarck, A., & Markides, C. N. (2016). On the drag reduction effect and shear stability of improved acrylamide copolymers for enhanced hydraulic fracturing. Chemical Engineering Science, 146, 135-143.

Lee, K., Kim, C. A., Lim, S. T., Kwon, D. H., Choi, H. J., & Jhon, M. S. (2002). Mechanical degradation of polyisobutylene under turbulent flow. Colloid and Polymer Science, 280(8), 779-782.

Lescarboura, J. A., Culter, J. D., & Wahl, H. A. (1971). Drag reduction with a polymeric additive in crude oil pipelines. Society of Petroleum Engineers Journal, 11(03), 229-235.

Li, F. C., Kawaguchi, Y., Segawa, T., & Hishida, K. (2005). Reynolds-number dependence of turbulence structures in a drag-reducing surfactant solution channel flow investigated by particle image velocimetry. Physics of Fluids, 17(7), 075104.

Li, W., & Graham, M. D. (2007). Polymer induced drag reduction in exact coherent structures of plane Poiseuille flow. Physics of Fluids, 19(8), 083101.

Liang, T., Yang, Z., Zhou, F., Liu, Z., Qu, H., Yang, K., & Sun, J. (2017). A new approach to predict field-scale performance of friction reducer based on laboratory measurements. Journal of Petroleum Science and Engineering, 159, 927-933.

Liberatore, M. W., Baik, S., McHugh, A. J., & Hanratty, T. J. (2004). Turbulent drag reduction of polyacrylamide solutions: effect of degradation on molecular weight distribution. Journal of non-newtonian fluid mechanics, 123(2-3), 175-183.

Lim, S. T., Choi, H. J., & Chan, C. K. (2005). Effect of Turbulent Flow on Coil-Globule Transition of λ-DNA. Macromolecular rapid communications, 26(15), 1237-1240.

Lim, S. T., Choi, H. J., Lee, S. Y., So, J. S., & Chan, C. K. (2003). λ-DNA induced turbulent drag reduction and its characteristics. Macromolecules, 36(14), 5348-5354.

Lim, S. T., Hong, C. H., Choi, H. J., Lai, P. Y., & Chan, C. K. (2007). Polymer turbulent drag reduction near the theta point. EPL (Europhysics Letters), 80(5), 58003.

Little, R. C., & Ting, R. Y. (1976). Number-average and viscosity-average molecular weights of popular drag reducing polymers. Journal of Chemical and Engineering Data, 21(4), 422-423.

Liu, F., Liu, D., Zhou, W., Chen, F., & Wei, J. (2018). Coarse-Grained Molecular Dynamics Simulations of the Breakage and Recombination Behaviors of Surfactant Micelles. Industrial & Engineering Chemistry Research, 57(27), 9018-9027.

Lueth, C. A., & Shaqfeh, E. S. (2009). Experimental and numerical studies of tethered DNA shear dynamics in the flow-gradient plane. Macromolecules, 42(22), 9170-9182.

Lumley, J. L. (1973). Drag reduction in turbulent flow by polymer additives. Journal of Polymer Science: Macromolecular Reviews, 7(1), 263-290.

Ma, Y., Zheng, X., Shi, F., Li, Y., & Sun, S. (2003). Synthesis of poly (dodecyl methacrylate) s and their drag-reducing properties. Journal of applied polymer science, 88(7), 1622-1626.

Madras, G., & Chattopadhyay, S. (2001). Effect of solvent on the ultrasonic degradation of poly (vinyl acetate). Polymer degradation and stability, 71(2), 273-278.

Malin, M. R. (1997). Turbulent pipe flow of power-law fluids. International communications in heat and mass transfer, 24(7), 977-988.

Malkin A. I., Malkin A. Y., and Isayev A. I., 2006, Rheology Concepts, Methods, and Applications. ChemTec Publishing, Toronto, CA, Chap. 2.

McComb, W. D., & Rabie, L. H. (1978). Drag-reducing polymers and turbulent bursts. Nature, 273(5664), 653-654.

Metzner, A. B., & Park, M. G. (1964). Turbulent flow characteristics of viscoelastic fluids. Journal of Fluid Mechanics, 20(2), 291-303.

Mizunuma, H., Ueda, K., & Yokouchi, Y. (1999). Synergistic effects in turbulent drag reduction by riblets and polymer additives. Journal of fluids engineering, 121(3), 533-540.

Motta, M. V. L., de Castro, E. V. R., Muri, E. J. B., Costalonga, M. L., Loureiro, B. V., & Filgueiras, P. R. (2019). Study of the mechanical degradation mechanism of guar gum in turbulent flow by FTIR. International journal of biological macromolecules, 121, 23-28.

Muth, C. L., Husen, G. J., Lewis, M. H., Stansberry, C. J., & Ziobro, M. S. (1985). Powerful new tool for pipeliners flow improver. Pipeline & Gas Journal, 212(6), 38-40.

Muth, C. L., Monahan, M. J., & Pessetto, L. S. (1986). Application of drag reducing agents effect cost savings. Pipe Line Industry, 65(1), 43-44.

Muthukumar, M. (1984). Concentration dependent relaxation times of linear polymers in dilute solutions. Macromolecules, 17(4), 971-973.

Myska, J., & Mik, V. (2003). Application of a drag reducing surfactant in the heating circuit. Energy and Buildings, 35(8), 813-819.

Nadolink, R. H., & Haigh, W. W. (1995). Bibliography on skin friction reduction with polymers and other boundary-layer additives. Applied Mechanics Reviews, 48(7), 351-460.

Nesyn, G. V., Sunagatullin, R. Z., Shibaev, V. P., & Malkin, A. Y. (2018). Drag reduction in transportation of hydrocarbon liquids: From fundamentals to engineering applications. Journal of Petroleum Science and Engineering, 161, 715-725.

Ng, J. C. Y., Cheung, W. H., & McKay, G. (2002). Equilibrium studies of the sorption of Cu (II) ions onto chitosan. Journal of Colloid and Interface Science, 255(1), 64-74.

Nguyen, T. C., Romero, B., Vinson, E., & Wiggins, H. (2018). Effect of salt on the performance of drag reducers in slickwater fracturing fluids. Journal of Petroleum Science and Engineering, 163, 590-599.

Nifant'ev, I. E., Shlyakhtin, A. V., Tavtorkin, A. N., Korchagina, S. A., Chinova, M. S., Vinogradov, A. A., Vinogradov, A. A., Roznyatovsky, V. A., Khaidapova, D. D. and

Ivchenko, P. V. (2018) The synthesis of ultra-high molecular weight poly (1-hexene) s by low-temperature Ziegler-Natta precipitation polymerization in fluorous reaction media. Polymer, 139, 98-106.

Oba, R., Ito, Y., & Uranishi, K. (1978). Effect of polymer additives on cavitation development and noise in water flow through an orifice. Journal of Fluids Engineering, 100(4), 493-499.

Oesterhelt, F., Rief, M., & Gaub, H. E. (1999). Single molecule force spectroscopy by AFM indicates helical structure of poly (ethylene-glycol) in water. New Journal of Physics, 1(1), 6.

Omrani, P. S., Delfos, R., & Boersma, B. J. (2012). Polymer induced drag reduction in a turbulent pipe flow subjected to a Coriolis force. Flow, Turbulence and Combustion, 4(89), 589-599.

Owolabi, B. E., Dennis, D. J., & Poole, R. J. (2017). Turbulent drag reduction by polymer additives in parallel-shear flows. Journal of Fluid Mechanics, 827.

Paschkewitz, J. S., Dimitropoulos, C. D., Hou, Y. X., Somandepalli, V. S. R., Mungal, M. G., Shaqfeh, E. S., & Moin, P. (2005). An experimental and numerical investigation of drag reduction in a turbulent boundary layer using a rigid rodlike polymer. Physics of Fluids, 17(8), 085101.

Paterson, R. W., & Abernathy, F. H. (1970). Turbulent flow drag reduction and degradation with dilute polymer solutions. Journal of Fluid Mechanics, 43(4), 689-710.

Pereira, A. S., & Soares, E. J. (2012). Polymer degradation of dilute solutions in turbulent drag reducing flows in a cylindrical double gap rheometer device. Journal of Non-Newtonian Fluid Mechanics, 179-180, 9-22.

Pereira, A. S., Andrade, R. M., & Soares, E. J. (2013). Drag reduction induced by flexible and rigid molecules in a turbulent flow into a rotating cylindrical double gap device: Comparison between Poly (ethylene oxide), Polyacrylamide, and Xanthan Gum. Journal of Non-Newtonian Fluid Mechanics, 202, 72-87.

Peyser, P., & Little, R. C. (1971). The drag reduction of dilute polymer solutions as a function of solvent power, viscosity, and temperature. Journal of applied polymer science, 15(11), 2623-2637.

Phukan, S., Kumar, P., Panda, J., Nayak, B. R., Tiwari, K. N., & Singh, R. P. (2001). Application of drag reducing commercial and purified guargum for reduction of energy requirement of sprinkler irrigation and percolation rate of the soil. Agricultural water management, 47(2), 101-118.

Pirih, R. J., & Swanson, W. M. (1972). Drag reduction and turbulence modification in rigid particle suspensions. The Canadian Journal of Chemical Engineering, 50(2), 221-227.

Polimeni, P. I., & Ottenbreit, B. T. (1989). Hemodynamic Effects of a Poly (Ethylene Oxide) Drag-Reducing Polymer, Poly ox WSR N-60K, in the Open-Chest Rat. Journal of cardiovascular pharmacology, 14(3), 374-380.

Polimeni, P. I., Ottenbreit, B., & Coleman, P. (1985). Enhancement of aortic blood flow with a linear anionic macropolymer of extraordinary molecular length. Journal of molecular and cellular cardiology, 17(7), 721-724.

Polverari, M., & van de Ven, T. G. (1996). Dilute aqueous poly (ethylene oxide) solutions: clusters and single molecules in thermodynamic equilibrium. The Journal of physical chemistry, 100(32), 13687-13695.

Poole R. J. (2012). The Deborah and Weissenberg numbers. The British Society of Rheology-Rheology Bulletin, 53(2), 32-39.

Pouranfard, A. R., Mowla, D., & Esmaeilzadeh, F. (2014). An experimental study of drag reduction by nanofluids through horizontal pipe turbulent flow of a Newtonian liquid. Journal of Industrial and Engineering Chemistry, 20(2), 633-637.

Procaccia, I., L'vov, V. S., & Benzi, R. (2008). Colloquium: Theory of drag reduction by polymers in wall-bounded turbulence. Reviews of Modern Physics, 80(1), 225.

Ptasinski, P. K., Boersma, B. J., Nieuwstadt, F. T. M., Hulsen, M. A., Van den Brule, B. H. A. A., & Hunt, J. C. R. (2003). Turbulent channel flow near maximum drag reduction: simulations, experiments and mechanisms. Journal of Fluid Mechanics, 490, 251-291.

Quan, Q., Wang, S., Wang, L., Shi, Y., Xie, J., Wang, X., & Wang, S. (2019). Experimental study on the effect of high-molecular polymer as drag reducer on drag reduction rate of pipe flow. Journal of Petroleum Science and Engineering, 178, 852–856.

Radin, I., Zakin, J. L., & Patterson, G. K. (1975). Drag reduction in solid-fluid systems. AIChE Journal, 21(2), 358-371.

Ram, A., Finkelstein, E., & Elata, C. (1967). Reduction of friction in oil pipelines by polymer additives. Industrial & Engineering Chemistry Process Design and Development, 6(3), 309-313.

Ramus, J., Kenney, B. E., & Shaughnessy, E. J. (1989). Drag reducing properties of microalgal exopolymers. Biotechnology and bioengineering, 33(5), 550-557.

Rasti, E., Talebi, F., & Mazaheri, K. (2019). A turbulent duct flow investigation of drag-reducing viscoelastic FENE-P fluids based on different low-Reynolds-number models. Physica A: Statistical Mechanics and its Applications, 526, 120718.

Reiner, M. (1964). The Deborah number. Physics today, 17(1), 62.

Reitzer, H., Gebel, C., & Scrivener, O. (1985). Effect of polymeric additives on cavitation and radiated noise in water flowing past a circular cylinder. Journal of non-newtonian fluid mechanics, 18(1), 71-79.

Rodriguez Corredor, F. E., Bizhani, M., & Kuru, E. (2015). Experimental investigation of drag reducing fluid flow in annular geometry using particle image velocimetry technique. Journal of Fluids Engineering, 137(8), 081103.

Rodriguez, J. M., Zakin, J. L., & Patterson, G. K. (1967). Correlation of drag reduction with modified deborah number for dilute polymer solutions. Society of Petroleum Engineers Journal, 7(03), 325-332.

Rowin, W. A., Sanders, R. S., & Ghaemi, S. (2018). A recipe for optimum mixing of polymer drag reducers. Journal of Fluids Engineering, 140(11), 111402.

Sachdev, S., Muralidharan, A., & Boukany, P. E. (2016). Molecular processes leading to "necking" in extensional flow of polymer solutions: Using microfluidics and single DNA imaging. Macromolecules, 49(24), 9578-9585.

Samanta, G., Beris, A. N., Handler, R. A., & Housiadas, K. D. (2009). Velocity and conformation statistics based on reduced Karhunen–Loeve projection data from DNS of viscoelastic turbulent channel flow. Journal of Non-Newtonian Fluid Mechanics, 160(1), 55-63.

Sar, N., & Rosenberg, E. (1989). Fish skin bacteria: production of friction-reducing polymers. Microbial ecology, 17(1), 27-38.

Savins, J. G. (1964). Drag reduction characteristics of solutions of macromolecules in turbulent pipe flow. Society of Petroleum Engineers Journal, 4(03), 203-214.

Savins, J. G. (1967). A stress-controlled drag-reduction phenomenon. Rheologica Acta, 6(4), 323-330.

Sawchuk, A. P., Unthank, J. L., & Dalsing, M. C. (1999). Drag reducing polymers may decrease atherosclerosis by increasing shear in areas normally exposed to low shear stress. Journal of vascular surgery, 30(4), 761-764.

Schmitt, G. (2001). Drag reduction by corrosion inhibitors–A neglected option for mitigation of flow induced localized corrosion. Materials and Corrosion, 52(5), 329-343.

Sedahmed, G. H., Abdo, M. S. E., Amer, M. A., & El-Latif, G. A. (1999). Effect of drag reducing polymers on the rate of mass transfer controlled corrosion in pipelines under developing turbulent flow. International communications in heat and mass transfer, 26(4), 531-538.

Sedahmed, G. H., Abdo, M. S. E., Farag, H. A., & Tantawy, S. G. (1979). The use of drag-reducing polymers as corrosion inhibitors in pipelines. Surface Technology, 9(5), 359-363.

Sedahmed, G. H., Farag, H. A., Abdo, M. S. E., & Tantawy, S. G. (1984). Inhibition of diffusion controlled corrosion in pipelines by drag reducing polymers under turbulent flow conditions. Journal of applied electrochemistry, 14(1), 75-78.

Sellin, R. H. J. (1978). Drag reduction in sewers: first results from a permanent installation. Journal of Hydraulic Research, 16(4), 357-371.

Sellin, R. H. J. (1983). Use of polymer additives to relieve overloaded sewers. Proceedings of the Institution of Civil Engineers, 74(4), 997-1006.

Selser, J. C. (1981). Dilute-solution hydrodynamic behavior of poly (α-methylstyrene) in a good solvent. Macromolecules, 14(2), 346-351.

Sever, F. A., & Metzner, A. B. (1967). Turbulent flow properties of viscoelastic fluids. The Canadian Journal of Chemical Engineering, 45(3), 121-126.

Seyer, F. A., & Catania, P. J. (1972). Laminar and turbulent entry flow of polymer solutions. The Canadian Journal of Chemical Engineering, 50(1), 31-36.

Shah, S. N., & Kamel, A. H. (2010). Investigation of flow behavior of slickwater in large straight and coiled tubing. SPE Production & Operations, 25(01), 70-79.

Shah, S. N., Tareen, M., & Clark, D. (2002). Effects of solids loading on drag reduction in polymeric drilling fluids through straight and coiled tubing. Journal of Canadian Petroleum Technology, 41(5), 63-69.

Shah, S., & Vyas, A. (2011). Temperature and Salinity Effects on Drag-Reduction Characteristics of Polymers in Coiled Tubing. SPE Production & Operations, 26(01), 55-66.

Shao, X. M., Lin, J. Z., Wu, T., & Li, Y. L. (2002). Experimental research on drag reduction by polymer additives in a turbulent pipe flow. The Canadian Journal of Chemical Engineering, 80(2), 293-298.

Shetty, A. M., & Solomon, M. J. (2009). Aggregation in dilute solutions of high molar mass poly (ethylene) oxide and its effect on polymer turbulent drag reduction. Polymer, 50(1), 261-270.

Smith, S. B., Finzi, L., & Bustamante, C. (1992). Direct mechanical measurements of the elasticity of single DNA molecules by using magnetic beads. Science, 258(5085), 1122-1126.

Soares, E. J., Siqueira, R. N., Leal, L. M., Barbosa, K. C., Cipriano, D. F., & Freitas, J. C. (2019). The role played by the aging of aloe vera on its drag reduction properties in turbulent flows. Journal of Non-Newtonian Fluid Mechanics, 265, 1-10.

Sreenivasan, K. R., & White, C. M. (2000). The onset of drag reduction by dilute polymer additives, and the maximum drag reduction asymptote. Journal of Fluid Mechanics, 409, 149-164.

Strelnikova, S., & Yushchenko, T. (2019). Adaptation of fluid motion mathematical model in pipelines using drag reducing agents. In PSIG Annual Meeting. Pipeline Simulation Interest Group.

Sung, H. J., Meredith, C., Johnson, C., & Galis, Z. S. (2004). The effect of scaffold degradation rate on three-dimensional cell growth and angiogenesis. Biomaterials, 25(26), 5735-5742.

Sylvester, N. D., & Smith, P. S. (1979). The concentration and friction velocity effects on drag reduction by Dowell-APE in kerosene. Industrial & Engineering Chemistry Product Research and Development, 18(1), 47-49.

Tabor, M., & De Gennes, P. G. (1986). A cascade theory of drag reduction. EPL (Europhysics Letters), 2(7), 519-522.

Tamano, S., & Itoh, M. (2011). Comparison of turbulence structures at large and small drag reduction ratios in turbulent boundary layer of surfactant solutions. Journal of Turbulence, 12(18), 1-22.

Teixeira, R. E., Babcock, H. P., Shaqfeh, E. S., & Chu, S. (2005). Shear thinning and tumbling dynamics of single polymers in the flow-gradient plane. Macromolecules, 38(2), 581-592.

Tesauro, C., B. J. Boersma, M. A. Hulsen, P. K. Ptasinski, and F. T. M. Nieuwstadt. "Events of high polymer activity in drag reducing flows." Flow, Turbulence and Combustion 79, no. 2 (2007): 123-132.

Test, F. L. (1974). Analytical Prediction of the Influence of Polymer Additives on the Shear Drag of Bodies of Revolution. Journal of Hydronautics, 8(2), 45-46.

Thais, L., Tejada-Martinez, A. E., Gatski, T. B., & Mompean, G. (2010). Temporal large eddy simulations of turbulent viscoelastic drag reduction flows. Physics of Fluids, 22(1), 013103.

Toms, B. A. (1948). Some observations on the flow of linear polymer solutions through straight tubes at large Reynolds numbers. Proceedings of International Congress on Rheology, 1948, 135-141.

Toms, B. A. (1977). On the early experiments on drag reduction by polymers. The Physics of Fluids, 20(10), S3-S5.

Tuan, N. A., & Mizunuma, H. (2013). High-shear drag reduction of surfactant solutions. Journal of Non-Newtonian Fluid Mechanics, 198, 71-77.

Unthank, J. L., Lalka, S. G., Nixon, J. C., & Sawchuk, A. P. (1992). Improvement of flow through arterial stenoses by drag reducing agents. Journal of Surgical Research, 53(6), 625-630.

Ushida, A., Hasegawa, T., Nakajima, T., Uchiyama, H., & Narumi, T. (2012). Drag reduction effect of nanobubble mixture flows through micro-orifices and capillaries. Experimental Thermal and Fluid Science, 39, 54-59.

Ushida, A., Murao, S., Hasegawa, T., Narumi, T., & Amaki, K. (2016). Anomaly of pressure drops of rod-like micelle surfactant solutions passing through small orifices. Experimental Thermal and Fluid Science, 70, 69-76.

Ushida, A., Ogawa, S., Narumi, T., Sato, T., & Hasegawa, T. (2018). Pseudo-laminarization effect of dilute and ultra-dilute polymer solutions on flows in narrow pipes. Experimental Thermal and Fluid Science, 99, 233-241.

Van Dam, P. H. J., & Wegdam, G. H. (1993). The role of small scale coherent structures in turbulent drag reduction. Applied Scientific Research, 51(1-2), 155-159.

Vanapalli, S. A., Islam, M. T., & Solomon, M. J. (2005). Scission-induced bounds on maximum polymer drag reduction in turbulent flow. Physics of Fluids, 17(9), 095108.

Virk, P. S. (1975). Drag reduction fundamentals. AIChE Journal, 21(4), 625-656.

Virk, P. S. (1976). Conformational effects in drag reduction by polymers. Nature, 262(5563), 46-47.

Virk, P. S., & Baher, H. (1970). The effect of polymer concentration on drag reduction. Chemical Engineering Science, 25(7), 1183-1189.

Virk, P. S., Mickley, H. S., & Smith, K. A. (1970). The ultimate asymptote and mean flow structure in Toms' phenomenon. Journal of Applied Mechanics, 37(2), 488-493.

Vleggaar, J., & Tels, M. (1973). Drag reduction by polymer threads. Chemical engineering science, 28(3), 965- 968.

Warholic, M. D., Heist, D. K., Katcher, M., & Hanratty, T. J. (2001). A study with particle-image velocimetry of the influence of drag-reducing polymers on the structure of turbulence. Experiments in fluids, 31(5), 474-483.

Wells Jr, C. S., & Spangler, J. G. (1967). Injection of a Drag-Reducing Fluid into Turbulent Pipe Flow of a Newtonian Fluid. The Physics of Fluids, 10(9), 1890-1894.

White, A. (1966). Effect of polymer additives on boundary layer separation and drag of submerged bodies. Nature, 211(5056), 1390.

White, C. M., & Mungal, M. G. (2008). Mechanics and prediction of turbulent drag reduction with polymer additives. Annu. Rev. Fluid Mech., 40, 235-256.

White, C. M., Somandepalli, V. S. R., & Mungal, M. G. (2004). The turbulence structure of drag-reduced boundary layer flow. Experiments in fluids, 36(1), 62-69.

White, D. A. (1970). Correlation of pressure drop data in pipe flow of dilute polymer solutions. Chemical Engineering Science, 25(7), 1127-1132.

Yang, B., Zhao, J., Mao, J., Tan, H., Zhang, Y., & Song, Z. (2019). Review of Friction Reducers used in Slickwater Fracturing Fluids for Shale Gas Reservoirs. Journal of Natural Gas Science and Engineering. 62, 302–313.

Yang, C., Changjun, L., Nechval, A. M., Peng, Y., & Zhukov, A. Y. (2018). Commercial field testing improves understanding of DRA degradation. Oil & Gas Journal, 116(3), 78-84.

Yang, K. S., Choi, H. J., Kim, C. B., Kim, I. S., & Jhon, M. S. (1994). Characterization of turbulent drag reduction in rotating disk system. Korean Journal of Chemical Engineering, 11(1), 8-13.

Yang, S. Q. (2009). Drag reduction in turbulent flow with polymer additives. Journal of Fluids Engineering, 131(5), 051301.

Yang, S. Q., & Ding, D. (2013). Drag reduction induced by polymer in turbulent pipe flows. Chemical Engineering Science, 102, 200-208.

Yang, S. Q., & Ding, D. (2014). Drag-reducing flows in laminar-turbulent transition region. Journal of Fluids Engineering, 136(10), 101202.

Yang, S. Q., & Dou, G. R. (2008). Modeling of viscoelastic turbulent flow in channel and pipe. Physics of fluids, 20(6), 065105.

Ying, Q., & Chu, B. (1987). Overlap concentration of macromolecules in solution. Macromolecules, 20(2), 362-366.

Zabihi, R., Mowla, D., & Karami, H. R. (2019). Artificial intelligence approach to predict drag reduction in crude oil pipelines. Journal of Petroleum Science and Engineering, 9, 586-593.

Zahran, R. R., & Sedahmed, G. H. (1997). Galvanic corrosion of zinc in turbulently moving saline water containing drag reducing polymers. Materials Letters, 31(1-2), 29-33.

Zahran, R. R., & Sedahmed, G. H. (1998). Effect of drag-reducing polymers on the rate of flow-induced corrosion of metals. Materials Letters, 35(3-4), 207-213.

Zakin, J. L., Myska, J., & Chara, Z. (1996). New limiting drag reduction and velocity profile asymptotes for nonpolymeric additives systems. AIChE Journal, 42(12), 3544-3546.

Zhang, K., Choi, H. J., & Jang, C. H. (2011). Turbulent drag reduction characteristics of poly (acrylamide-co-acrylic acid) in a rotating disk apparatus. Colloid and Polymer Science, 289(17-18), 1821-1827.

Zhang, K., Lim, G. H., & Choi, H. J. (2016). Mechanical degradation of water-soluble acrylamide copolymer under a turbulent flow: Effect of molecular weight and temperature. Journal of Industrial and Engineering Chemistry, 33, 156-161.

Zhang, M., Lashgari, I., Zaki, T. A., & Brandt, L. (2013). Linear stability analysis of channel flow of viscoelastic Oldroyd-B and FENE-P fluids. Journal of Fluid Mechanics, 737, 249-279.

Zhang, Y., Qi, Y., & Zakin, J. L. (2005). Headgroup effect on drag reduction and rheological properties of micellar solutions of quaternary ammonium surfactants. Rheologica acta, 45(1), 42-58.

Zhao, J., Chen, P., Liu, Y., Zhao, W., & Mao, J. (2018). Prediction of Field Drag Reduction by a Modified Practical Pipe Diameter Model. Chemical Engineering & Technology, 41(7), 1417-1424.

Zhu, L., Schrobsdorff, H., Schneider, T. M., & Xi, L. (2018). Distinct transition in flow statistics and vortex dynamics between low-and high-extent turbulent drag reduction in polymer fluids. Journal of Non-Newtonian Fluid Mechanics, 262, 115-130.

Zimm, B. H. (1956). Dynamics of polymer molecules in dilute solution: viscoelasticity, flow birefringence and dielectric loss. The journal of chemical physics, 24(2), 269-278.

Appendix

Appendix 1 How to Obtain the Weissenberg Number from μ_S, u, d, and N

TABLE A1 Detailed procedure of combining these four variables as one dimensionless number, the Weissenberg number, based on Zimm's theory (1956)

Step	Parameter /Group	Unit	Parameter /Group	Unit	Parameter /Group	Unit	Parameter /Group	Unit
1	μ_S	kg · m^{-1} · s^{-1}	u	m · s^{-1}	d	m	N	...
2	$N^{1.8}\mu_S$	kg · m^{-1} · s^{-1}	u	m · s^{-1}	d	m	...	...
3	$\frac{a^3}{k_BT}N^{1.8}\mu_S$	s	u	m · s^{-1}	d	m	...	...
4	$\frac{(aN^{0.6})^3}{k_BT}\mu_S$	s	u	m · s^{-1}	d	m	...	...
5	$\frac{(aN^{0.6})^3}{k_BT}\mu_S$	s	$8u$	m · s^{-1}	d	m	...	...
6	$\frac{(aN^{0.6})^3}{k_BT}\mu_S$	s	$\frac{8u}{d}$	s^{-1}	...	...	...	...
7	$\frac{(aN^{0.6})^3}{k_BT}\mu_S\frac{8u}{d}$	...						

NOTES: 1: Four remaining parameters are listed; 2: The degree of polymerization, N, and solvent viscosity, μ_S, are combined. The unit of the new group $N^{1.8}\mu_S$ has the same unit as μ_S; 3: The monomer length of the PEO, a, Boltzmann constant, k_B, and temperature, T, are constants in each experiment. Therefore, these constants, a^3/k_BT and $N^{1.8}\mu_S$ are combined; 4: This new group, $a^3N^{1.8}\mu_S/k_BT$, is rearranged to $(aN^{0.6})^3\mu_S/k_BT$; the latter one is equal to the relaxation

time from Equation (2); 5: A constant 8 is multiplied by u; 6: To eliminate the unit of length, $8u$ is divided by d. Therefore, a new group $8u/d$ forms, which is equal to the shear rate at the wall in Equation (4); and 7: $(aN^{0.6})^3\mu_S/k_BT$ and $8u/d$ are combined to have the Weissenberg number.

Appendix 2. Why the Correlation Format of Eq. 4-8 Is Proposed

In addition to the main reasons related to previous experimental and analytical results explained in the paper, the format can be further explained from a statistic point of view. If one assumes that C_P and Wi follow a second order polynomial (without a constant, since DR should be 0 when no polymers are added) in Equation (A1), the P values for C_P, C_P^2, Wi, Wi^2 and $C_P Wi$ are 1.47×10^{-6}, 0.86, 0.62, 0.07, and 0.68, respectively. A lower P value (usually < 0.05) means that a variable is more relevant to the equation. From these five P values, it can be seen that C_P is the most relevant to Eq. A1 since its P value is the lowest. C_P^2, Wi, and $C_P Wi$ are not relevant since their P values are much greater than 0.05. The P value of Wi^2 is 0.07, slightly greater than 0.05, which means that this variable has a high potential of relevance to the drag reduction correlation if a proper correlation format is used, Eq. 4-8 as an example. If Eq. 4-8 format is used, the P values for C_P and Wi^2 are 3.05×10^{-27} and 1.09×10^{-10}, meaning C_P and Wi^2 are relevant to the correlation. In this condition, it is believe that Wi^2 not Wi should be chosen for the correlation, as shown in Eq. 4-8:

$$DR = A_1 C_P + A_2 C_P^2 + A_3 Wi + A_4 Wi^2 + A_5 C_P Wi \quad \text{(A1)}$$

Appendix 3. List of Publications

Published Journal Papers

- Zhang, X., Duan, X., & Muzychka, Y. (2018). Analytical upper limit of drag reduction with polymer additives in turbulent pipe flow. Journal of Fluids Engineering, 140(5), 051204. https://doi.org/10.1115/1.4038757
- Zhang, X., Duan, X., & Muzychka, Y. (2018). New mechanism and correlation for degradation of drag-reducing agents in turbulent flow with measured data from a double-gap rheometer. Colloid and Polymer Science, 296(4), 829-834. https://doi.org/10.1007/s00396-018-4300-4
- Zhang, X., Duan, X., & Muzychka, Y. (2019). Degradation of flow drag reduction with polymer additives—A new molecular view. Journal of Molecular Liquids, 292, 111360. https://doi.org/10.1016/j.molliq.2019.111360
- Zhang, X., Duan, X., & Muzychka, Y. (2020). Drag reduction by linear flexible polymers and its degradation in turbulent flow: A phenomenological explanation from chemical thermodynamics and kinetics. Physics of Fluids, 32(1), 013101. https://doi.org/10.1063/1.5132284
- Zhang, X., Duan, X., Muzychka, Y., & Wang, Z. (2020). Experimental correlation for pipe flow drag reduction using relaxation time of linear flexible polymers in a dilute solution. The Canadian Journal of Chemical Engineering, 98(3), 792-803. https://doi.org/10.1002/cjce.23649

Journal Papers under Preparation

- Zhang, X., Duan, X., & Muzychka, Y. Mini-review of drag reduction and degradation by polymers: history, application, research and theory.

Published Conference Papers

- Zhang, X., Duan, X., Muzychka, Y. (2017, May). Analytical solution of drag reduction by chemical additives in turbulent pipe flow. In 26th Canadian Congress of Applied Mechanics. Canadian Congress of Applied Mechanics.
- Zhang, X., Duan, X., Muzychka, Y., & Wang, Z. (2018, November). Predicting drag reduction in turbulent pipe flow with relaxation time of polymer additives. In 2018 12th International Pipeline Conference. American Society of Mechanical Engineers.

Posters and Presentations

- Zhang, X., Duan, X., Muzychka, Y., & Wang, Z. (2017, May). A possible mechanism for degradation of drag-reducing agents in turbulent flow in rheometers. Memorial University of Newfoundland and Canadian Society for Mechanical Engineering Symposium.
- Zhang, X., Duan, X., Muzychka, Y. (2018, May). Degradation of drag-reducing polymers from chemical dynamics view. Memorial University of Newfoundland Engineering Research Day.